General Disclaimer

One or more of the Following Statements may affect this Document

- This document has been reproduced from the best copy furnished by the organizational source. It is being released in the interest of making available as much information as possible.

- This document may contain data, which exceeds the sheet parameters. It was furnished in this condition by the organizational source and is the best copy available.

- This document may contain tone-on-tone or color graphs, charts and/or pictures, which have been reproduced in black and white.

- This document is paginated as submitted by the original source.

- Portions of this document are not fully legible due to the historical nature of some of the material. However, it is the best reproduction available from the original submission.

08710-6023-R0-00
NOVEMBER 1968

TEST PLAN
for
NAVSTAR NAVIGATION SYSTEM

VOLUME I
TEST PLAN DESCRIPTION

Prepared under Contract NAS-12-539 for
ELECTRONICS RESEARCH CENTER
NATIONAL AERONAUTICS AND SPACE ADMINISTRATION

TRW
SYSTEMS GROUP

Mr. Peter Engels
Technical Coordinator
NAS 12-539
Electronics Research Center
Cambridge,
Massachusetts 02139

Requests for copies of this report
should be referred to:

NASA Scientific and Technical
Information Facility
P.O. Box 33
College Park,
Maryland 20740

08710-6023-R0-00
November 1968

TEST PLAN FOR NAVSTAR NAVIGATION SYSTEM

Volume I. Test Plan Description

Prepared Under Contract NAS 12-539 for

ELECTRONICS RESEARCH CENTER
NATIONAL AERONAUTICS AND SPACE ADMINISTRATION

TRW Systems Group
One Space Park
Redondo Beach, California

CONTENTS

CONTENTS (cont)

1. INTRODUCTION

The test plan described here in Volume I develops a series of tests for evaluating the NAVSTAR navigation system. These tests are aimed at establishing a high degree of confidence in the ultimate performance of navigation sat llite systems operating in the frequency range from 1540 to 1660 MHz.

The specific tests proposed in this plan follow a logical sequence from the laboratory to the field to spaceborne testing using a small piggy-back-launched satellite. In addition, a demonstration test of the NAVSTAR position location technique using the Initial Defense Communications Satellite Project (IDCSP) satellite nerwork is discussed. The ultimate goal of the test plan is development of sufficient data and confidence to permit the deployment of a full scale prototype NAVSTAR satellite system for the area coverage described in Reference 1.

The test sequence, discussed in detail in Section 3, includes the following four types:

1) Laboratory Tests, using a precision oscillator, BINOR code generator, and low power L-band transmitter, connected through an attenuator to a BINOR TDM (time division multiplex receiver and range acquisition unit. Another test uses an antenna test range and model antennas and aircraft to measure user antenna pattern characteristics.

2) Field Tests, using a receiving aircraft and/or helicopter to simulate a user and such signal sources as aircraft, balloons, or ground transmitters simulating the satellite(s).

3) ERS (piggyback-launched satellite) Test, using a low-orbiting satellite carrying the BINOR code signal portion of the N NAVSTAR navigation signal subsystem plus supporting subsystems. The satellite design is covered in Volume II of this report. A ground station network and an aircraft simulating a user form the remaining components of the test. The aircraft can be the same as that used in the field tests.

4) IDCSP Demonstration Test, using four of the IDCSP satellites for transponding range signals among a network of ground stations, one of which simulates a user while others simulate the NAVSTAR ground tracking network.

Budgetary and planning type cost estimates plus schedules for the laboratory and field tests are given in Section 4.

2. TEST OBJECTIVES

NAVSTAR is a complete radio navigation system incorporating satellites in lieu of ground beacons. Potential users range from low speed ships to SST's; the complexity of user equipment will vary significantly, depending on the user's dynamics and need for precision navigation. Because of the diversity of speeds, altitudes, and precision requirements, the system test plan needs to provide data on all of the basic operating characteristics of the system, from which the results to be achieved by a particular user can be determined from individual user operating characteristics.

The objective of the test phase is to formulate and understand the system model. A model of the ranging measurement error sources for the NAVSTAR system is given in Appendix A. This model is an updated version of the error model given in Volume II of Reference 1.

Each test is designed to verify certain portions of the range error model (as tabulated in Table 1). In addition, Table 1 shows the other objectives of each specific test which are connected with the operating performance of key elements of the user and satellite electronics and with demonstration of position determination.

Each test provides for the maximum number of objectives at minimum cost. In this regard, presently operational satellites were surveyed to determine whether any are applicable to the objectives of the ERS test. For example, a transponding satellite operating at or near L band could meet some of the ERS objectives, such as tropospheric, ionospheric, and multipath errors. Appendix B reports the results of the survey, which concludes that no suitable satellites exist at this time. Future launches as provided for in NASA's Application Technology Satellite Program could change this conclusion.

A demonstration pf high accuracy position fixing using the near-synchronous IDCSP X-band satellite network is also discussed. The value of this test in in demonstrating position location techniques using a network of tracked synchronous satellites such as that proposed for the NAVSTAR SYSTEM.

Table 1. Objectives of Each Test

Test	Error Model	Other
Laboratory	• Receiver thermal noise • Receiver drift and bias • Quantization • Satellite oscillator	• Receiver acquisition times • User antenna coverage • User antenna multipath reception
Field	• Multipath • User oscillator	• Operation of user equipment in aircraft and/or helicopter • Airborne RFI environment • Refinement of satellite ERP requirements • Limited test of position determination
ERS	• Tropospheric retardation • Ionospheric refraction • Multipath • Overall model*	• Further refinement of satellite ERP requirements
IDCSP		• Tracking station and user software • Demonstration of NAVSTAR position determination technique

*The overall error will be measured at a ground station so that it will not contain multipath errors or any errors that may be peculiar to an aircraft environment.

3. TEST DESCRIPTIONS

3.1 LABORATORY TESTS

The laboratory tests are designed to verify the performance of the user receiving equipment and the satellite precision oscillator. Included are tests to measure the acquisition properties of the L-band carrier and BINOR range code signals and to determine the magnitude of the range measurement error sources (random and bias) in the receiver range code acquisition unit, and satellite precision oscillator prediction. In addition, a test to measure user antenna patterns with scale model aircraft and antennas is described. The measurements not only determine coverage patterns for the tested antennas but also can be used to predict the multipath rejection characteristics of the antenna with the aid of a computer program written for this purpose.

The following equipment is required for the laboratory tests:

1) Low-power L-band transmitter

   RF bandwidth $\geq$ 2 MHz
   Power output: 10 milliwatts

2) Phase modulator

3) BINOR code generator

4) Precision oscillator (two identical units)

5) Phase lock receiver–time division multiplex (TDM)

6) BINOR range code acquisition unit

7) Acquisition sequence control logic (special built test equipment)

8) Scale model aircraft

9) Scale model user antenna

10) Instrumented antenna range

The first seven items are for the user receiving equipment and satellite oscillator tests while the last three are for the antenna pattern measurements. In addition, standard commercial test equipment, e.g., voltmeters, power meters, counters, attenuators, will be required.

Many of the tests require knowledge of the various noise bandwidth and signal-to-noise ratios in the equipment being tested. Appendix C describes procedures for measuring these parameters.

The receiver and oscillator tests should be repeated for various environmental conditions expected to be encountered by the equipment in the field.

3.1.1 Receiver Acquisition

The acquisition sequence for the received signal from the satellites is described in detail in Volume I of Reference 1. Briefly, the sequence can be divided into three sequential parts. First, the carrier phase is acquired by a phase lock loop in the receiver which searches for the carrier by sweeping continuously over a frequency range about the nominal carrier frequency. At the start of each satellite transmission, an unmodulated carrier is transmitted for a time equal to or slightly greater than one sweep period of the receiver so that the loop must acquire the carrier in one sweep period if it is not to miss that satellite transmission. After carrier acquisition, the phase lock loop automatically disables the sweep and switches from a wideband loop search mode to a narrowband loop tracking mode.

The next step is the acquisition of the BINOR code clock frequency by the clock loop in the range code acquisition unit. The BINOR code appears as modulation on the carrier after one sweep period of the carrier loop. After clock acquisition, the last step in the sequence is the acquisition of the code phase by sequential correlations of the code subfrequency components with the received BINOR code sequence. Twelve of these correlations in sequence are required for a 13-component BINOR code. After the twelfth correlation, the code phase is acquired and a range measurement can be made.

To summarize, the total acquisition time for a range measurement can be written as

$$\tau = T + \tau_{c1} + \tau_{c2} + 12\tau_s$$

where $T = \Delta f/\dot{f}$ = sweep period of receiver phase lock loop

Δf = total receiver sweep range

$\dot{f}$ = sweep rate of carrier loop

τ_{c1} = transient time in carrier loop for locking to carrier once sweep places carrier frequency within the loop bandwidth

τ_{c2} = pull-in time for clock loop

τ_s = correlation times of each subfrequency component

The sweep range is preset in the receiver to correspond to the expected frequency uncertainty in the arriving signal. The sweep rate which determines the sweep period is given by

$$\dot{f} = KB_L^2$$

where K = a constant whose value determines probability of acquisition on one sweep

B_L = loop noise bandwidth (one-sided)

The carrier loop transient time is proportional to $1/B_L$. The clock loop pull-in time is also proportional to $1/B_L$ for that loop (Volume III, Appendix B of Reference 1 shows values for τ_{c2} calculated from phase plane trajectories). The correlation times τ_s are preset and are a multiple of the code period; the value of the multiple depends on the signal-to-noise ratio and the desired probability of correct code phase acquisition.

The testing will be set up to measure the acquisition time of each of the three parts of the acquisition sequence separately as a function of certain key parameters. The test setup shown in Figure 1 measures the acquisition times of the carrier and clock loops. The lock indication signals C_o and G_o are taken from the quadrature detectors of both loops. The acquisition sequence is initiated by a start button on the control logic box. At T seconds from the start, the control logic switches the modulation on with a carrier modulation index of 1.2 radians peak. The value of T should always be set equal to or slightly greater than the carrier loop sweep period in the receiver. After a preset time determined by the estimated time for code acquisition, the control logic box switches the signal

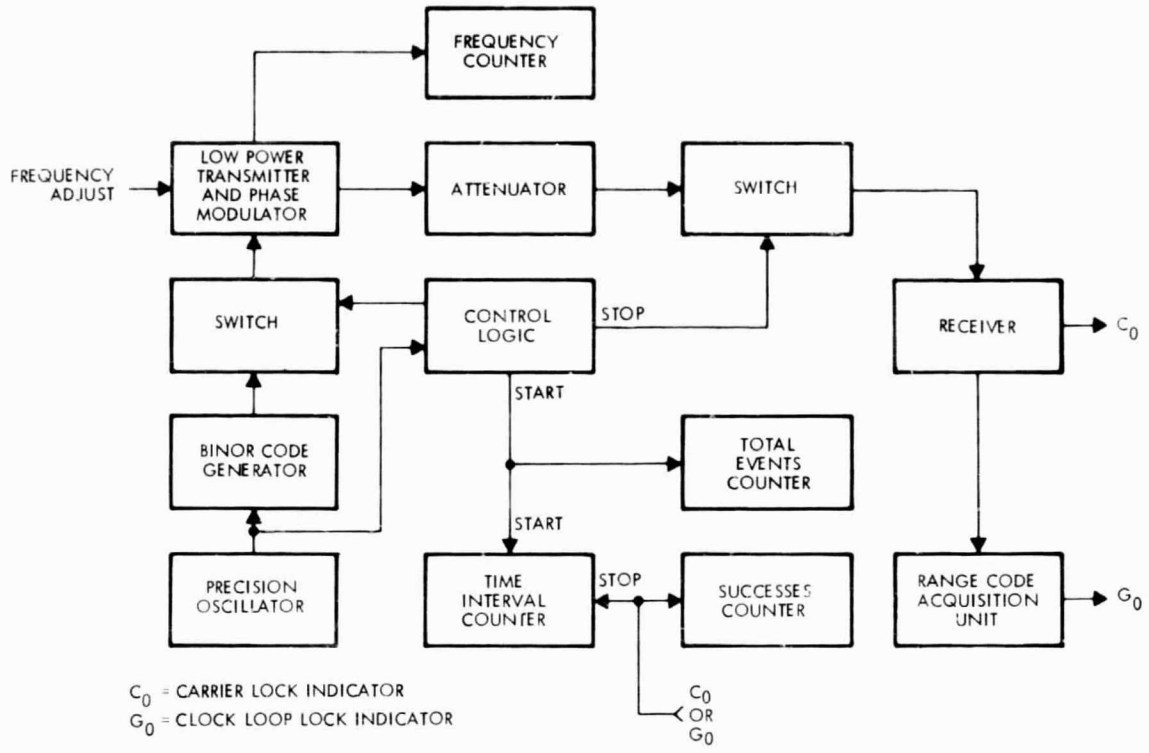

Figure 1. Test Setup for Acquisition Times

off to the receiver and then repeats the sequence 0.1 second later in order to simulate the time division multiplexed signals from the satellites. The time interval counter measures the elapsed time between the start of the sequence and the occurrence of the loop lock indicator signals C_o and G_o. These two times can be measured either in separate trials or simultaneously by using two time interval counters. C_o measures

$$\frac{\Delta f}{\dot{f}} + \tau_{c1}$$

and G_o measures

$$\frac{\Delta f}{\dot{f}} + \tau_{c1} + \tau_{c2}$$

The "total events" and "successes" counters indicate the probability of occurrence of C_o and G_o in one transmitted sequence.

The measurements of C_o and G_o should be repeated enough times to obtain statistically meaningfu. counts of the "total events" and "successes." The measurements should be repeated for different values of

IF signal-to-noise ratio and frequency offset between the transmitter and receiver (Δf) at a fixed carrier loop sweep period and fixed carrier and clock loop noise bandwidths. The effects of changing the two loop noise bandwidths and the sweep period should also be determined. Changes in the loop bandwidths from the nominal values shown below may require readjustment of the carrier modulation index from 1.2 radians to redistribute the power between the two loops.

The final portion of the total acquisition time is fixed by the length of the subfrequency correlations. The nominal correlation time selected in the system design of Reference 1 is two code periods, i.e.,

$$\tau_s = 2\left(\frac{1}{78.125}\right) = 0.026 \text{ second}$$

However, a plot of the correlation time (in multiples of the code length) versus the probability of correct code phase acquisition should be made for different values of IF signal-to-noise ratio. Correct code phase acquisition can be determined by comparing the phases of the lowest frequency components in the code (78.125 Hz) from the BINOR code generator and the range acquisition unit, respectively, on a dual trace oscilloscope or a phase meter. Except for time delays in the test setup, the phase comparison should equal zero. This test can also be considered as part of the test to determine range measurement errors due to thermal noise since an error in code phase acquisition causes an error in the range measurement.

The resulting data from these measurements determines the variation of acquisition time and the probability of acquisition with each parameter. The best set of system design parameters can then be selected.

The nominal values for the test parameters are (based on design calculations in Reference 1):

$2B_L$ (carrier loop)	= 1650 Hz (during sweep) 50 Hz (after acquisition)
$2B_L$ (clock loop)	= 26 Hz
Δf (frequency offset)	= ±26 kHz (52 kHz total)

Carrier loop sweep period	= 0.38 sec
Receiver IF SNR	= -29 db (5 MHz noise bandwidth)
Carrier loop SNR	= 6 db (during sweep) 10 db (after acquisition)
Clock loop SNR	= 21 db

For the proposed tests the IF SNR should be changed in 2-db increments from -6 to +10 db about the nominal IF SNR. The carrier frequency offset should be adjusted in approximately 5-kHz steps from -26 to +26 kHz.

3.1.2 Receiver Error Source

The magnitude of the range measurement errors in the user receiver is determined by the tests proposed here. The following sources of error are measured (see Appendix A): receiver thermal noise, receiver bias, and quantization.

The same oscillator is used for both the BINOR code generation and the range measurement reference in the receiver in order to eliminate the error source from a separate user oscillator. For each range measurement, a separate user oscillator is a major error source. However, as shown in Appendix A, for range differences the user oscillator error is negligible and therefore need not be considered in these tests.

The three error source measurements are combined in one test but are isolated with the aid of two other tests. The measurements are repeated for different IF signal-to-noise ratios and frequency offsets between the transmitter and receiver. The thermal noise error depends only on the signal-to-noise ratio while the bias error depends on both the signal-to-noise ratio and frequency offset. The quantization error, of course, is independent of both and depends only on the frequency of the clock used to obtain the range count (actually a time interval count). As such, the quantization error is easy to calculate and represents the limit on measurement accuracy.

Only the thermal noise error due to carrier and clock loop phase jitter is measured here. The thermal noise error due to false acquisition of the BINOR code phase is discussed in conjunction with the acquisition

tests. Since this error is easy to recognize because of its magnitude, it can easily be isolated from the other error sources.

The error measurement tests are divided into three parts:

1) Measurement of time delay in the test setup, which includes quantization error.

2) Measurement of clock loop phase jitter at different values of IF signal-to-noise ratio and fixed carrier and clock loop noise bandwidths determined by the results of the acquisition tests.

3) Measurement of total rms error in the receiver and range acquisition unit (which includes the thermal noise, bias, and quantization errors) at different values of IF signal-to-noise ratio (the same values used in Part 2) and different frequency errors between the transmitted carrier and the receiver (Δf).

The first test determines the reference from which the errors in Part 3 are determined. The test setup is shown in Figure 2. The range measurement should be made with very high signal-to-noise ratio (the strong signal end of the receiver dynamic range) and with the frequency error Δf set to zero. Enough data should be taken to determine statistically significant mean and rms values for the range measurement.

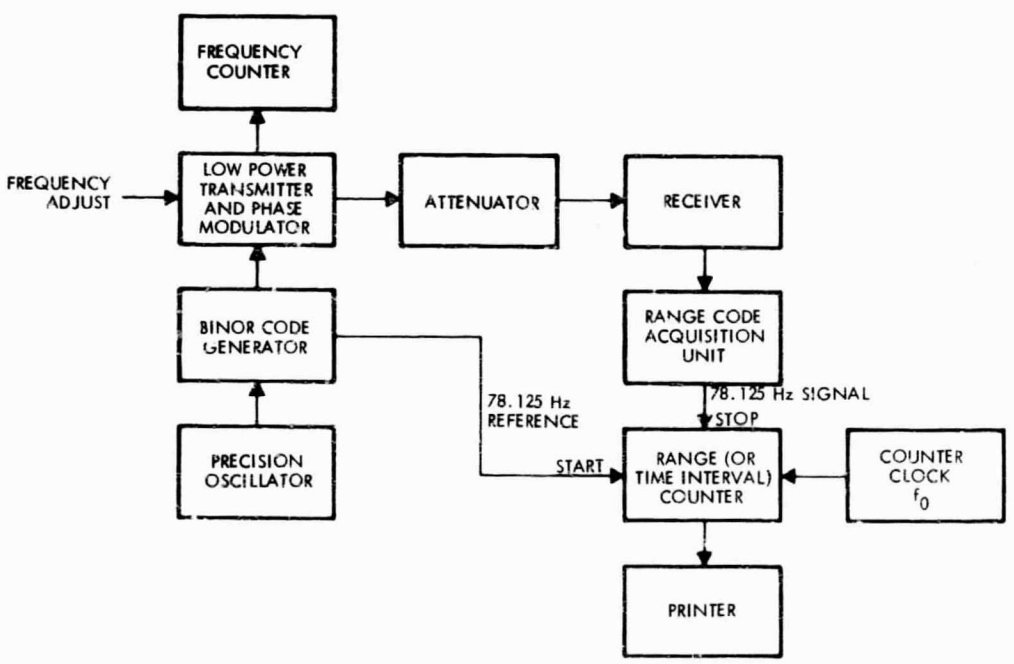

Figure 2. Test Setup for Measuring Receiver Errors

The mean value should represent the time delay in the test setup while the rms value should represent the quantization error in the range count measurements. The rms quantization error is easily computed from the equation in Appendix A.

$$\sigma_R = \frac{c}{\sqrt{12}\, f_o}$$

and can be compared with the measured rms error to determine if other unaccounted errors are present.

The test setup for Part 2, the measurement of phase jitter, is shown in Figure 3. The following procedure is used. With the switch in the

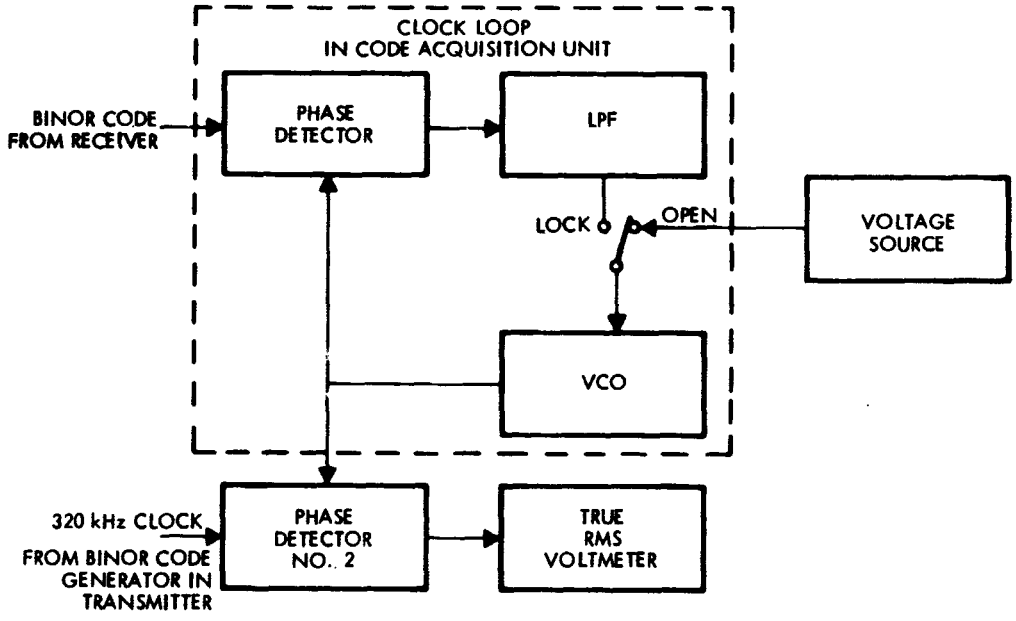

Figure 3. Test Setup to Measure Clock Loop Phase Jitter

"open loop" position, the maximum positive and negative peak error voltage excursions out of the second phase detector are measured by adjusting the voltage source to provide $\pm(\pi/2)$ phase errors between the VCO and the 320-kHz clock frequency. Phase errors which lie between the peak positive and negative phase errors can be defined by a linear function (phase detector No. 2 is assumed to have a linear transfer function with the square-wave inputs).

$$\theta_{rms} = e_{rms} \left(\frac{\pi}{e_{pp}}\right)$$

where e_{rms} = the rms voltage measured

e_{pp} = peak-to-peak voltage measured

The switch is now placed in the "lock" position and the phase jitter voltage e_{rms} is measured (to determine θ_{rms}) at different values of IF signal-to-noise ratio. The IF signal-to-noise ratio should be changed in 2-db increments between -6 and +10 db about the nominal value of -29 db. The carrier and clock loop noise bandwidths at the nominal IF SNR should be the same as used in the acquisition tests.

The test setup for the third part is the same as for the first part (Figure 2). However, now range measurements are made at different values of IF signal-to-noise ratio (the same values used to measure the clock loop phase jitter). At each IF signal-to-noise ratio, the measurements are repeated for different frequency errors in 5-kHz steps between -26 and +26 kHz.

Having determined the test setup time delay and the quantization error in Part 1 and the thermal noise error in Part 2, these errors are removed from the measurements in Part 3. The remaining error in Part 3 is equal to the receiver bias error as a function of the signal output, i.e., the IF signal-to-noise ratio and the frequency error or doppler shift of the carrier. Enough data should be recorded to determine mean and rms values for the bias error.

3.1.3 Satellite Precision Oscillator Prediction Error

The error in predicting the satellite oscillator drift ahead to $+\tau$ based on a quadratic polynomial fit to oscillator time observations at $-\tau$, -2τ, and 0 is discussed in Appendix A. The laboratory test setup shown in Figure 4 is used to measure the rms residual error from such a prediction. The BINOR code generator and range acquisition unit are used as a convenient means of obtaining the cumulative time error between two identical oscillators to an adequate resolution. Since two identical oscillators are used, the measured error will be $\sqrt{2}$ larger than if one of

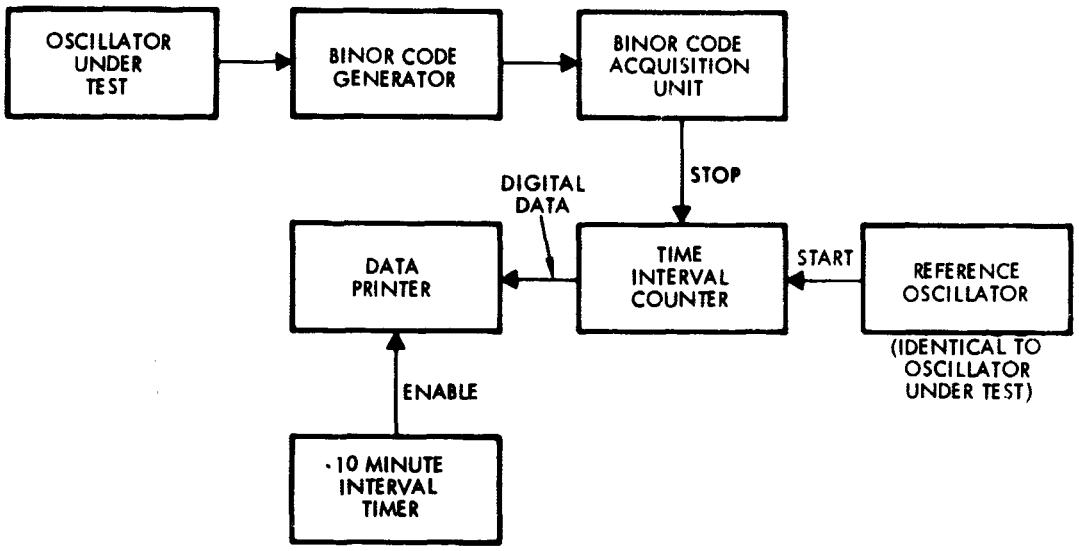

Figure 4. Test Setup for Measurement of Satellite Oscillator Prediction Error

the oscillators was measured against a more precise oscillator such as a cesium beam or hydrogen maser standard.

The digital data from the time interval counter will be recorded by a printer at 10-minute intervals over about a five-day period. The time interval counter should have a resolution of at least 0.05 microsecond (20 MHz clock in the counter). The recorded data will be subjected to the following analyses:

- Find the third variate difference of the data at intervals from 10 minutes to 12 hours per the procedures discussed in Reference 2.
- Fit quadratic polynomials to all available data over spans of from 2 to 24 hours. Study variation of the second order term (C_2) in the quadratic fit with time. Using the quadratic fit coefficients to extrapolate for periods of from 1 to 24 hours ahead of the data, evaluate the actual rms prediction error and compare with theory (Reference 2) as a function of the fitting and extrapolation span.

3.1.4 Antenna Pattern Measurements

User antenna pattern coverage and multipath rejection capabilities are measured in the tests proposed here. The antenna performance should be evaluated to include radiation interactions with the user structure which is assumed to be an aircraft. Since radiation measurements

cannot be performed in the laboratory using a full-scale aircraft, the measurements must be conducted on a frequency scaling basis using models. To do this successfully, the aircraft antennas and aircraft models must be carefully fabricated to maintain the same electrical behaviors as those of the physical system. The scale antenna model must have the same radiation patterns as the full-size antenna. Similarly, the dimensions of the aircraft model must be scaled. A maximum scaling factor of about seven is recommended. This scaling factor is considered to be an upper limit at which the scale model antennas can be readily fabricated. The operating frequency of the antennas then increases from L band (1.6 gHz) to X band (11 gHz).

The antenna range to conduct the measurement patterns must be long enough to insure far field conditions. Far field conditions occur at a distance given by the following relationship:

$$F = \frac{2D^2}{\lambda}$$

where D = length of radiating aperture

λ = operating wavelength

For example, a 10-foot long 5:1 scale model aircraft (50-foot long full size) would be expected to require an antenna range of 1600 feet. Actually, a 100-foot range is adequate since the resulting 2.5-foot aperture is equivalent to 20 wavelengths at 8 gHz, The current magnitude around the aircraft skin at 6 wavelengths distance from the antenna location is sufficiently low so that it should not affect the resultant aircraft pattern.

The three element slot dipole, curved arm turnstile, and conical spiral antennas described in Volume III of Reference 1 are recommended for testing. The antenna measurement tests should include the following:

1) Principal plane patterns of the full-scale L-band antennas and the corresponding scale model antennas measured on a ground plane. These measurements are required in order to match the radiation characteristics of the scale models to the full-size antennas.

2) Principal plane patterns of the scale model antennas mounted in several locations on the aircraft. These measurements show the change in the radiation patterns in going from a ground plane to the aircraft model.

3) Contour plots of each scale model antenna mounted on the aircraft which show both the upper and lower hemisphere radiation patterns. Contour plots should be made for vertical, horizontal, right hand and left hand circular incident polarizations. Several locations on the aircraft should be tested in an attempt to find an optimum location.

The contour plots, in addition to giving detailed antenna patterns over the entire sphere, can be used to compute multipath rejection ratios as described in Appendix D. The multipath rejection ratio for an antenna is defined here to mean the ratio of the direct signal strength to the ground reflected signal strength received by the antenna from a signal arriving from a satellite.

3.2 FIELD TESTS

The field test program will be conducted to evaluate the performance of the NAVSTAR system under typical operational environments. Two user type aircraft, such as a four engine jet transport and a helicopter, will be appropriately equipped to receive L-Band BINOR code signals in flight. BINOR transmitter equipment will be installed at accurately surveyed locations on the ground for testing the navigational accuracy of the NAVSTAR system in the aircraft environment. Additional tests will be made with BINOR transmitter equipment located in a high altitude aircraft or balloon to measure L-Band BINOR signal and noise characteristics under conditions more closely approximating the operational NAVSTAR satellite geometry. These field tests will be an integrated outgrowth of the laboratory test program.

The specific test configurations to be used and the objectives of each configuration are summarized as follows:

Configuration 1

a. Transmitters - None required.

b. Receivers - A calibrated noise source and radiometer type receiver located in a jet transport for measurement of the L-Band noise environment. Also several user candidate quartz crystal oscillators and a cesium beam frequency standard are to be flown on the aircraft.

c. Flight Paths - Multiple flights at various operational altitudes over typical terrains under benign and extreme weather conditions.

d. Objectives -

1) To investigate the contribution of aircraft generated RFI, ground RFI, atmospheric RFI and precipitation static to the user antenna noise temperature.

2) To investigate the relative stability and performance of various quartz oscillators in the aircraft environment. Results of this investigation will provide data for ultimate selection of a NAVSTAR user oscillator.

Configuration 2

a. Transmitters - None required.

b. Receivers - Same as Configuration 1 using helicopter instead of jet transport aircraft.

c. Flight Paths - Same as Configuration 1 except that flight paths will be typical for helicopter rather than jet transport.

d. Objectives - Same as Configuration 1 in helicopter environment except that it may not be necessary to repeat the oscillator tests.

Configuration 3

a. Transmitters - BINOR code transmitter equipment located in a single high altitude aircraft (40,000 feet or higher if possible).

b. Receiver - BINOR code receiver equipment located in a jet transport user type aircraft. A three receiving antenna configuration is required for the multipath signal measurements.

c. Flight Paths - Multiple flights over various terrains and with different geometries of the receiver aircraft with respect to the transmitter aircraft. In the case of all flights the transmitter aircraft altitude will be at least five times that of the receiver aircraft to simulate the satellite configuration.

d. Objectives -

1) To investigate the performance of the antenna reception, TDM phase lock receiver, and BINOR code range acquisition unit in a jet transport aircraft environment.

2) To investigate ground multipath signal reception as a function of aircraft altitude, elevation angle to the transmitter or signal source, and the type of terrain or sea state.

Configuration 3a

Same as Configuration 3 except that a balloon is used for the transmitter equipment test bed instead of a high flying aircraft. Either Configuration 3 or 3a will be used but not both.

Configuration 4

a. Transmitters - Same as Configuration 3.

b. Receiver - Same as Configuration 3 using a helicopter for BINOR receiver equipment instead of a jet transport type aircraft. Receiving antennas will be located above and below the rotor blades.

c. Flight Paths - Same as Configuration 3 except that flight paths will be typical for helicopter rather than jet transport.

d. Objectives - Same as Configuration 3. Particular attention will be given to the effect of receiver antenna location with respect to the rotor blades on system performance.

Configuration 4a

Same as Configuration 4 except that a balloon is used for the transmitter equipment test bed instead of a high flying aircraft. Either Configuration 4 or 4a will be used but not both.

Configuration 5

a. Transmitters - Three sets of BINOR transmitter equipment located at accurately surveyed positions on the ground each separated from the others by approximately 50 or 100 miles.

b. Receiver - BINOR code receiver equipment located in a jet transport user type aircraft. A computer and appropriate instrumentation will be required in order to make navigation measurements in real time.

c. Flight Paths - Multiple flights over the transmitter complex at various altitudes, velocities and approach angles during inclement and fair weather extremes.

d. Objectives -

1) To evaluate NAVSTAR system accuracy under more realistic operational circumstances than can be simulated in the laboratory.

2) To identify and further investigate NAVSTAR error sources.

3) To investigate the NAVSTAR capability and software requirements for real time navigation computations.

Configuration 6

a. Transmitters - Same as Configuration 5.

b. Receiver - Same as Configuration 5 using a helicopter instead of a jet transport for the receiver test bed.

c. Flight Paths - Same as Configuration 5 except that flight paths will be typical for a helicopter rather than a jet transport.

d. Objectives - Same as Configuration 5.

Configuration 7

a. Transmitters - Three sets of BINOR transmitter equipment located at accurately surveyed positions on the ground each separated from the others by several hundred feet to several miles. Different geometries for the transmitters including the possibility of locating one or two at altitudes of several hundred feet will be used.

b. Receiver - Same as Configuration 6 (i.e., BINOR receiver equipment located in a helicopter).

c. Flight Paths - Multiple flights to simulate VSTOL final approach and landing configurations under inclement and fair weather conditions.

d. Objectives -

1) To investigate the capability of NAVSTAR for navigation of VSTOL type aircraft during final approach and landing.

2) To evaluate different geometries of transmitter equipment for ILS.

The above configurations can all be implemented with one properly instrumented jet transport and one helicopter. In addition a high flying aircraft or balloon will be required for the high altitude transmitter tests

and an instrumented range for the ground transmitter tests. The field tests are described further in the following sections and include some additional test configurations which were investigated but are not recommended.

3.2.1 User Aircraft Requirements

The jet transport type user aircraft should be one with sufficient payload capacity to carry the necessary instrumentation and test personnel. An aircraft of the Lockheed Jetstar class, grossing about 40,000 pounds including 3000 pounds of useful payload, is adequate for test purposes. An H-19 Sikorsky helicopter will provide adequately for the helicopter user tests.

Figure 5 is a block diagram of the equipment and other test instrumentation required aboard the user aircraft. The three antennas shown in Figure 5 are in the 0 db turnstiles described in Volume III of Reference 1. They will be mounted on the top and sides of the aircraft in a manner identical to that proposed in Reference 3. The top antenna will normally (but not always) be connected to the phase lock receiver used for the BINOR code range measurements while the side-mounted antennas are used to measure the presence and magnitude of multipath. The antenna switching unit permits the switching of any receiver to any antenna.

In the case of the helicopter tests, two receiving antennas will be mounted, one above the rotor blades and a second below the rotor blade on the top side of the aircraft. These antennas will provide for evaluation of the effects of rotor noise on receiver performance.

The receiving equipment for the range measurements consists of an RF preamplifier (noise figure of 5.7 db), a TDM phase lock receiver, and a BINOR code range acquisition unit for measuring range. The multipath receivers provide coherent amplitude detection and AGC outputs for monitoring signal strength variation. These units will normally be connected to the horizontal and vertical polarization elements of the side-mounted turnstiles. The radiometer receiver employs a calibrated noise source as a reference for measuring the temperature of the receiving antennas. An off-line quartz oscillator test is also provided using a cesium beam

frequency standard and precision frequency comparator to evaluate the stability of various candidate user crystal oscillators.

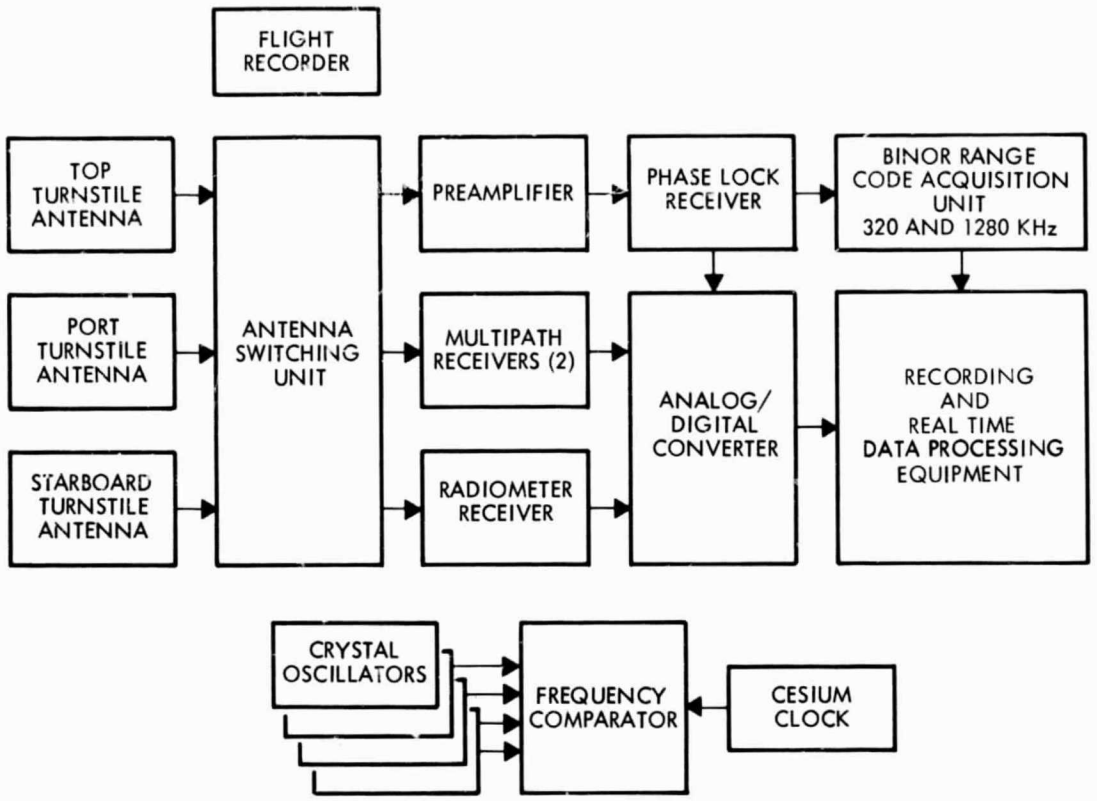

Figure 5. Block Diagram of Equipment in User Aircraft

The flight recorder shown in Figure 5 should be capable of recording speed, heading, attitude and altitude as a function of time. This data is necessary so that the relative geometry between the user aircraft and signal source can be reconstructed for analysis of multipath effects and phase/amplitude variations in received signal as a function of antenna pattern "holes" and irregularities.

3.2.2 Transmitter Test Bed Requirements

The test bed for the signal source in Configurations 3 and 4 can either be a free balloon at 60,000 feet or an aircraft capable of maintaining an altitude of 40,000 feet or better. The Lear Jet appears to be a good choice for an aircraft signal source since it can easily accommodate one to two racks of equipment and one test operator and can sustain flight at 40,000 feet.

The choice between a balloon and an aircraft as a signal source for the environmental field tests requires further study. A free balloon has the advantage of attaining greater heights for the multipath tests while an aircraft has the advantage of being able to change test parameters such as radiated signal power during tests. (The balloon could provide this capability with a command link.) The free balloon would be preferable for the multipath tests if the relative velocity between the user aircraft and a slowly drifting balloon can be controlled as tightly as the realitive velocity between two aircraft (see Appendix E). However, the flexibility of the aircraft in adjusting test parameters at the transmitter is a highly desirable feature. The addition of a command link to the balloon can solve this problem but at the expense of added complexity to the balloon equipment. The problems associated with the use of a balloon are discussed in more detail in the next subsection (Paragraph 3.2.3).

Figure 6 is a block diagram of the equipment and other test instrumentation required aboard the test bed for the field tests. The flight recorder is necessary for the same functions as described for the user aircraft.

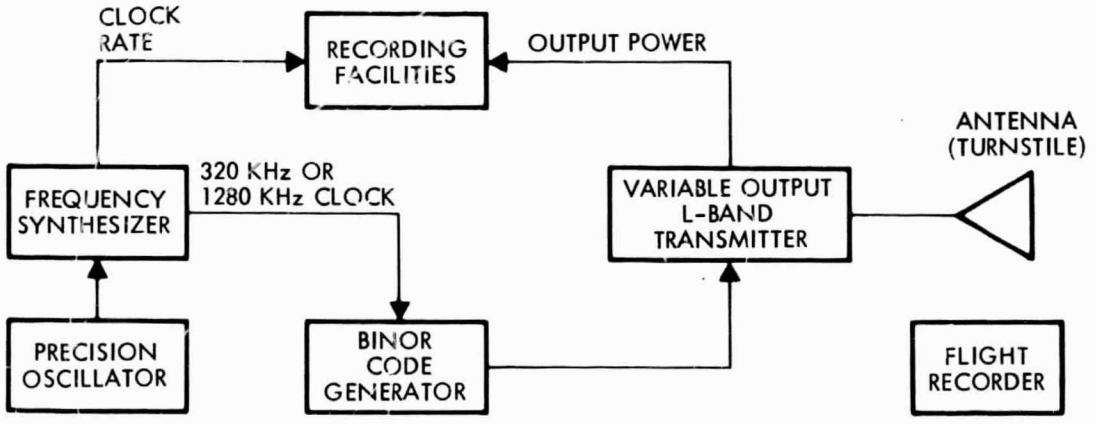

Figure 6. Block Diagram of Signal Source Equipment

The frequency synthesizer will output 320 and 1280 kHz tones for the BINOR code generator. The code generator will provide code lengths of 2^{13} or 2^{15} bits. The L-Band transmitter is a solid state unit, with a variable output of up to four watts maximum. It will transmit the code in the time division multiplexed format of the NAVSTAR satellites.

A constant gain final output stage will be employed using PIN diodes to control the input signal. The antenna will be a circularly polarized 0 db gain turnstile.

The 4-watt transmitter output will be more than adequate for these tests, as shown by the power budget in Table 2. The maximum radio line of sight distance between a balloon at 60,000 feet and an aircraft at 40,000 feet is 550 nautical miles. In actual tests, the distances involved will be considerably less in order to obtain elevation angles between the signal source and aircraft of at least 10 degrees. Distances of 5 to 50 nautical miles will be more typical.

Table 2. Signal Source to User Aircraft Power Budget

Parameter	Value
Maximum transmitter power (4 watts)	+36.0 dbm
Signal source antenna gain	0 db
Space loss (1600 MHz, 550 nmi)	155.9 db
User antenna gain	0 db
Polarization loss	0.3 db
Circuit losses	2.0 db
Total transmission loss	-158.2 db
Received signal strength	-122.2 dbm
Required signal strength for BINOR code	-131.8 dbm (Vol I, Ref 1)

3.2.3 Balloons Versus Aircraft

The use of balloons instead of aircraft has been investigated for airborne signal sources. Balloons offer certain advantages in that their positional stability can be made better than aircraft and consequently are easier and more accurate to track. Moreover, they can reach higher altitudes, which is advantageous to the multipath test (see Appendix E). Potential disadvantages are the possible limitations on location because of hazards to aviation and the public, dependence of launch time on weather (wind) conditions, the possible loss of the equipment, and the difficulty of adjusting parameters such as signal power during test runs. Two types of balloons exist, tethered and free flight. Data on balloon technology was

obtained in discussions with Sea-Space Systems, Inc., of Torrance, California, a manufacturer of advanced balloon technology systems used in military and civil test programs.

3.2.3.1 Tethered Balloons

Tethered balloons cannot be deployed above 5000 feet without a major engineering effort. If altitudes up to 20,000 feet are desired, engineering design and development efforts of $250,000 to $500,000 would be involved. At the 5000-foot level, fairly significant launching costs in equipment and crew are required. Estimated cost to support a single balloon station during a test period is $15,000 per month.

Tethered balloons display unusual dynamics and accurate tracking would be required in spite of their tethering. The balloons can be launched only under certain restricted wind states.

Maximum altitudes of 5000 feet will not add significantly to test goals; at these altitudes multipath cannot be tested effectively. Consequently, there is no reason why transmitters located at 5000 feet will be any better than transmitters fixed to the ground except for measuring the upper hemisphere antenna pattern on the receiving aircraft. Conclusions on tethered balloons are:

1) A test designed around tethered balloons moored at 5000 feet or less can be formulated.

2) Such a test is not recommended because:

   a) Altitude of 5000 feet does not add anything significant to test goals.

   b) Cost of supporting the balloon runs to $15,000 per month per balloon.

   c) There are significant deployment and tracking problems with tethered balloons.

3.2.3.2 Free Floating Balloons

Free balloons can achieve altitudes in excess of those practical for jet aircraft. Although altitudes of over 100,000 feet are obtainable, experience shows that maximum positional stability is obtained at near 60,000 feet. At this altitude, winds tend to be lowest. This altitude is 50 percent higher than the 40,000 feet obtainable with normal jet aircraft.

Specialized aircraft such as the U-2 or stretched span RB-57 can reach such altitudes (60,000 feet) but would probably be difficult to obtain for this test program. At 60,000 feet positional stability of $\pm$ 50 miles (with respect to a ground site) per day is achievable. That is, the balloon could be released 50 miles upwind of a test site and drift only 100 miles in a day. This kind of positional stability makes the free balloon a good candidate for both the multipath test (which requires high altitudes) and position location tests.

There are limitations to the areas in which such tests can be performed; specifically, California desert areas are recommended. Edwards AFB is equipped with tracking instrumentation capable of supporting the position location portion of the test.

The use of balloons in such tests requires experienced field test crews and very careful attention to meteorological factors. Extensive upper atmosphere wind surveys are needed prior to the actual balloon launching to obtain the low drift levels. Balloons cannot, obviously, be put on station as quickly as aircraft; free balloons intended to reach 60,000 feet would be launched about six hours prior to the test initiation.

If the equipment carried on the balloon is expensive, there is naturally concern about the possibility of losing it, a problem not faced with a tethered balloon. However, recoverability of instrument packages from high-altitude free balloons can be accomplished with good reliability.

The cost of material expended in the free balloon flight is about $700 per flight and a manpower level of 10 man days per flight is required to support the system. This level of cost and manpower support is somewhat less than the operating cost of a large jet aircraft for a several hour flight.

Conclusions on free balloons are:

1) Free balloons are a feasible means of reaching 60,000 feet with a transmitter.

2) Costs will be less than with a jet aircraft capable of reaching 40,000 feet for a short program.

3) The balloon operating region can be within $\pm$50 miles of a test site for a day, given careful meteorological planning and observation.

4) Free balloons can be tracked by theodolite or radar.

3.2.4 Instrumented Range Requirements

All field tests will require reliable voice communications between the pilot and test crew of the user aircraft, the pilot and test crewmen of the signal source aircraft and a ground control station. It is desirable that one or more ground radars capable of measuring coarse time space-position history of the two aircraft or aircraft and balloon be available, since this capability could be a valuable adjunct to the flight recorders in reconstructing the relative geometry of the two aircraft for analysis of multipath effects. A single three-dimensional surveillance type radar or two instrumentation tracking radars would suffice for this purpose.

In addition the ground transmitter tests of Configurations 5 and 6 will require a range of approximately 50 to 100 miles square. Communication links between the three transmitter locations and the ground control station would be desirable. A standard for measuring ground transmitter frequency and phase before, during and after the aircraft fly-by tests will be required. This standard can be a portable cesium beam atomic standard such as manufactured by Hewlett-Packard which is carried between the three ground sites by helicopter.

3.2.5 Potential Field Test Sites

The following is a summary of the desirable facilities and attributes of the field test site:

a. Ground control station availability.

b. A GCI radar or two tracking radars.

c. A variety of weather conditions.

d. Proximity to many different types of terrain, including high density urban areas, forested, arid and mountainous areas, and oceans.

e. Suitable facilities for logistically supporting aircraft and possibly free balloons.

Based on these criteria, the following locations have been considered:

- The Air Force Eastern Test Range (ETR) in Florida.

- The "West Coast Complex" consisting of the Air Force Western Test Range (WTR), the Pacific Missile Range (PMR), and the Air Force Flight Test Facility (FTC) at Edwards AFB, Calif.
- The Eglin AFB complex in Florida.
- The Wallops Island and Langley Field complex in Virginia.

Table 3 compares these sites. The table indicates that the Wallops-Langley complex is the most attractive. The "West Coast complex" is very attractive except for its relatively good weather which does not often result in the high sea states desired for multipath tests. Additionally, lack of electrical storms is a drawback for RFI measurements.* While ETR and Eglin AFB are considered adequate sites, Wallops-Langley is considered superior because of its proximity to more types of terrain. Additionally, it is a NASA facility, which should result in less test coordination activity than if a DOD facility were used.

Table 3. Comparison of Potential Field Test Sites

	ETR	WTR/PMR/FTC Complex	Wallops Island Langley Field	Eglin AFB
Control Facilities	Adequate. Variety of facilities available.	Adequate. Variety of facilities available.	Adequate. Variety of facilities available.	Adequate. Variety of facilities available.
Tracking Facilities	Adequate. Multiple tracking and surveillance radars available.	Adequate. Multiple tracking and surveillance radars available.	Adequate. Multiple tracking and surveillance radars vavilable.	Adequate. Multiple tracking and surveillance radars available.
Aircraft Logistic Facilities	Patrick AFB has adequate facilities.	All bases have adequate facilities.	Adequate.	Adequate.
Proximity to Varied Terrain Types	No nearby mountainous or arid terrain. Proximity to forest terrain. Nearest large urban area is Miami.	Excellent – forests, mountains, deserts, ocean, and ultra high density urban area (Los Angeles) is nearby.	Good proximity to forests, mountains, oceans, and two urban areas (Washington DC and Baltimore).	Same as for ETR, except that nearest urban area is New Orleans.
Variability of Weather	Good. High Incidence of electrical storms.	Poor. Very low incidence of electrical storms. High sea states seldom occur.	Good.	Good.
Remarks	Adequate, but not as attractive as Wallops Island/ Langley Field.	Lack of poor weather is only drawback. Balloon support is good.	Probably best all-around test site. Lack of nearby arid area is not a serious drawback.	Adequate, but not as attractive as Wallops Island/ Langley Field.

*However, these measurements do not require test site support and can be done elsewhere.

3.2.6 RFI Noise Measurement Tests

RFI noise measurement tests will be conducted in the jet transport environment of Configuration 1 and the helicopter environment of Configuration 2. A calibrated noise source and radiometer will be used to measure the noise temperature of the antennas aboard the user aircraft under a variety of environmental conditions. By switching the receiver from one of the antennas to the known noise source, a difference at the receiver output can be obtained from which the antenna noise temperature can be derived. The expected values of noise temperature due to RFI vary from 50°K (when pointing at a quiet part of the sky) to as high as 3000°K (above urban areas). The prediction of small effects at L-Band due to precipitation static is based on extrapolation from data at other frequencies, and if this extrapolation is incorrect or if aircraft or external RFI contribute greater noise than expected, the actual experienced noise temperature could be well above 3000°K. For this reason, it is desirable to provide a capability for measuring noise temperatures to 10,000°K and beyond. The ATS-F experiment (Reference 3) proposed to provide several calibrated noise sources so that direct measurement could be made of noise temperatures from 50 to 10,000°K. By providing a 6 db fixed attenuator which could be switched in series with the antenna, even higher noise temperatures can be measured.

To obtain a complete range of noise temperatures as a function of terrain and weather conditions, it is desirable to obtain noise measurements from extremely dense urban areas, broad ocean areas, and forested and desert terrain. Measurements over each of these terrain types should be made during both day and night in conditions of clear weather and storms with a high degree of electrical activity. If possible, flights should also be made during conditions of high sun spot activity.

3.2.7 Crystal Oscillator Tests

Crystal oscillator tests will be performed in the jet transport environment of Configuration 1 and if desired in the helicopter environment of Configuration 2 also.

The "absolute standard" against which candidate quartz oscillators will be compared will be a cesium beam frequency standard. By using

frequency and phase difference meters, the phase and frequency difference between each quartz oscillator and the cesium beam unit can be obtained. The quartz oscillators to be tested may include any units whose accuracy and cost are believed to be commensurate with NAVSTAR user needs. As in the case of the noise temperature experiment, this experiment does not require the use of a signal source and can be conducted off line from the other tests.

3.2.8 BINOR System Evaluation Tests

BINOR system functional checkout and evaluation tests will be conducted using Configurations 3 and 4 (or 3a and 4a). The primary objective of these tests will be to insure that user equipment performance in an aircraft environment conforms to the results of the laboratory tests. The signal source should be at an altitude of 20,000 to 40,000 feet. In order to measure the receiving antenna pattern, the user aircraft should be flown in a manner that allows a range of elevation and azimuth angles which encompass all portions of the top-mounted turnstile antenna pattern. For this test the signal source should transmit an unmodulated CW signal. For the BINOR code tests, the signal source should provide code transmissions once every 1.5 seconds (simulating satellite time division multiplexing), and the power level of the transmitted signal should be adjusted so that the received signal at the receiver is about -127 dbm, the anticipated signal level from an actual satellite. By varying the received signal level, it will be possible to verify the acquisition performance of the receiver as a function of scintillation rate and amplitude, and phase perturbations induced by antenna pattern anomalies. Also, it will be possible to investigate the thermal noise content of the received signal and the minimum usable signal level for successful BINOR code reception/processing in an aircraft environment.

Acquisition at both BINOR clock rates should be attempted from signal levels of about -120 dbm down to receiver threshold. It is important that throughout the test, the entire user antenna pattern is exercised to provide insight into phase and amplitude perturbation effects caused by pattern nulls. A signal source is preferred which allows adjustments of the transmitted signal to be made during tests. The adjustments can be coordinated by voice links between the aircraft and the ground during flights.

3.2.9 Ground Multipath Tests

Ground multipath tests will be conducted in the jet aircraft user environment of Configuration 3 (or 3a) and if desired the helicopter environment of Configuration 4 (or 4a) also. The geometry required for multipath tests is discussed in Appendix E. For a signal source at 60,000 feet, multipath at the user aircraft can be tested up to a maximum altitude of about 12,000 feet. The multipath receivers will record the received signal strengths using different polarizations of the side-mounted and top turnstile antennas. For these tests, the BINOR code modulation is removed and the signal source transmits a CW signal only, except when a check of the BINOR code acquisition performance is desired under multipath reception conditions. Data from the multipath receivers will be recorded on the aircraft and processed post-flight.

During the test it is important that the geometric constraints discussed in Appendix E be adhered to, and that a precise time record of relative geometry between signal source and receiver be available so that in post-flight, multipath effects can be correlated with the geometry that actually occurred. This is one reason for the desirability of tracking radar(s); another is that the radar(s) may assist the aircraft in maintaining their planned flight profiles. The tests should be conducted over all kinds of terrain, including oceans in different sea states.

3.2.10 BINOR System Accuracy Tests

BINOR system accuracy tests will be performed with the jet transport aircraft using Configuration 5 and with the helicopter using Configuration 6. For these tests only one turnstile antenna, plus the BINOR receiving equipment and flight instrumentation are required on the user aircraft. For real time demonstration of in-flight position location the instrumentation must include a digital computer and display unit. Three signal transmitting sources located 50 to 100 miles apart are required on the ground. The three ground transmitters which transmit the BINOR code in time sequence are received by the user aircraft. Figure 7 illustrates the configuration. Since the ranging signals now arrive from below the horizon, the receiving turnstile antenna should be located underneath the aircraft. Radar tracking of the aircraft is required to evaluate the accuracy of the BINOR code ranging in this configuration. The primary

utility of this test is demonstration of user software for in-flight computations of position location.

It should be noted that these accuracy tests will not fully evaluate NAVSTAR system accuracy because ionospheric errors are not present and because of the difficulty in obtaining accurate tracking data on the user aircraft from ground-based radars.

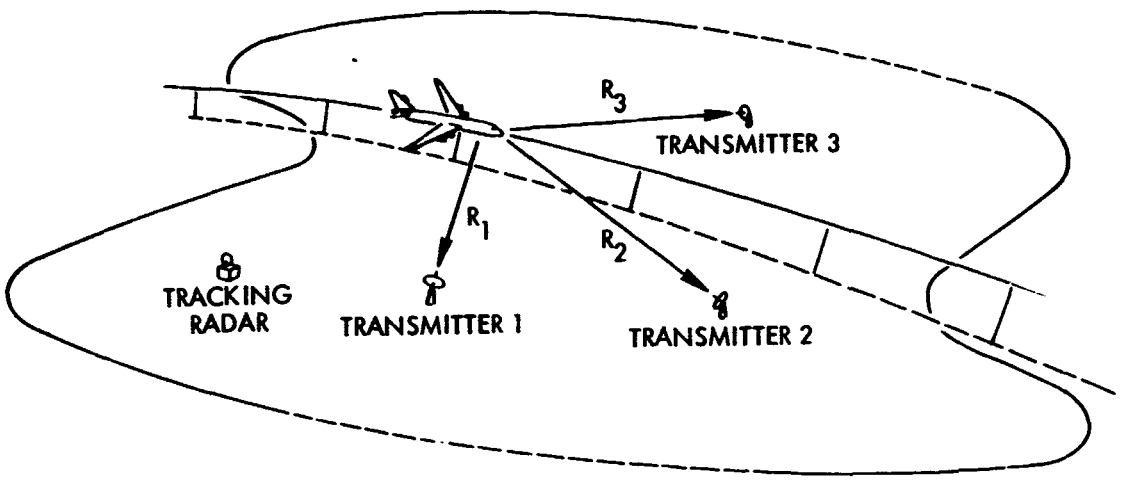

Figure 7. Position Location Using Ground Transmitters

3.2.11 VSTOL ILS Tests

VSTOL ILS tests will be conducted using the helicopter in the environment of Configuration 7. These tests will provide for demonstration of an instrument landing system (ILS) using the aircraft BINOR receiving equipment. The three ground transmitters can be located in the vicinity of an airport runway. In conjunction with a radar altimeter on the aircraft which can also utilize the down-looking turnstile antenna, a complete ILS landing system is possible. Therefore, it may be possible for the NAVSTAR user equipment to serve as an ILS as well as a navigation system increasing its utility and value. The test can evaluate whether sufficient accuracy is possible to achieve such a dual purpose role.

3.2.12 Other Test Configurations

Two other test configurations for BINOR system accuracy measurements were considered as follows:

a) The user aircraft and three transmitting balloons or aircraft stationed around the perimeter of a 30 to 50 nautical mile diameter circle. The user aircraft flies at lower altitudes inside the circle and again makes range or range difference measurements. Position will be determined by post-flight analysis.

b) The user aircraft and one transmitting aircraft. The user aircraft makes range measurements to the moving transmitter so that multiple signal sources are simulated by different locations of the transmitter at different times. Again position is determined by post-flight analysis.

The first of the above two configurations is complicated and presents severe requirements on the ground tracking facility for handling the user aircraft and three signal sources. Furthermore, in this configuration real time in-flight position computation is impractical because of the necessity of the user aircraft to know in real time the position of the three signal sources. This would only be possible if data communication links to the user aircraft were available. The second configuration results in poor accuracy because of the geometry involved with only a single transmitter and is therefore not recommended.

In order to demonstrate position location, range measurements from three directions must be made. The accuracy of the position fix depends on the geometry of the three or more ranges as well as on the accuracy of the range or range difference measurement itself. In order to get three noncolinear range measurements in this demonstration, it is necessary to use three transmitting sources or to move a single transmitter from place to place.

The first concept, using three sources, is more realistic and will provide a better demonstration of operational techniques, but is more expensive in equipment. It would involve placing three aircraft or free balloons on station at high altitude, each equipped with BINOR code transmitters time sequenced just as if satellites were being used. Sequential transmission to the user aircraft would enable the aircraft to determine its position using computation techniques similar to those that would be employed in the NAVSTAR system.

A major problem with this configuration is the requirement to track all three signal sources with sufficient accuracy to provide the transmitter positions with time required for the position location computations plus

the tracking of the user aircraft well enough to evaluate the position location accuracy. Such a tracking task would place a practically impossible load on any known tracking range. However, the use of aircraft with inertial systems on board could alleviate this problem. The use of balloons would simplify the problem because the large, slow moving free balloons could be tracked by theodolite.

Another possible solution to the tracking problem is to use ground-based BINOR code receivers to track the transmitters in a manner similar to the NAVSTAR ground tracking system; three would be required and would receive the signals transmitted from the three aircraft in the same fashion as the user aircraft. Since the signals are time sequenced, each ground receiver would be able to receive all three transmitters.

This technique would also demonstrate to a limited degree satellite ephemeris determination by ground tracking, as well as the basic user position determination aspect of the NAVSTAR system, although the orbit determination aspect of the job would not be demonstrated. However, a possible disadvantage is that using ground NAVSTAR receivers may not provide the same accuracy of transmitter position determination as in the satellite case, for the transmitter trajectories are not amenable to the orbital "smoothing," although better geometry can be provided. More importantly, the inclusion of the NAVSTAR equipment in both the user and the transmitter position measurements portion of the test without additional independent verification of the positions may leave the source of any observed errors very difficult to find.

The following conclusions can be made:

a) A configuration of three airborne transmitters or station around the perimeter of a 30- to 50-mile circle with a user aircraft flying at lower altitudes inside the circle can demonstrate techniques of position fixing.

b) Operating costs for the three transmitters and user aircraft would represent a substantial sum, and the availability of four aircraft for the test may be questionable.

c) Tracking support is the major problem. NAVSTAR receivers on the ground could fulfill this role, but could be considered a "safe" design feature only after they had been well tested in this mode.

d) On-board computation of user position is not practical with this test unless sophisticated computation-communication links are established. These links are felt to be outside the scope of the tests. This problem is not present in the "transmitters on the ground" configuration previously described.

An alternative configuration is to use only a single transmitting aircraft, but to let its motion make it "different" sources at different times, thus representing multiple sources. This design reduces the need for three transmitters to one.

The major difficulty with this scheme is that it appears that at reasonable transmitter aircraft velocities, the variation in transmitter location cannot be made large enough to adequately represent different sources in a time acceptable to any reasonable user position extrapolation. In the geometry shown in Figure 8, one measurement is made when the elevation angle is 30 degrees. At the speed and altitudes shown, 23 seconds would elapse until the angle was 60 degrees which would provide a "geometry" change required for position fixing, and 11.5 seconds more to reach, say, 90 degrees for the third measurement necessary (out-of-plane maneuvers would also be required). Thus, times on the order of 35 seconds would be required to make the measurements in this single-aircraft case, during which the user aircraft would travel about 3 miles. This would place a severe strain on the position extrapolation software required to obtain position "fixes." The altitude differential could be reduced, but to obtain reasonable geometry variations (corresponding to multiple satellites) in anything like the 3 to 6 seconds required for the NAVSTAR system, requires impractical aircraft separation and maneuvering requirements. For example, if the aircraft of Figure 8 were to be at the 30, 60, and 90 degree points not more than 2 seconds apart (simulating the operational case), an altitude separation of only 2300 feet would be required. Similar arguments apply to changes in azimuth angle when the aircraft are flying in opposite directions on parallel tracks.

It can be concluded that such a test could demonstrate multiple signal position computation, but that the accuracy would probably be poor because of the long intervals required for the single transmitter aircraft to modify the geometry. Based on this preliminary look it is not recommended.

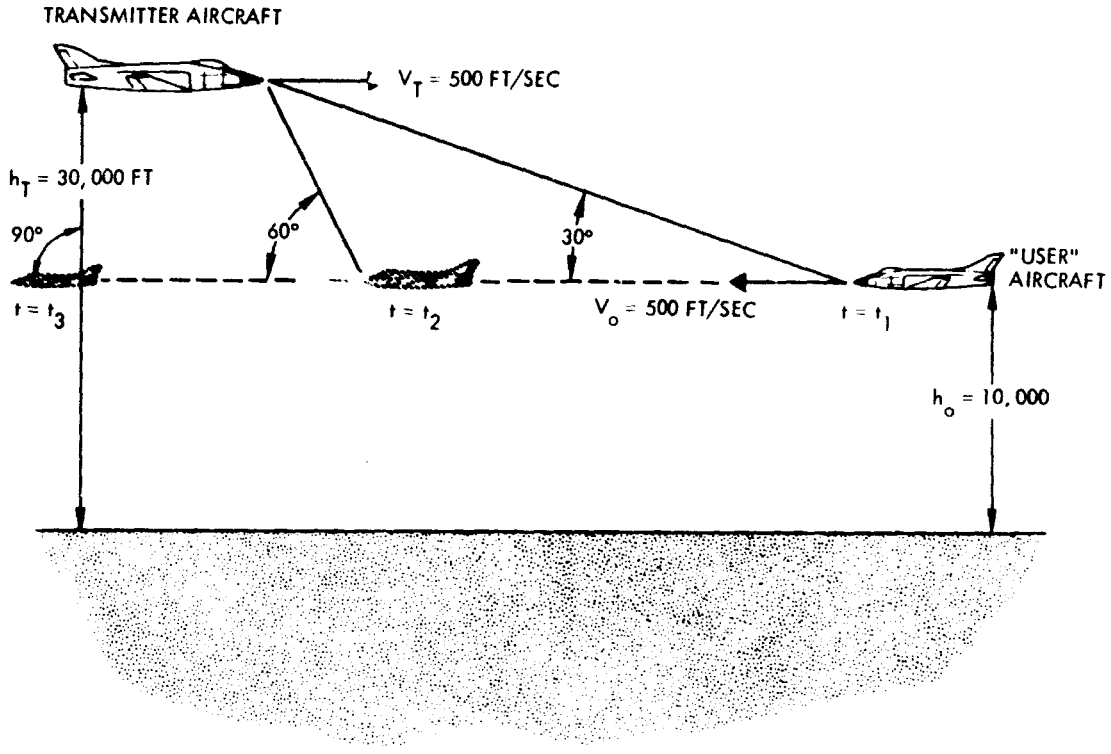

Figure 8. Geometry Between Transmitter and User Aircraft

3.3 ERS TEST

The ERS test is centered around a small piggyback-launched satellite designed to carry the basic NAVSTAR navigation equipment package: precision oscillator, BINOR code generator, and L-band transmitter. The satellite is one member of an existing family of Environmental Research Satellites (ERS) of which 15 have been placed in orbit as secondary payloads on other launches. Two alternative satellite designs have been made. The first design carries as the payload only the NAVSTAR navigation equipment. The second design carries, in addition to the NAVSTAR equipment, a MISTRAM transponder which allows for tracking the satellite by the Missile Trajectory Measurement System (MISTRAM). This latter design results in a larger and more costly satellite (still piggyback, however) but provides attractive features to the ERS test. Descriptions of the two satellite designs are given in Volume II.

The laboratory and field tests are assumed to have been completed prior to the satellite tests so that the operating characteristics of components will be well understood. However, testing of NAVSTAR equipment performance with a satellite is desirable to gain full confidence in the system. The test objective is to evaluate the system performance model, not to demonstrate a prototype navigation system. The tests will lead to:

- Evaluation of each error source predicted for the ranging model
- Positive confirmation that no error source exists that is not predicted by theory, or
- Modeling of any errors which become apparent.

The test described here assumes use of the MISTRAM satellite design. If only the NAVSTAR equipment (BINOR) is flown, a BINOR self calibration test instead of a MISTRAM/BINOR calibration test would be conducted. Other tests such as satellite reception in an aircraft and the orbit selection would be the same for either satellite design. The MISTRAM system is an X-band, CW, interferometer, transponder-aided tracking system. It consists of a transmitting site and three receiving sites together with the satellite transponder.* The three receiving sites are arranged in an L configuration, with the transmitting site close to the central receiving site. The system measures the range sum from the transmitter to the transponder and back to the central receiving site. Since the central site and the transmitter are close together, this range sum divided by two is approximately a standard range measurement. The signal received by the central site is mixed with that at each of the outlying receiver sites to obtain two range difference measurements. These three measurements locate the transponder. Derivatives of these measurements can be used to determine the velocity of the transponder. MISTRAM was selected for the following reasons:

*The two existing MISTRAM systems are located at Valkaria, Florida, and Eleuthera Island, Bahamas.

- The transponder is not significantly heavier nor does it require more power than competing systems such as a C-band instrumentation radar.
- MISTRAM has been in operation for four years and is the most accurate known U.S. tracking system.
- Operating at X-band, MISTRAM should have negligible ionospheric errors. The L-band NAVSTAR signal will provide a standard for comparing test data.
- Data handling and reduction processes for MISTRAM are established.
- A space-rated transponder exists. The current inventory is assigned to the Minuteman program.

The primary test procedure is to compare the MISTRAM-measured range with the NAVSTAR-measured range. The indicated error will be analyzed to formulate and validate the ranging model for NAVSTAR. Given that the ranging model is understood, the navigation performance of the system under a variety of operating conditions may be predicted. The satellite transmitting equipment will be designed so that reception of the signal by an aircraft will also be possible; reception by an aircraft will constitute a series of tests different from the ranging accuracy test at the MISTRAM site.

The better MISTRAM accuracy, up to an order of magnitude improvement over NAVSTAR, makes it possible to use a direct measurement or "yardstick" test philosophy. It will not be necessary to use the conventional orbit determination techniques which rely on estimation procedures that are very sensitive to the error models. Omission or erroneous form of an error term may generate false answers for many other terms in the model.

The NAVSTAR objectives should not be met by a technique which requires high confidence in a model. As examples in the following section demonstrate, the consequence of uncertainty in the system modelling can be disasterous; the characteristics of any new or unmodelled errors can be distorted or unmodelled errors could be undetected.

The conclusion is that self-calibration through orbital fitting would be an uncertain means of verifying the BINOR code ranging performance. A direct ranging measurement verification is required. The MISTRAM system can provide more than adequate accuracy and, when colocated with a ground-based BINOR code receiver, can fulfill the requirement of an accurate measurement device for the NAVSTAR system with an order of magnitude better measurement quality. Data produced on NAVSTAR accuracy by direct and simple comparison to MISTRAM can be confidently treated as actual NAVSTAR performance, untroubled by questions of correlated and unmodelled error terms, wrong estimates, erroneous weighting, and disappearing covariance matrix inverses.

The recommended test facility is the MISTRAM I site at Valkaria, Florida, about 30 miles south of Cape Kennedy. A BINOR code receiver, characteristic of proposed user equipment will be installed with the receiving antenna as close as possible to the MISTRAM receiving site. The antenna selection should be alterable between the proposed user antenna and ground station antenna. Additionally, an aircraft should be outfitted with user equipment and be available for the satellite tests. The aircraft portion of these tests can be carried out after MISTRAM/NAVSTAR calibration.

Figure 9 shows the ground trace of three successive passes of a 30-degree inclination orbit at an altitude of about 280 nautical miles. Each of these three consecutive passes generate substantial viewing periods for the test site. The elevation angles and ranges from the site are shown in Figures 10 and 11.

On each pass, MISTRAM data will be processed in the same manner as on current missile flights which use MISTRAM to determine the vehicle position relative to the test site. These data reduction procedures are well established. After the MISTRAM position data has been obtained, orbital fits may be demonstrated to illustrate the precision of the data. It is expected that values of position along the NAVSTAR range coordinate (i.e., a ranging calibration standard) of an order of magnitude better than NAVSTAR (better than 5 feet) will be demonstrated by the MISTRAM system in normal operation. If required, orbital fits

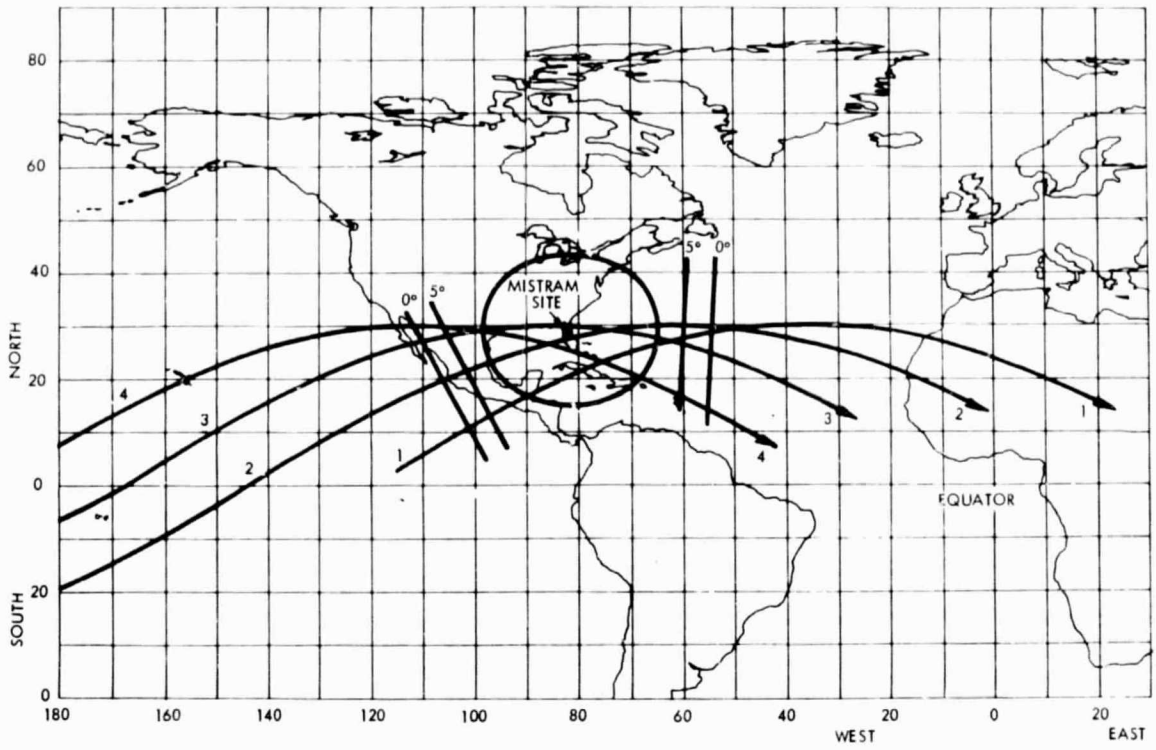

Figure 9. Orbit Ground Trace

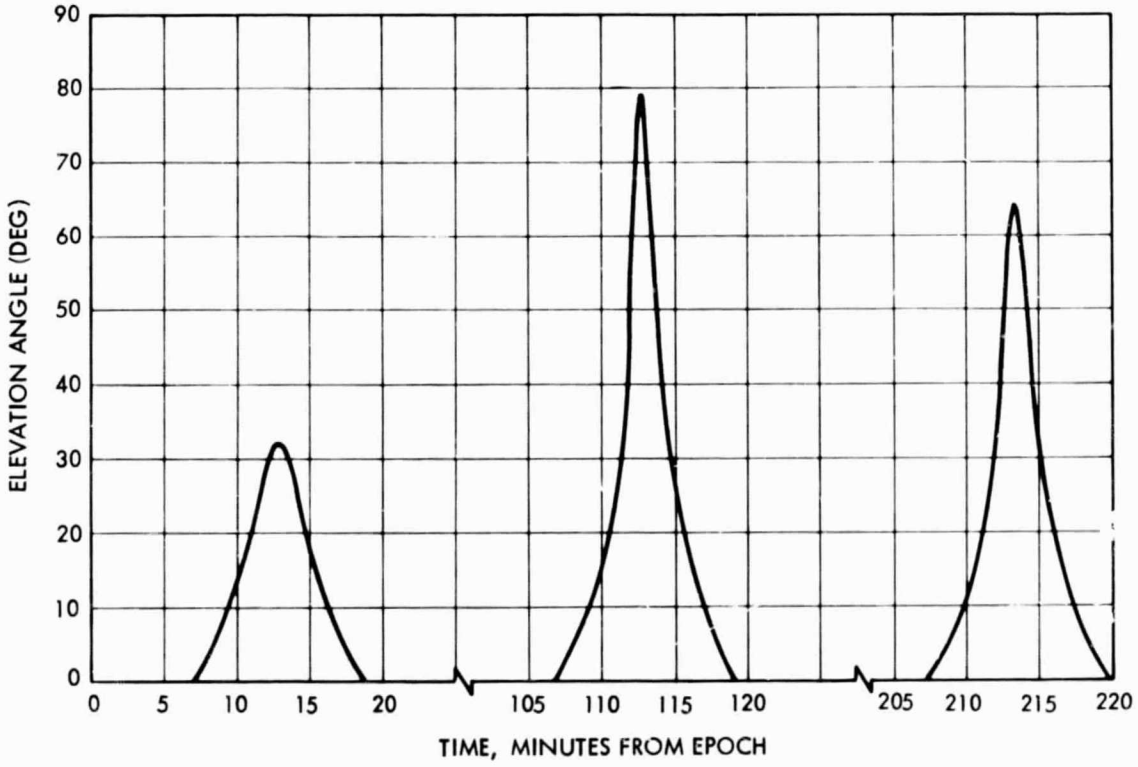

Figure 10. Elevation Angles from Test Site

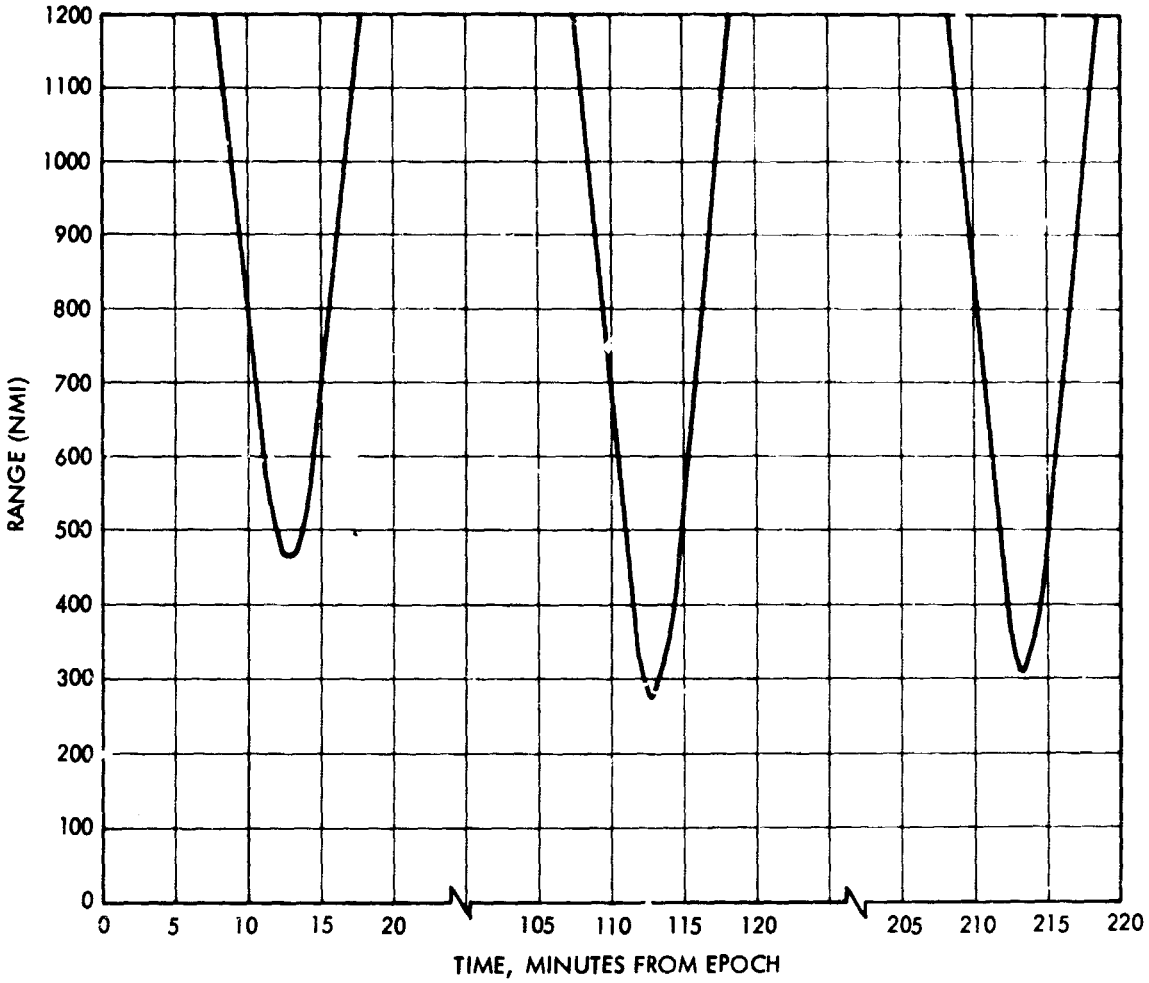

Figure 11. Range from Test Site

may be made to resolve error levels and confirm accuracy; the MISTRAM performance levels and error model are well understood after four years of operation at the Eastern Test Range.

The measured values of range from the NAVSTAR equipment at the test site will be compared with the MISTRAM position data. An accurate timing tie between the two sites must be established. To remove this potential error source from the comparisons, a timing tie between the two sites accurate within at least 0.2 millisecond is recommended.

The indicated values of range error (Appendix A) for the NAVSTAR unit are the raw material for the system's accuracy analysis. Each error source in the model will be modelled on the indicated trajectory and attempts made to correlate the anticipated error with the actual error level, shape, and magnitude. The classical parameter estimation

computer programs will be used. The influence of antenna changes and of day-night ionospheric differences will be examined with the data to verify and improve the models. If ideal fits to the error using the hypothesized error model are not achieved, the remaining errors will be subjected to rigorous analysis by the electronic hardware designers and test designers to isolate the causes of the unmodelled errors.

The rapid movement of the satellite will yield short experiment times per pass, about 10 to 12 minutes, during which the satellite moves from horizon to horizon. Hence, tests of aircraft multipath reception will not have the reasonably stationary geometry obtainable in the field tests. However, the capability to receive the signal from the satellite in the aircraft should definitely be demonstrated and multipath measurements can be made for short time intervals per pass. Tracking the aircraft by the radar at the Eastern Test Range would yield data for measuring the accuracy of the airborne ranging signal reception. Such tracking would confirm the general airborne accuracy with the satellite transmission.

The aircraft tests in conjunction with the satellite would be similar to first two tests in the field: general reception characteristics of the BINOR code system and the multipath reception characteristics. A test plan combining both the satellite-ground and satellite-aircraft phases could rely on the first phase (satellite-ground) to meet the ranging signal calibration objective, and the subsequent satellite-aircraft tests could then feature ground reception of the BINOR code signal as a calibration of the airborne link. In this case, the MISTRAM would not be required after positive validation of a ranging error model and the satellite would remain as a useful experimental tool for NAVSTAR testing.

3.3.1 MISTRAM Accuracy

MISTRAM performance has demonstrated that negligible systematic errors exist in this system apart from refraction. A range difference ambiguity has been a frequent interferometer problem in the past, but is not anticipated to be a problem in these tests; the strength of the orbital

fit would provide additional capability for ambiguity resolution. The MISTRAM data will be compared with the BINOR code data point by point to determine the accuracy with which such comparisons can be made. The MISTRAM range value can be used reliably to ± 5 feet. This kind of accuracy in determining the BINOR code residuals can be anticipated. The random error components in the MISTRAM range has been demonstrated to be about 0.3 feet.

The MISTRAM measures range sum to a transmitter positioned about 120 feet from the receiver. To calculate range exactly to the satellite from the BINOR code receiving site, the full system set of a range sum and two range differences would be used. Figure 12 shows a sketch of the MISTRAM site. Using the range sum and range difference measurements, the accuracy of position computation on the first pass

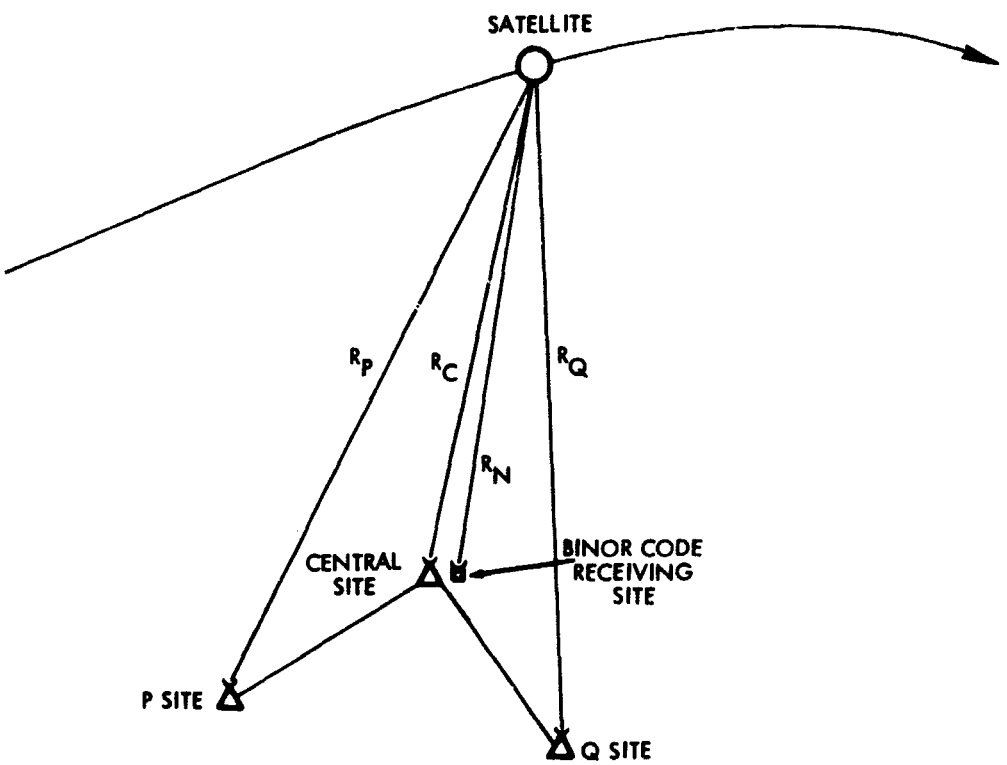

MISTRAM MEASUREMENTS:

R_C

$P = R_C - R_P$

$Q = R_C - R_Q$

Figure 12. MISTRAM Test Site

shown in Figure 9 was computed (Table 4). Since this is not the minimum range pass the answers on this pass will be worse than for passes 2 and 3 (see Figure 11). The accuracies were computed for two cases: with orbital constraints (i.e., fitting the equations of motion) and without. The second case represents a single point in time solution and is the primary solution mode. It does not require any assumptions on the gravity field, initial vehicle state, or drag.

Table 4. Error Model Uncertainty from First Pass MISTRAM Calibration with Orbital Constraints

Term		A Priori Uncertainty	Recovered Uncertainty
Initial	X_o, ft	1000	18
	Y_o, ft	1000	11
	Z_o, ft	1000	25
	$\dot{X}_o$, ft/sec	10	0.012
	$\dot{Y}_o$, ft/sec	10	0.014
	$\dot{Z}_o$, ft/sec	10	0.026
	Range (sum) bias, ft	10	2.2
	(P) range difference bias, ft	2	0.012
	(Q) range difference bias, ft	2	0.022
	Refraction	10 n-units	3 n-units
Internal Survey	Length, ppm	1	0.15
	Azimuth, ppm	1	1.99
	Elevation, ppm	1	0.33

The following error model for MISTRAM was set up for tests of the orbital fit case:

	1σ Random Error	1σ Bias Error
Range sum, ft	0.3	10
Range difference, ft	0.03	2

Other errors:

10 n-units (1σ) refraction

1 ppm internal survey in baseline length and direction

The bias values are conservative. The 2-foot range difference bias represents the basic ambiguity level in the system and was used to show how an ambiguity could be solved using orbital calibration. The random (noise) values are also conservative, since MISTRAM has demonstrated better values in free-flight tracking.

In computing the accuracy obtainable on the first pass with the orbital fitting technique, solutions were obtained of the six initial conditions $(xyz, \dot{x}\dot{y}\dot{z})_o$ with a priori uncertainties of 1000 feet and 10 ft/sec. The covariance matrix of these quantities was propagated through the pass to compute the accuracy.

The position accuracies in downrange, crossrange and vertical (relative to the orbit plane) shown in Figure 13 are obtained if the full 6 x 6 initial state covariance matrix is propagated through the pass. These values are smaller than the position components of the initial state estimation because the initial condition covariance matrix has some strong negative cross correlations. As Table 4 shows, uncertainties in ambiguity resolution in the MISTRAM can be clarified by orbital fits. The orbit position accuracies shown in Figure 13 rss to less than 6 feet as the vehicle passes the longitude, south, of the test site.

The MISTRAM capability to provide position data without the aid of the equations of motion was also analyzed. The rss position error history for this case is shown in Figure 14. The accuracy at the point of closest approach is very nearly the same as for the case using orbital constraints (Figure 13). At the extended ranges, the solution is degraded by less than a factor of two. This is a particularly meaningful result

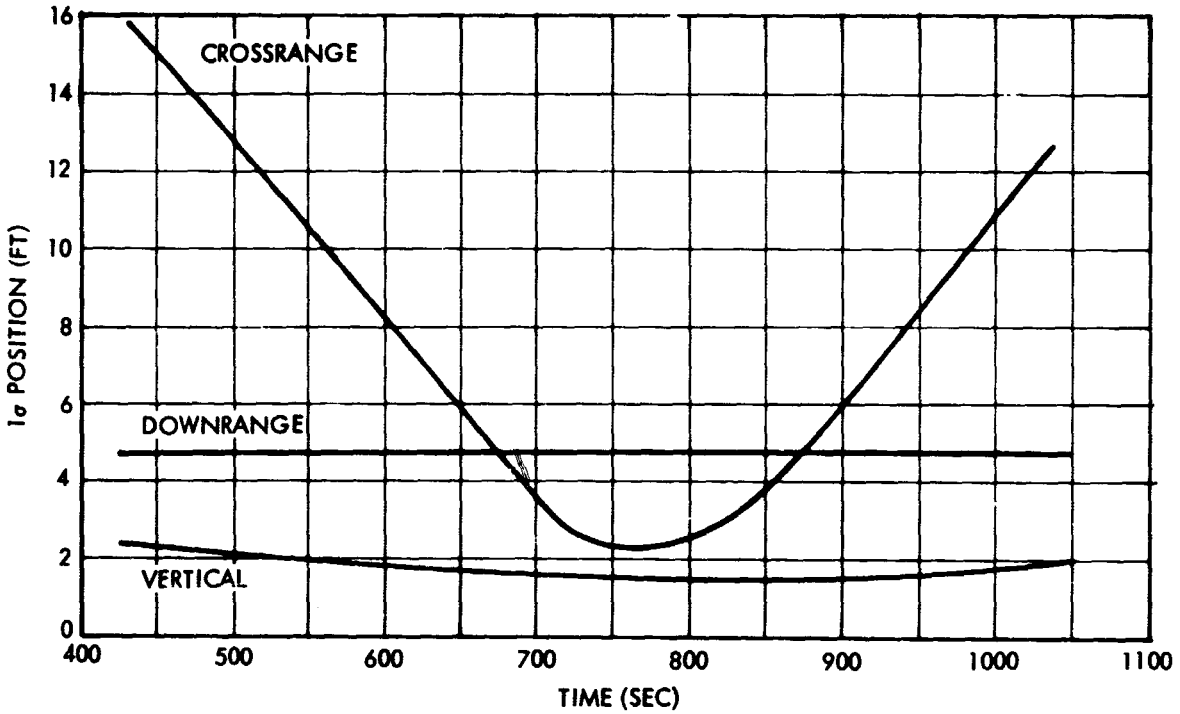

Figure 13. Orbital Uncertainties, First Pass with MISTRAM

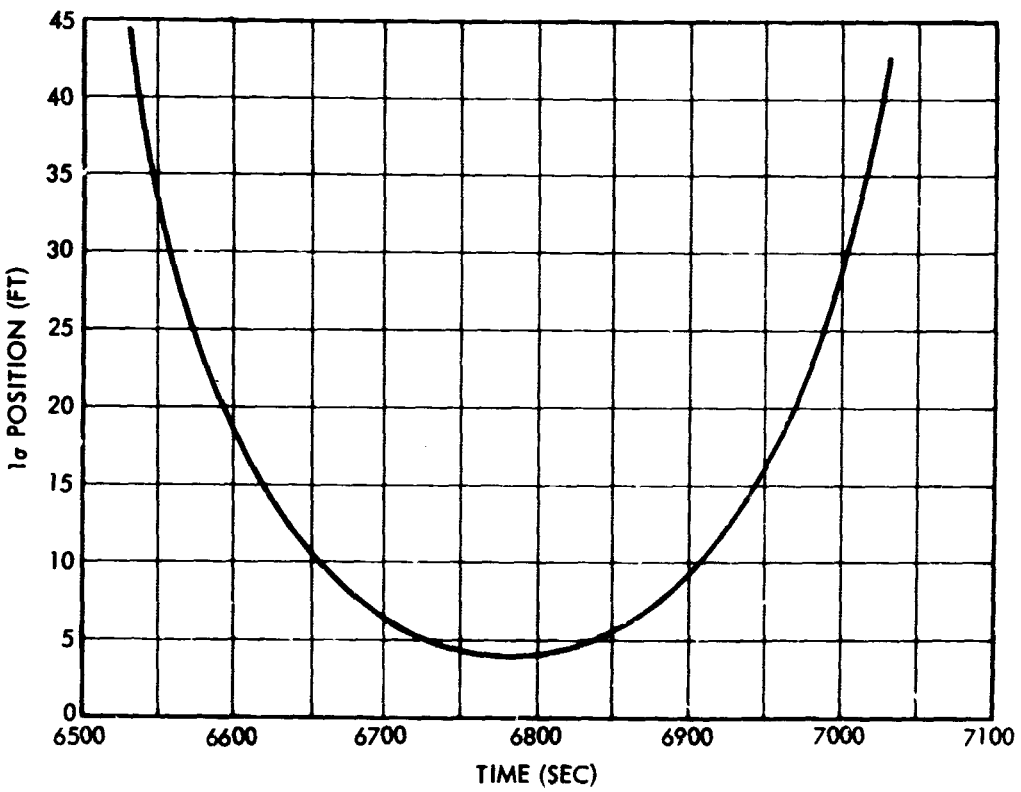

Figure 14. RSS Position Uncertainty, Single-Point-in-Time

showing that the MISTRAM system is of such high quality that the application of the laws of motion only slightly enhance the solution. For passes where the satellite range from MISTRAM is relatively short, orbital constraints may not be required.

3.3.2 BINOR Code Self-Calibration

In evaluating the possibility of BINOR code self-calibration, the potential accuracies and problems were studied. For the same first pass as considered in the MISTRAM example, the capability of recovering the BINOR code system modelled errors was evaluated in a standard regression program. The accuracy of the calibration depends heavily on the model. A random 1σ error assumption of 50 feet in range was used for the test cases. Initial condition uncertainties were solved for in all cases with 0.25 ft/sec a priori standard deviations on velocity to represent the result of iterations on the data to refine the initial state estimates. The following cases illustrate the results:

Case 1: Bias, Refraction Modelled Only

Term	a priori σ	Recovered σ
Range bias, ft	100	33
Refraction, n	10	10

Case 2: Range and Oscillator Bias Modelled Only

Term	a priori σ	Recovered σ
Range bias, ft	100	57
Oscillator bias, ft/sec	0.1	0.077

Case 3: Extended Model

Term	a priori σ	Recovered σ
Range bias, ft	100	62
Scale factor, ppm	2	1.98
Timing, ms	2	1.91
Oscillator bias, ft/sec	0.1	10
Refraction, n	10	10
East site survey, ft	10	10

Term	a priori σ	Recovered σ
North site survey, ft	10	10
Vertical site survey, ft	10	10
Range acceleration error, ft/sec^2	1	0.392

These cases indicate that a very restricted model is required even to assure confidence in estimating a range bias error of 100 feet a priori to one-third that value, and that if an extended model is used the initial uncertainty is cut only by a third. Significantly, such terms as ionospheric error and receiver phase drift during the pass are not included in the model.

To illustrate more clearly some of the problems that unmodelled error terms could cause in a BINOR code self-calibration procedure, a sample range residual was invented to simulate the data which would be obtained from the BINOR code receiving station differenced with an assumed orbit. Then the normal regression program was run on this data with various forms of deliberate mismodelling to illustrate potential hazards.

Figure 15 shows the simulated residual data for the first orbital pass. The data is made up of the following components:

Range random noise	50 ft
Range bias	100 ft
Timing	2 msec
Oscillator bias	0.1 ft/sec
Refraction	10 n-units
East survey	10 ft
North survey	10 ft
Vertical survey	10 ft
Range acceleration lag	1/sec^2
X initial condition	200 ft
Y initial condition	0
Z initial condition	0
$\dot{X}$ initial condition	-0.25 ft/sec
$\dot{Y}$ initial condition	0.10 ft/sec
$\dot{Z}$ initial condition	0

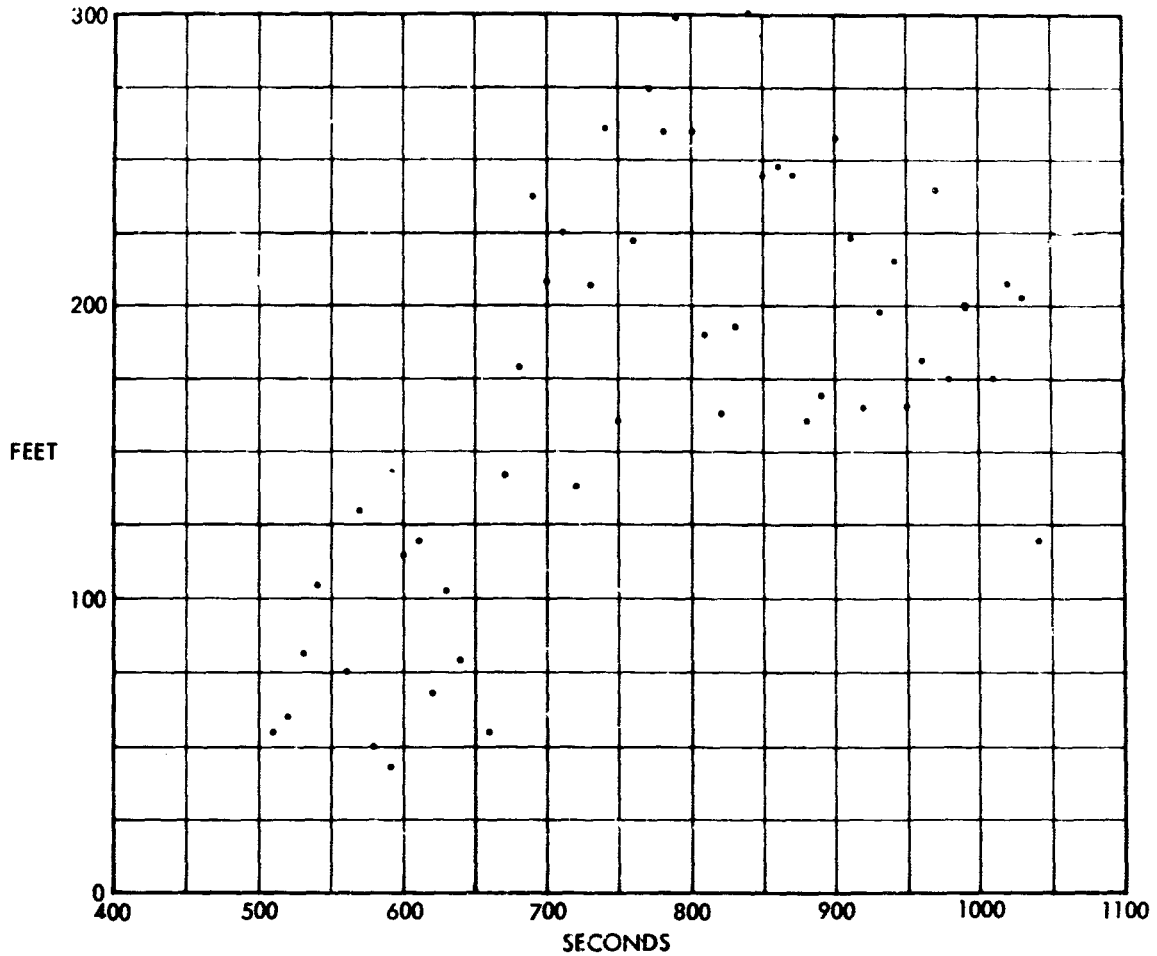

Figure 15. Simulated Range Error of BINOR Code

It is interesting to determine how well this error model could be estimated if the existence of certain components were not known. In this case white Gaussian noise is assumed, which might not be the case in practice. The problem is to separate the modelled errors and hope that no unmodelled errors will get lumped in with the modelled errors. Initial condition errors were included in the solution in every case.

- Case 1

  Assume that only range bias and refraction are in the model. Using these two terms (and initial conditions) in the solution, the following values are obtained:

Term	Actual Value	Solved For	Error
Range bias, ft	100	42	58
Refraction, n	10	-0.1	10.1

The solution for the standard deviation of range bias, however, was only 33 feet, so a nearly 2σ answer has been obtained for this term.

- Case 2

Assume that only range and oscillator biases are in the model. The solution is:

Term	Actual Value	Solved For	Error
Range bias, ft	100	15	85
Oscillator bias, ft/sec	0.1	0.045	0.055

The oscillator bias standard deviation was 0.077, so less than a 1σ error has been made for this term.

- Case 3

Assume that the makeup of the model is well known, even to the selection of a priori variances, but that the random noise is underestimated by a factor of two. In this case, the following results are produced:

Term	Actual Value	Solved For	Error
Range bias, ft	100	24	76
Scale factor, ppm	2	0.03	1.97
Timing, rms	2	0.14	1.86
Oscillator bias, ft/sec	0.1	0.07	0.03
Refraction, n	10	0.07	10
East survey, ft	10	0.2	9.8
North survey, ft	10	-0.14	9.0
Vertical survey, ft	10	0.14	9.9
Range acceleration lag, ft/sec^2	1	0.312	0.688

Term	Actual Value	Solved For	Error
X_o, ft	200	56	144
Y_o, ft	0	-34	34
Z_o, ft	0	-18	18
$\dot{X}_o$, ft/sec	-0.25	0.078	0.172
$\dot{Y}_o$, ft/sec	0.10	-0.026	0.126
$\dot{Z}_o$, ft/sec	0	-0.061	0.061

3.3.3 Accuracy Conclusions

Most of these terms are not multi-sigma errors and from a statistical standpoint are not considered a bad solution. All the cases reviewed provide a fairly good fit to the data. Figures 16-19 show the fits (residuals) obtained with these solutions. The fits for the deliberately mismodelled cases are not significantly different from the case in which the correct model was used. The residual rms values, a typical figure of merit, vary only slightly. The point made by this simple example is that in spite of the good fit to the data in orbital self-calibration, the errors made in the individual error sources are significant as far as interpreting BINOR code hardware performance. It will be of importance to know whether the bias is 100 feet or 24 feet, even though the fits may be comparable. Worse is the concealing of the character of unmodelled terms. Consider Case 2, for example, in which the presence of a term proportional to range acceleration (R) is represented in the data but not in the solution. This error, at the level at which it was included in the simulated data, would cause an error in range as shown in Figure 20. It is not implied that any error of this type does not exist, but imagine for a moment that an unmodelled error of the size and shape of Figure 20 existed in the system unsuspected. Now observe the residuals from Case 2 (Figure 17) in which the error was not modelled in the solution. No hint of the characteristics of the unmodelled error is contained in the residuals. Most of the unmodelled error has been absorbed by the other terms in the model.

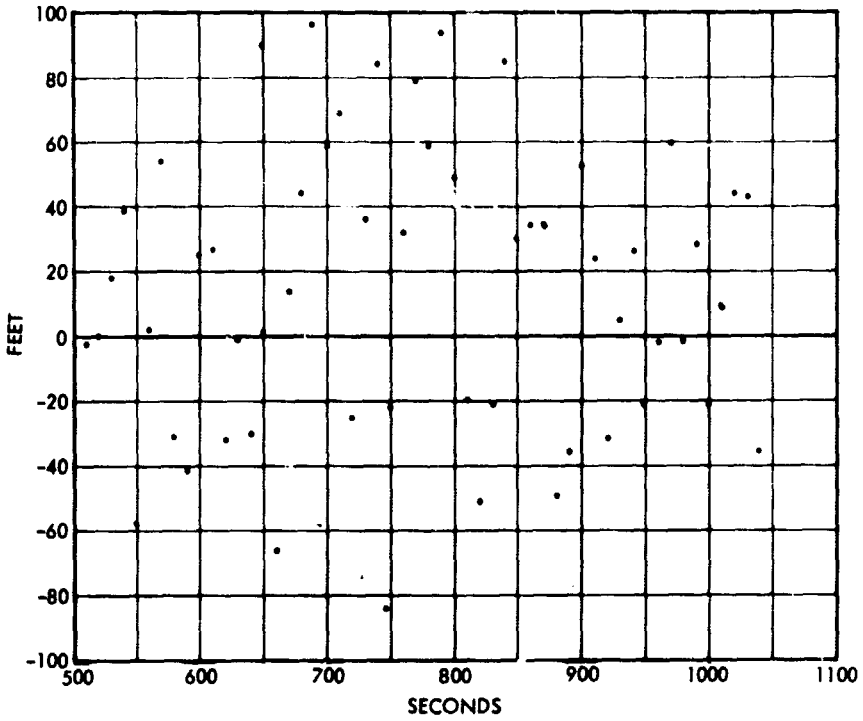

Figure 16. Residuals from Fit with Range Bias and Refraction Only (Case 1)

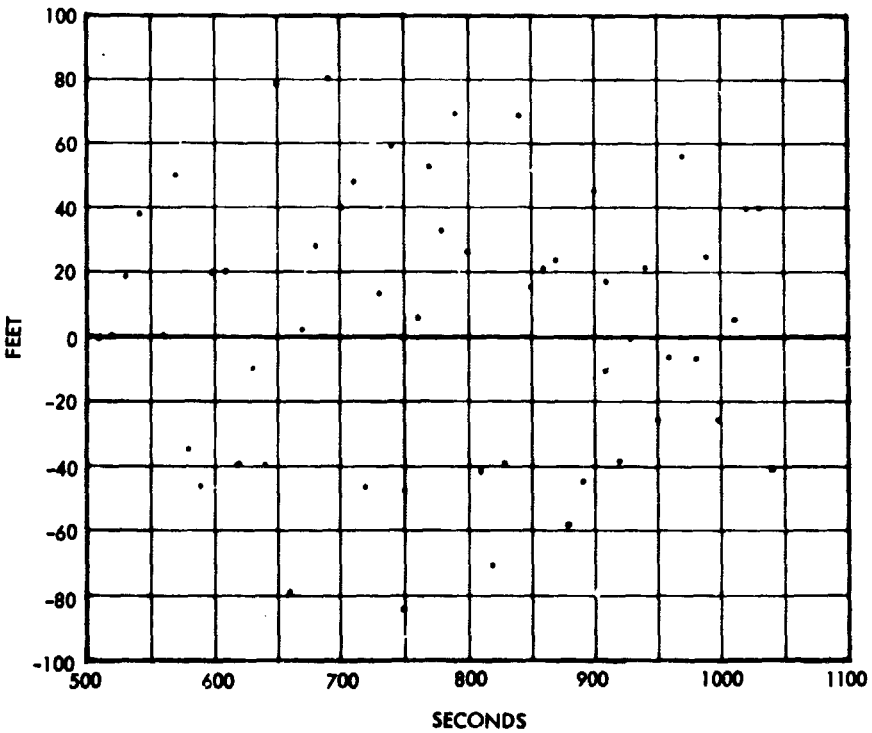

Figure 17. Residuals from Fit with Range and Oscillator Biases Only (Case 2)

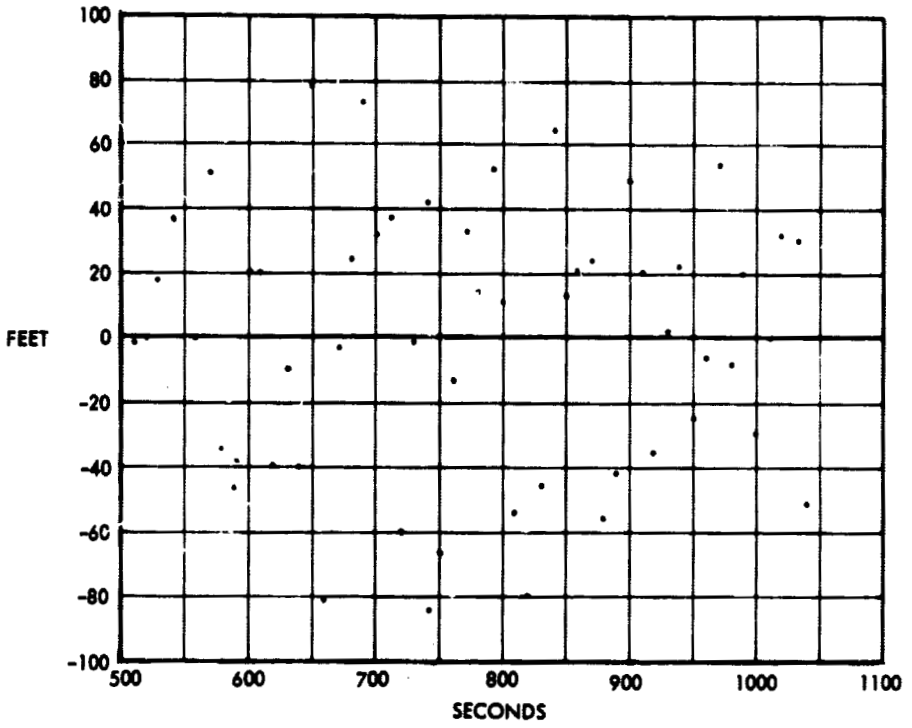

Figure 18. Residuals from Fit with Half-Sigma Noise Estimate (Case 3)

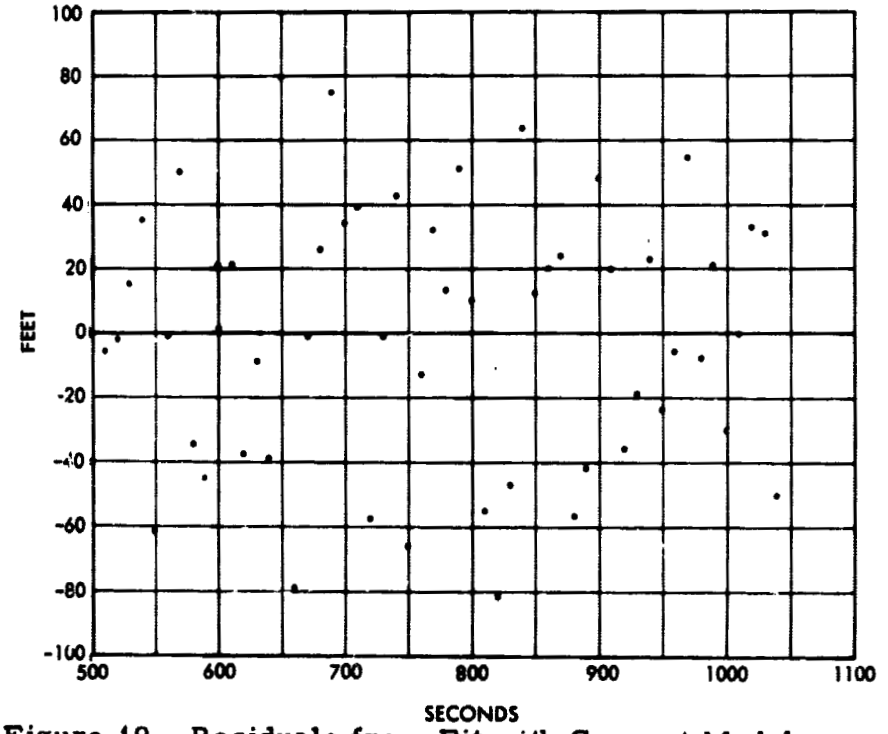

Figure 19. Residuals from Fit with Correct Model

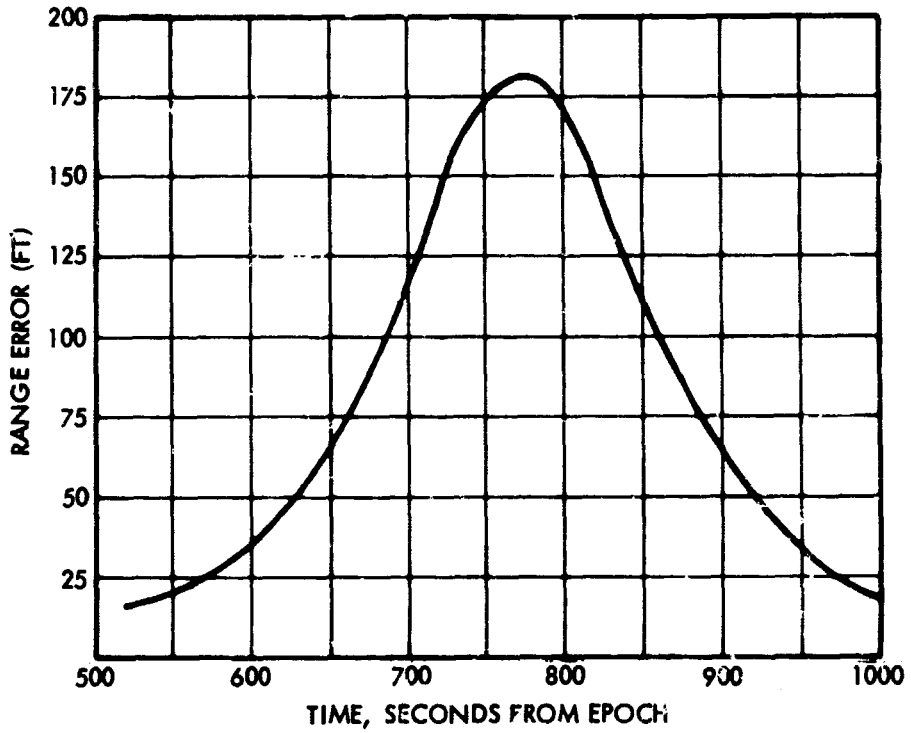

Figure 20. Range Error Due to Unit Simulated 'Unmodelled Error' (Proportional to $\dot{R}$)

This is a perfectly acceptable state of affairs for many orbit determination exercises, but only serves to emphasize the hazards of this form of system testing in cases where the error models themselves are of primary interest. This is the reason that an independent tracking system (MISTRAM) is felt to be far superior to self-calibration for determining overall accuracy of the BINOR code.

3.3.4 Satellite Signal Characteristics at Aircraft

Figures 21 and 22 show the elevation angle, range rate, and path difference range rate ($\dot{\Delta}$ defined in Appendix E) from the satellite with time as received in an aircraft at a 40,000-foot altitude. The plots assume no aircraft motion and the aircraft positioned in a plane perpendicular to the midpoint of the satellite ground trace. The plots are symmetrical about zero time since this time is referenced to the maximum elevation angle of the satellite above the horizon. Two cases were plotted: with the maximum elevation angle at 10 degrees and at 20 degrees; in both cases the satellite orbit is the nominal 300 n mi orbit and the aircraft altitude is 40,000 feet.

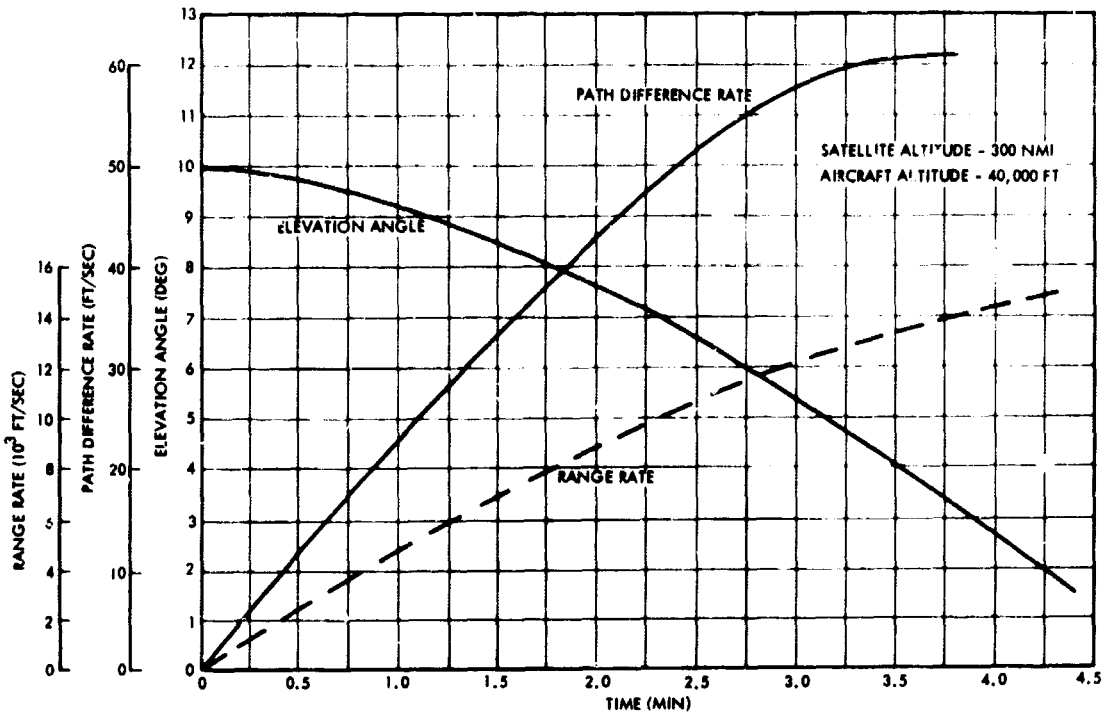

Figure 21. Signal Characteristics at Aircraft from Satellite for Maximum 10-Degree Elevation Angle

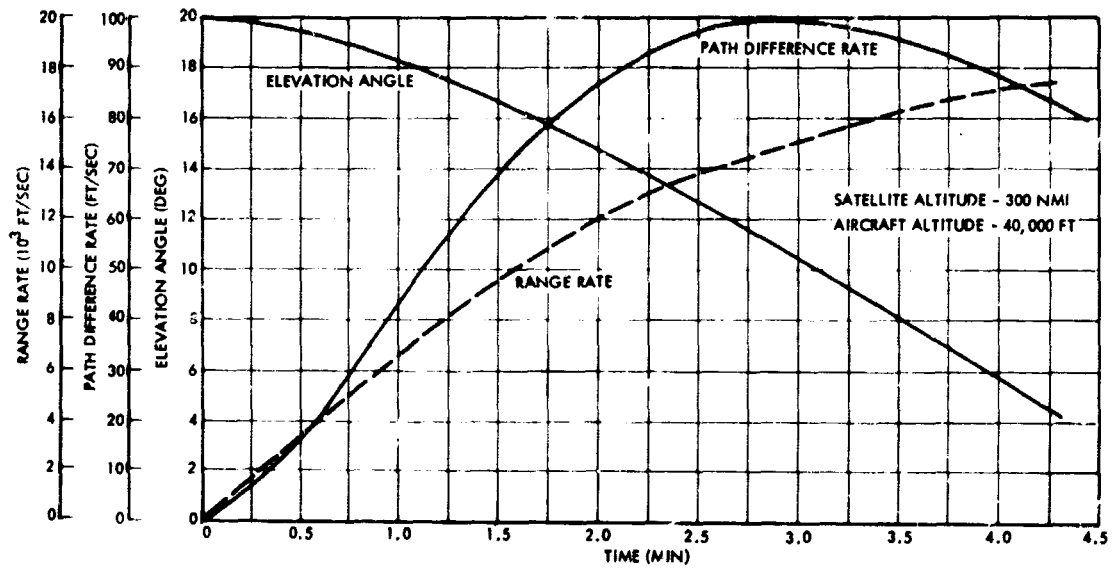

Figure 22. Signal Characteristics at Aircraft from Satellite for Maximum 20-Degree Elevation Angle

The plots show that the range rate is less than 3,000 ft/sec for only about 2.5 minutes in the 10-degree elevation angle case and about one minute in the 20-degree elevation angle case. The path difference rate which determines the multipath induced amplitude and phase rates on the received signal is less than 10 ft/sec for about 1.5 minutes in the 10-degree elevation angle case and less than a minute in the other case. Consequently, in order to observe carrier doppler and multipath rates similar to the synchronous satellite case, a short time (on the order of 1 - 2 minutes) is available during each pass to obtain data. Since the plots assume a motionless aircraft, which is hardly realistic, the aircraft may be able to move in a path which can increase the data observation time by partially canceling the coppler and/or multipath rate. The amount of increase will be small, however, since the maximum velocity of the aircraft is small compared with the satellite. The aircraft positioned in a plane perpendicular to the midpoint of the satellite ground trace is thought to be the most favorable geometry to minimize doppler and multipath rate. Further investigation of the most favorable satellite and aircraft geometry including the effects of aircraft motion should be made prior to the aircraft-satellite tests in an attempt to increase data time per satellite pass.

3.4 IDCSP SATELLITE DEMONSTRATION

Described here is an experiment to demonstrate the concept of self determination of position by making use of range and/or range difference measurements to a network of tracked satellites in synchronous or near synchronous orbits. The existing network of IDCSP satellites is proposed for use in this demonstration. Complete determination of NAVSTAR L-band navigation accuracy will not be possible since the satellites operate at X-band, are repeaters, and do do not have sufficient ERP to enable reception by low-gain antennas mounted on aircraft. However, the payoff in this test would be primarily the demonstration of high accuracy position determination including the effects of satellite tracking errors using a receiving terminal with a high-gain antenna to simulate a user. In addition, NAVSTAR software designs for determining satellite ephemeris and position location can be exercised.

The Initial Defense Communications Satellite Project network consists of a total of 26 satellites (one of which is only partially operable), several permanent ground stations, and numerous transportable ground terminals. The satellites are 3 feet in diameter and 3 feet high, weigh 105 pounds each, are spin stabilized, require 42 watts prime power, employ redundant 3-watt TWT transponders (see Figure 23), and have omni-toroid, circularly polarized, 4 db gain antennas. Uplink communications are in the 7975 to 8025 megahertz band, where the signals are frequency translated in a pseudo-coherent manner and retransmitted in the 7250 to 7300 MHz band. System bandwidth is 20 MHz, and the front end noise figure is 9.5 db. The satellites have no command capability, but do telemeter 62 functions on a 400 MHz link. A block diagram of the satellite communications equipment is shown in Figure 23. The IDCSP satellites are at altitudes in the vicinity of 18,300 nautical miles, and drift at about 30 to 35 degrees per day. Stations between 30 and 40 degree latitude typically see each satellite 4 to 5 days. Three of the 26 satellites (including the partially operable one) reach inclinations as high as 6 degrees, the remaining 23 do not exceed 2 degrees.

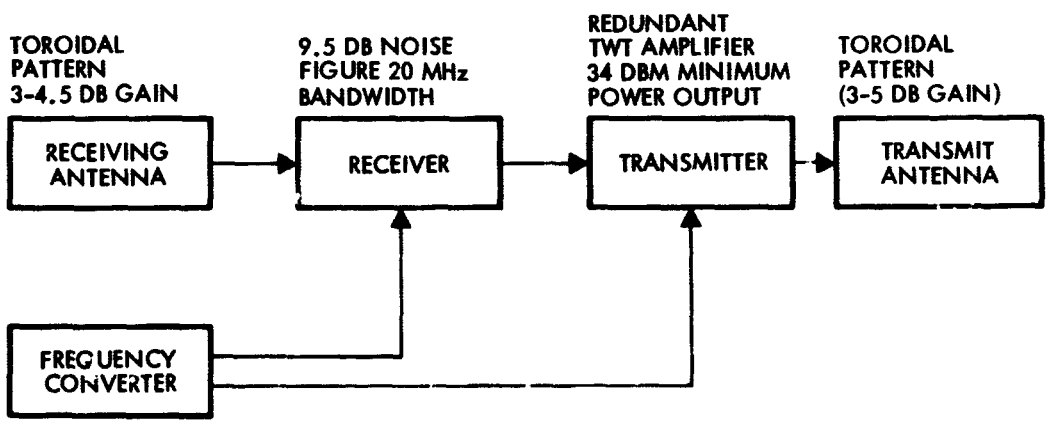

Figure 23. Simplified Block Diagram of the IDCSP Satellites

There are several classes of ground terminals that can be used with the satellites. The primary ones are the permanent terminals at Camp Roberts, California, and Fort Dix, New Jersey. These employ 60-foot parabolic antennas and 10 kw transmitters. Similar stations are believed to be under construction at Hawaii, the Phillipines, West Germany and Ethiopia. Additionally, two transportable terminals, designated AN/MSC-46 and employing 40-foot antennas, will be located at Hawaii. Both the 60- and 40-foot antennas are 4 horn cassegrain monopulse trackers. At present, the tracking of the satellites and calculation of satellite ground traces is the responsibility of the Air Force Satellite Control Facility (SCF). The 60-foot Philco tracking and data acquisition antennas at the Hawaii, Vandenberg AFB (California), New Hampshire and Indian Ocean SCF stations are used for this purpose. IDCSP epheremis is crude due to the use of angle tracking data, obtained by tracking the 400 MHz telemetry source to an accuracy of about 1 milliradian. The epheremis of each satellite is updated weekly, and the published ground traces are updated monthly. The purpose of the epheremis data is to provide acquisition information to IDCSP users, and no special attempt is made to refine the data for trajectory reconstruction purposes.

3.4.1 Proposed Demonstration

In order to demonstrate the feasibility of position determination by passive ranging to multiple satellites, essentially two items must be supplied to the user equations to arrive at a position fix: ephemeris data on three or four satellites, and pseudorange or range difference measurements from the satellites. To obtain these measurements, the following scheme is proposed.

One of the IDCSP ground stations will transmit a ranging signal (the BINOR code modulated onto the X-band carrier) to each of the four satellites sequentially. These satellites will, in turn, retransmit the signals in sequence (simulating the time division multiplexing of NAVSTAR) to four specially instrumented receiver terminals. One terminal will simulate a user attempting to determine his position while the other three terminals will simulate the NAVSTAR ground

tracking network. Precision frequency standards will be used to note the time at which the signals are transmitted and the time at which they are received at the tracking sites. The user terminal will measure arrival times with a crystal oscillator of the quality proposed for the actual NAVSTAR users. The tracking site data will furnish the satellite ephemeris information which will therefore require known locations for the tracking sites. The user measurements together with the ephemeris data will furnish the basis for calculating user position as proposed in NAVSTAR. The calculated user position can be compared with the actual knowledge of user position.

It is desirable (but not necessary) to transmit the range code to the satellites at 1.5 second intervals so that the time between retransmitted signal matches that of the NAVSTAR satellites. A potential problem exists here since the terminals require narrow beam antennas which contain only one satellite in their fields of view. Rapid switching between satellites necessitates either four antennas tracking each satellite separately or rapid steering of one antenna between satellites. The best time interval that would be possible with the IDCSP satellite transmissions remains to be determined.

The receiver terminals must be located such that four satellites are mutually visible to all of the terminals. This is not considered a serious constraint, since if either Fort Dix or Camp Roberts is employed as the transmitter, the receiver terminals may be located virtually anywhere in the continental United States.

3.4.2 Required Equipment

The proposed demonstration requires a transmitting terminal, three receiving terminals for satellite tracking (one of which can be co-located with the transmitter), and a receiving terminal for making the user pseudorange or range difference measurements. The transmitter terminal must contain a BINOR range code generator which can phase-modulate the IDCSP uplink carrier and a portable time or frequency standard such as a Hewlet-Packard 5061A cesium beam atomichron. The times of transmission to each satellite will be recorded using the

standard and will serve as an input to the satellite ephemeris determinations. In addition, the transmitter terminal must be capable of switching rapidly between four satellites by either steering of one antenna or switching between four antennas tracking each satellite separately.

The receiver terminals for tracking will require the BINOR code acquisition and range measurement unit plus a time standard similar to the transmitter to act as a reference for the range measurements. Suitable recording equipment is also required to record the range readings and the time of each reading.

The receiver terminal which simulates the user can be identical to the other receiver terminals except that a crystal oscillator will be used as the reference for the range measurements. The terminal can be located at either a fixed site or in a mobile van. Another possibility is to use a large aircraft capable of receiving the IDCSP signals. The mobile terminals have the advantage of demonstrating NAVSTAR capability for position location with moving users such as ships and aircraft.

The receiver terminals, including the user terminal, have the following problems in common. First, the same antenna problem of switching between the four satellites exists as for the transmitter terminal. Second, the terminals must be at locations which are geodetically well known (also applies to the transmitter). In particular, the user terminal, if mobile, must move along a well-determined path which, in the aircraft case, will require an instrumented flight range.

The size of the receiving antennas can be determined from the satellite-to-ground power budget based on the requirement of -131.8 dbm signal strength for the BINOR code (see Volume I of Reference 1). Actually, this value is based on a receiving system noise temperature of 730°K. Since the IDCSP ground stations, which use parametric preamplifiers, will have smaller noise temperatures, this signal strength is probably larger than will be required. Table 5 indicates that a 12 db margin results with an eight-foot parabolic antenna which is easily mounted on top of a van.

Table 5. IDCSP to Ground Power Budget

Maximum transmitted power (3 watts)	+ 34.8 dbm
IDCSP antenna gain	+ 4.0 db
Space loss (19,000 n mi, 7275 MHz)	-199.8 db
Polarization loss (estimate)	- 0.3 db
Ground antenna gain (8-foot dish)	+ 43.0 db
Assumed circuit losses	- 1.5 db
Received signal level	-119.8 dbm
Required signal level	-131.8 dbm
Margin	12 db

3.4.3 Accuracy

The accuracy with which the position of the user terminal can be determined is generally a function of: the individual range measurement errors associated with the equipment and transmission media of each system the geometric dilution of precision or GDOP effect associated with user-satellite geometry, and the contamination of the user position fix by uncertainties in satellite epheremis. The two largest error terms for the high accuracy user, multipath and ionospheric effects, will be negligible in the IDCSP demonstration because of the large ground antennas and X-band frequencies employed. Assuming refraction correction, the tropospheric error will be small, as indicated in Appendix A. Receiver drift and oscillator errors will be comparable to those of NAVSTAR and receiver noise will probably be less due to the relatively large satellite-to-ground link margin. In the area of GDOP, some degradation in position uncertainties will occur due to the fact that the IDCSP satellites are essentially equatorial instead of in inclined orbits such as the case with NAVSTAR, but results can be extrapolated to the NAVSTAR case. In summary, high accuracy position fixes can be anticipated.

4. LABORATORY AND FIELD TEST COST ESTIMATES

Following are budgetary and planning type cost estimates for the laboratory and field tests desceibed in previous sections. The total period of time from start of work to test completion, including data analysis and reporting, is estimated to be about 18 months. The total cost is estimated to be approximately 1.3 million dollars with a jet transport type aircraft used in the field tests. An additional 0.5 million dollars will be required to complete the helicopter field tests (including the VSTOL ILS test).

4.1 COST SUMMARY

Table 6 summarizes estimated laboratory and field test program costs assuming that only the jet transport is used in the field tests. Table 7 provides incremental costs of adding a user helicopter to the field test program. The latter costs include VSTOL ILS tests as well as NAVSTAR system tests in the instrumented helicopter configuration.

It should be noted that both tables show a small difference in cost when a balloon is used instead of an aircraft for a high altitude signal source. The estimated difference is 20,000 dollars in favor of a balloon source for the jet transport user tests and 4,000 dollars in favor of a jet aircraft source for the helicopter tests. The slight advantage to a jet aircraft source in the latter case accrues because the aircraft need not be tied down for installation and checkout of the signal source instrumentation; installation and checkout are included in the costs for the jet transport user field tests. The balloon costs assume a total of five flights each for the jet and helicopter tests. If problems occur in system performance, however, five flights may not be enough.

4.2 TEST SCHEDULE

Figures 24 and 25 provide a feasible schedule for the laboratory and field tests.

Table 6. Summary of NAVSTAR Test Program Costs (Jet Transport User Aircraft)

	Cost ($000)						
	Integrated System Lab Tests	Precision Oscillator Lab Tests	Antenna Pattern Lab Tests	RFI and ser ...ilator Field Tests	*Aircraft to Aircraft Field Tests	Ground to Aircraft Field Tests	Total
1. Test Planning and Project Coordination	51.5	12.5	15.0	30.0	75.0	75.0	259.0
2. Procure Test Hardware							
a. Oscillator	8.0	8.0					16.0
b. Transmitter	34.7					74.8	109.5
c. Receiver	57.4						57.4
d. BINOR Code Generator	6.0					17.8	23.8
e. BINOR Code Processor	15.2						15.2
f. Antennas			6.3	27.7	12.9	7.3	54.2
g. Antenna Switching Unit					8.9		8.9
h. RFI Measurement Instrumentation				12.5			12.5
i. Test User Oscillators				1.0			1.0
j. Multipath Measurement Instrumentation					15.4		15.4
k. Model Aircraft and Range			9.6				9.6
l. Generator Instrumentation	28.6	7.0		28.1		80.2	143.9
3. Leased Test Equipment							
a. Jet Transport				40.0	40.0	40.0	120.0
b. Signal Source Aircraft (Signal Source Balloon)*					36.0		36.0
					(16.0)*		(16.0)*
c. General Instrumentation	20.5	0.6				3.7	24.8
d. Helicopter (Ground Test Support)						8.8	8.8
4. Equipment Installation, Integration, and Check Out							
a. Laboratory	5.8		2.2				8.0
b. Jet Transport Antennas				5.1	11.8		16.9
c. Jet Transport Receivers and Instrumentation				18.0	3.7	2.0	23.7
d. Signal Source Antennas					6.2		6.2
e. Signal Source Transmitters and Instrumentation					6.1		6.1
f. Ground Antennas						2.6	2.6
g. Ground Transmitters and Instrumentation						23.6	23.6
5. Software Development						79.5	79.5
6. Test Operations	35.7	5.5	5.8	7.0	14.0	51.0	119.0
7. Data Reduction, Analysis, and Reporting	19.3	8.0	8.1	9.0	24.6	33.5	102.5
Total	282.7	41.6	47.0	178.4	254.6 (234.6)*	499.8	1304.1 (1284.1)*

*The cost of using a balloon for the signal source (instead of an aircraft) is given in parenthesis.

Table 7. Incremental Cost to NAVSTAR Test Program For Helicopter User Aircraft Tests

	Cost ($000)				
	Antenna Pattern Lab Tests	*Aircraft to Helicopter Field Tests	Ground to Helicopter Field Tests	VSTOL ILS Field Tests	Total
1. Test Planning and Project Coordination	10.0	30.0	30.0	60.0	130.0
2. Procure Test Hardware					
a. Oscillator b. Transmitter c. Receiver d. BINOR Code Generator e. BINOR Code Processor f. Antennas g. Antenna Switching Unit h. RFI Measurement Instrumentation	2.1	8.6			10.7
i. Test Oscillators j. Multipath Measurement Instrumentation k. Model Aircraft and Range l. General Instrumentation	9.6				9.6
3. Leased Test Equipment					
a. Helicopter		16.0	16.0	16.0	48.0
b. Signal Source Aircraft (Signal Source Balloon)*		12.0 (16.0)*			12.0 (16.0)*
c. General Instrumentation			3.7		3.7
d. Helicopter (Ground Test Support)			8.8		8.8
4. Equipment Installation, Integration, and Check Out					
a. Laboratory	2.2				2.2
b. Helicopter Antennas		9.1			9.1
c. Helicopter Receivers and Instrumentation		21.7	2.0		23.7
d. Signal Source Antennas e. Signal Source Transmitters and Instruinentation f. Ground Antennas g. Ground Transmitters and Instrumentation				11.8	11.8
5. Software Development					
6. Test Operations	5.8	14.0	51.0	39.3	110.1
7. Data Reduction, Analysis, and Reporting	8.1	24.6	31.5	9.9	76.1
Total	37.8	132.3 (140.0)*	145.0	117.0	455.8 (459.8)*

*The cost of using a balloon for the signal source (instead of an airplane) is given in parenthesis.

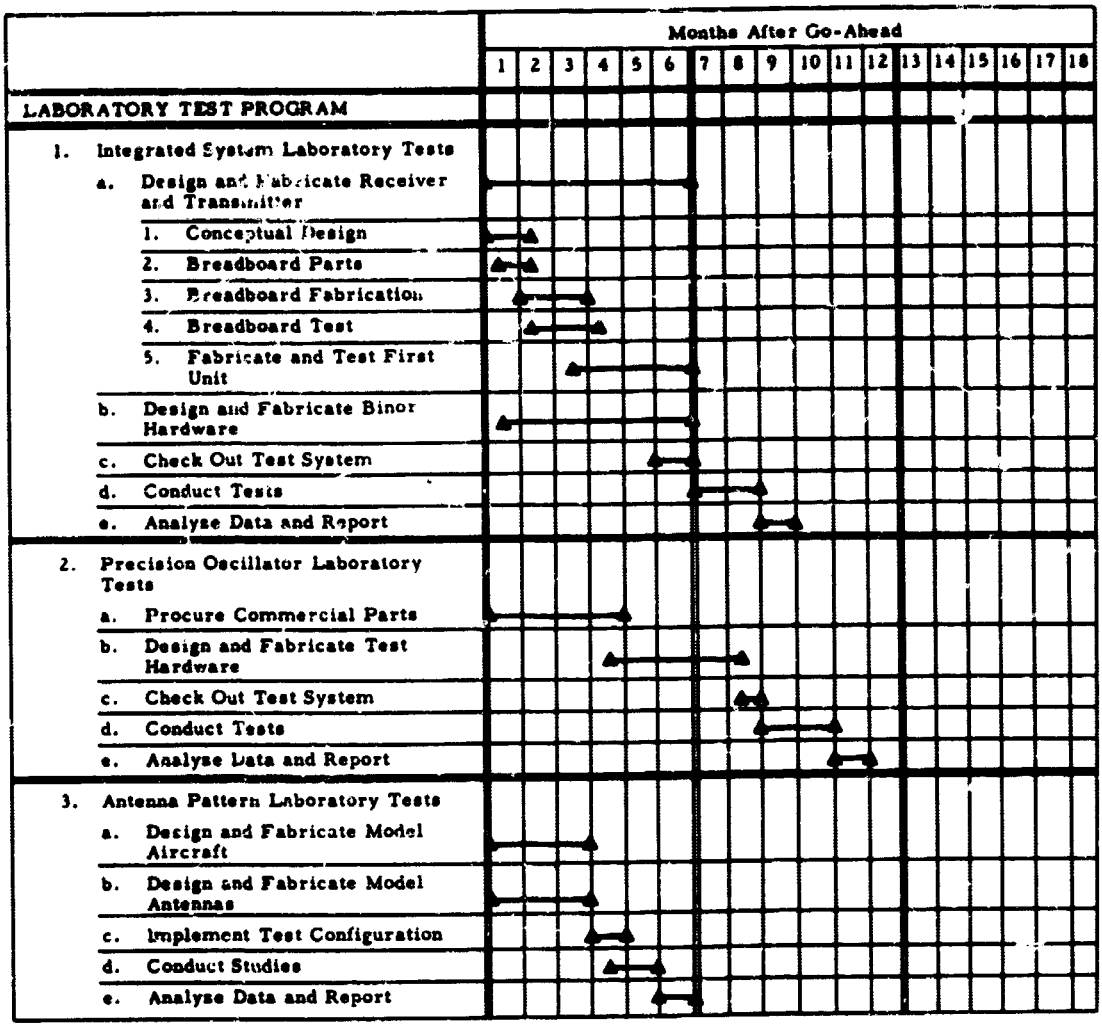

Figure 24. NAVSTAR Laboratory Test Program Schedule

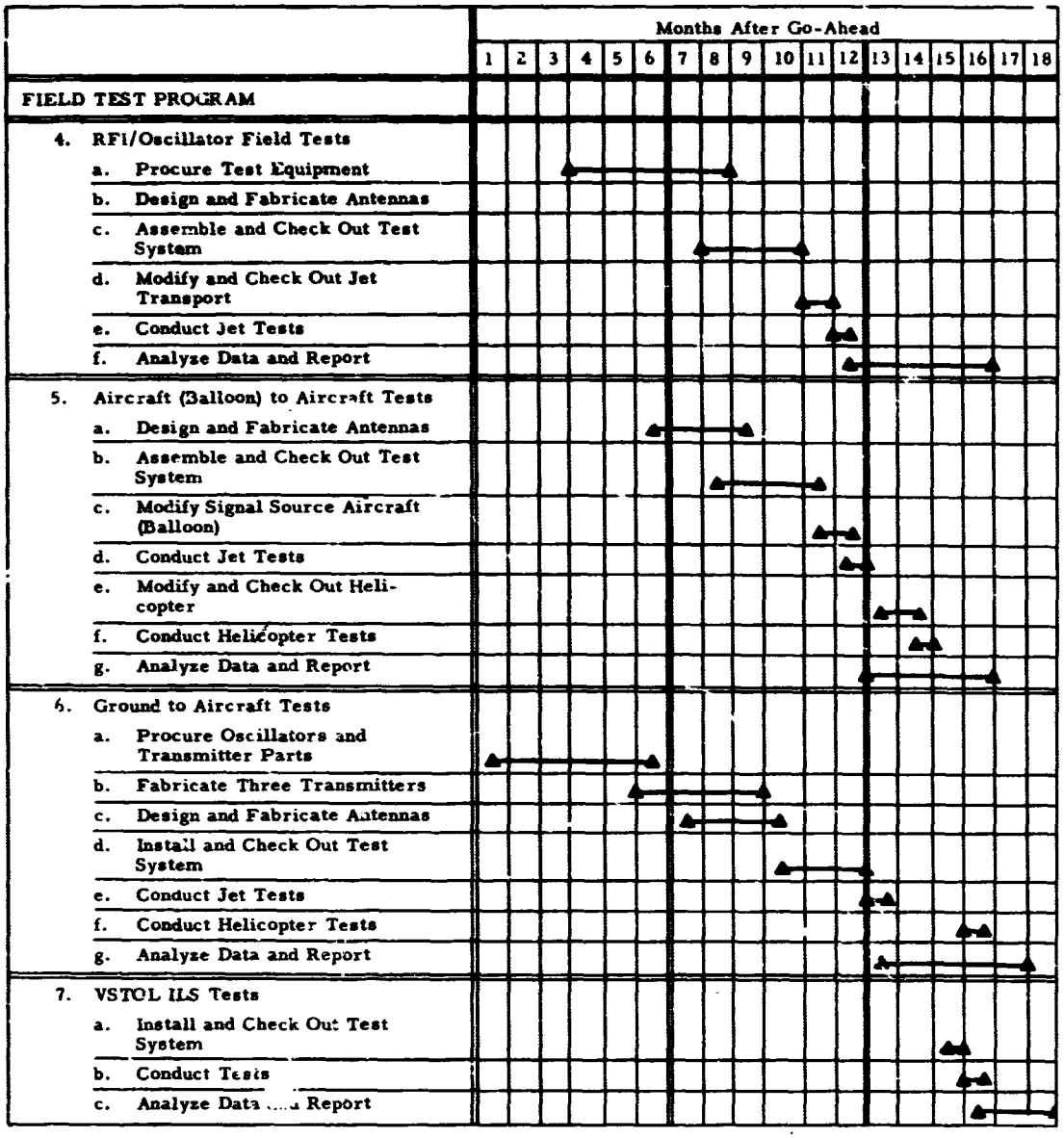

Figure 25. NAVSTAR Field Test Program Schedule

4.3 ASSUMPTIONS

The costs estimates in Tables 6 and 7 are based on the following assumptions:

1) The cost of an engineer for one year is 60,000 dollars (including clerical support, overhead, and contractor's fee).

2) The cost of a technician, fabricator, or draftsman for one year is 18,000 dollars (including clerical support, overhead, and contractor's fee).

3) The test program will be conducted over an 18 month period.

4) Only one BINOR code processor and receiver system is required for all tests. The same system will be used for the laboratory tests first, then for the jet transport user field tests, then for the helicopter user field tests.

5) A total of four oscillators, four BINOR code generators, and four transmitting systems are required. One set of equipment will be installed in the signal source aircraft or balloon while the remaining three systems will be used on the ground for the position location field tests.

6) The test program will conducted in the chronological order shown in Figure 25. Equipment associated costs (Tables 6 and 7) are included under the test phase for which the equipment is first required. Succeeding tests requiring the same equipment do not include those costs again.

7) A less expensive oscillator than the one indicated can be used for the integrated system laboratory tests. Table 6, however, reflects a precision oscillator since it will be required for subsequent laboratory and field tests.

8) Receiver and transmitter costs are based on the assumption that no hardware can be "borrowed", but that there are some designs which can be modified to save design time.

9) The transmitter design will use commercial components for the stable oscillator and 4-watt power amplifier. The phase modulator and multiplier will be laboratory developed for the system.

10) The receiver will be completely laboratory developed.

11) Costs have been included to insure that the transmitter and receiver are flightworthy for airborne environments.

12) Test equipment costs are based on monthly leasing rates. For some general purpose test equipment, which may be used throughout the program, it may be cheaper to purchase rather than lease.

13) Receiver engineering tests will include: (a) time delay variation vs temperature and input signal, (b) dynamic range, (c) noise figure vs temperature, (d) phase lock loop performance in the presence of doppler and doppler rate, and (e) carrier acquisition times.

14) No major subcontracts are required.

15) Capital equipment and instrumentation costs include material handling.

16) Fabrication costs include model shop labor as well as part costs.

17) Product Assurance participation is limited to workmanship inspection in the model shop.

18) Formal documentation of fabricated equipment is not included in the estimates.

19) Fabricated equipment will not be accepted and delivered. It will, of course, be structurally compatible with the aircraft environment and its appearance will be consistent with purchased equipment.

20) The airborne computer will process real-time data and output a printed record of computed position at a rate consistent with computer capability.

21) The airborne computer will be used to process postflight and other test data.

22) The BINOR equipment to be fabricated will be similar in concept to that already available at TRW. No increase in operating speed or performance capability is covered.

23) Basic power sources available to all test locations (i.e., 110 volt, 60 Hz, with a power capacity of at least 2 KVA).

24) The scale model aircraft and range for the antenna laboratory tests assumes a one-seventh scale model of the Boeing 707 type jet transport. The model can be constructed or leased, whichever is least expensive.

25) Four antennas are required on the jet transport user aircraft - one on the top, two on the sides, and one on the bottom. Design and installation is estimated under the RFI field tests. The increment for fabrication and installation of three additional antennas is estimated under the aircraft to aircraft tests.

26) Two antennas are required on the helicopter user aircraft - one over the rotor blades and one on the bottom of the aircraft.

27) The jet transport user aircraft (Jetstar class) will be required for approximately 12 weeks at an average estimated rental cost of 10,000 dollars per week.

28) The signal source aircraft (Lear Jet type) will be required for 6 weeks at an average cost of 6,000 per week.

29) The helicopter user aircraft will be required for 16 weeks at an average cost of 4,000 per week. The helicopter tests will be conducted after the jet tests to minimize costs.

30) All software for the airborne computer is estimated under the ground to aircraft position location tests. Some of this software, however, will be used for reduction of post-flight data from other field and, possibly, laboratory tests.

31) Specification development and design or qualification tests are not included because they are not considered necessary.

32) Design or qualification test costs are not included and are not considered necessary.

A possible test configuration which has not been estimated is that of using only the helicopter for the user aircraft field tests. This configuration is not recommended because the jet transport is believed to be the most representative of the user aircraft. If it is desired for other reasons, however, to conduct the field tests using only a helicopter for the user aircraft, the costs would be comparable to those of the jet aircraft only (Table 6).

REFERENCES

1. TRW Systems, "Study of a Navigation and Traffic Control Technique Employing Satellites," Volumes I through IV, Contract NAS 12-539, Report 8710-6012-R000, December 1967.

2. TRW Systems, "High Power L-Band Transmitter and Ultrastable Oscillator for the NAVSTAR Satellites," Contract NAS 12-539, Report 08710-6021-R000, October 1968

3. TRW Systems, "Applications Technology Satellite F L-Band Air Traffic Control Communications-Navigation Experiment," Contract NAS 12-539, Report 08710-6015-R000, June 1968.

APPENDIX A

NAVSTAR RANGING ERROR BUDGET

The error model for the satellite range (difference) measurements is given in Volume II of Reference 1. The model is updated here, particularly in regard to the oscillator and ionospheric errors, and put in more general form which can be used in predicting test results.

The sources of range measurement error are

- Tropospheric retardation
- Ionospheric refraction
- Receiver thermal noise
- Quantization
- Receiver drift and bias
- Satellite oscillator
- User oscillator
- Multipath

The errors are divided into two categories, systematic and random errors. Systematic errors have important correlation properties between range measurements, while random errors are uncorrelated between range measurements. Each of the error sources is uncorrelated with the others.

Troposphere

The tropospheric range error (Ref. 2) is frequency independent and can be estimated rather accurately for elevation angles E above 10 degrees by

$$\Delta R = 8.8 \csc E \text{ (ft)}$$

The correction to this error is subtractive, i.e., the correction equation is

$$R_{true} = R_{meas.} - 8.8 \csc E$$

The residual from such a correction may be characterized by a standard deviation of about 10 percent or

$$\sigma_R = 0.88 \csc E \text{ (ft)}$$

Since the range residual error itself is small, on the order of a few feet, it is conservative (but not unduly so insofar as final error results are concerned) to ignore all correlations and consider the error as independent between successive measurements and between measurements over different paths, i.e., as a random error.

At an elevation angle of 10 degrees, the tropospheric error will be

$$\sigma_R = 50.5 \text{ ft uncorrected}$$

$$= 5.05 \text{ ft corrected}$$

Since the correction is simple must users will probably apply it in their position computations.

Ionosphere

In estimating the ionospheric error and the error in correcting it, the approach of Freeman (Refs. 3 and 4) is used. The "ionospheric predictions" of Reference 5 provide graphs of the parameters f_i (the F2 layer maximum vertical incidence critical frequency) and MUF (4000) (the F2 layer 4000 km maximum usable frequency), as functions of latitude, longitude, local time, and for the applicable month. From these the total ionospheric columnar electron content is estimated by the semi-empirical relationship

$$N_T = 0.157 \times 10^{17} f_i^2 \; e^{-0.5596M} \text{ (electrons/m}^2\text{)}$$

where

$$M = \frac{\text{MUF (4000)}}{1.1 f_i}$$

The range error estimate is given by (Ref. 6)

$$\Delta R = \frac{K}{f^2} Q(E) N_T$$

where $K = 1.3 \times 10^{-16}, \frac{\text{ft (gHz)}^2}{\text{e/m}^2}$

f = carrier frequency, gHz

N_T = estimated columnar electron constant, e/m^2

E = elevation angle, deg

$Q(E) = \csc \sqrt{E^2 + (18^\circ)^2}$ (Ref. 4)

The ionosphere is subject to much larger variations than the troposphere. Some preliminary estimates of the electron content are (Ref. 7)

$$N_T \begin{cases} \text{(90 percentile)} = 6\ 5 \times 10^{17}\ \text{e/m}^2 \\ \text{(median)} = 2.5 \times 10^{17}\ \text{e/m}^2 \\ \text{(10 percentile)} = 1 \times 10^{17}\ \text{e/m}^2 \end{cases}$$

The corresponding range errors for $f = 1.6$ gHz are

$$\Delta R = 33 \csc \sqrt{E^2 + (18^\circ)^2}\ \text{ft (90 percentile)}$$

$$= 12.7 \csc \sqrt{E^2 + (18^\circ)^2}\ \text{ft (median)}$$

$$= 5.1 \csc \sqrt{E^2 + (18^\circ)^2}\ \text{ft (10 percentile)}$$

Assuming a correction to the ionosphere error using the above equations, the rms residual error based on extensive comparisons with actual total electron content measurements is 25 percent of the correction, or

$$\sigma_R = \frac{1}{4} \Delta R$$

Temporal and spatial correlations of the ionospheric correction residual are analyzed in Reference 8. For the purpose of range difference measurements the covariance structure is modelled as (Ref. 6)

$$\overline{\sigma_{R_1}\sigma_{R_2}} = \sigma_{R_1}\sigma_{R_2}\rho_\tau(\tau)\rho_D(D)$$

where σ_{R_1}, σ_{R_2} are two successive correction residuals

τ = time difference between measurements 1 and 2

D = absolute position difference (range) between the points at which range and range "pierce" the ionosphere taken as a thin shell at 350 km height

The correlation functions $\rho_\tau(\tau)$ and $\rho_D(D)$ are given graphically in References 6 and 8 or may be represented by any of several approximations:

$$\rho_D(D) = \begin{cases} e^{-D/2500} \\ \\ 1 - D/4625 \end{cases} \quad (D \text{ in km})$$

$$\rho_\tau(\tau) = \begin{cases} 0.45\, e^{-\tau/2.5} + 0.55\, e^{-\tau/28} \\ \\ \rho^{-\tau/7.2} \end{cases} \quad (\tau \text{ in hours})$$

Receiver Thermal Noise

Receiver thermal noise causes two types of errors in the range measurement which are a function of the received signal-to-noise ratio. First, the code clock loop possesses a phase tracking error caused by noise on the clock signal, called phase jitter. Phase jitter is specified as the amount of rms phase error in radians present in the phase lock loop. Assuming a good SNR in the carrier loop (10 db or better), the rms range error caused by the phase jitter is

$$\sigma_R = \frac{1}{\sqrt{2\,(SNR)}}\left(\frac{c}{2\pi f_c}\right)$$

where SNR = clock loop signal-to-noise ratio

f_c = clock frequency, Hz

c = velocity of light, ft/sec

For a clock loop SNR of 21 db and a clock frequency of 320 kHz, the rms range error from this source is 31 feet. The error is random for each measurement and can be reduced by averaging several measurement samples.

Second, thermal noise can cause errors in the subfrequency correlations of the BINOR code components causing false code phase acquisition and consequently an error in the range measurement. However, a wrong correlation decision or error on one or more of the subfrequency components causes a large error in the range measurement which is detectable by comparing the values of adjacent range measurements for unusual changes. These range readings can be deleted from the position determination calculations. Therefore, the only effect of the second thermal noise error source is the loss of some of the range measurements. Since the probability of a false range acquisition will be designed for a low value (0.001 or less) this source of error is not significant and does not enter into the overall error budget.

Quantization

The quantization error in the range measurement is a function of the user oscillator frequency that is the basis for the range measurement count. The rms error due to quantization is random and expressed as

$$\sigma_R = \frac{c}{\sqrt{12}\, f_o}$$

where c = velocity of light, ft/sec

f_o = count frequency, Hz

For a 10 MHz count frequency, the quantization error is 29 feet However, this error can be reduced by averaging several measurement samples.

Receiver Drift and Bias

The long-term receiver drift and biases affect the accuracy of each range measurement but tend to cancel for range difference measurements and as such are not important. However, receiver biases which change from measurement to measurement because of variations in the received signal levels and carrier doppler shifts from each satellite will be a

source of error. The magnitude of this error is difficult to predict since it depends on the receiver design. The error will be small compared to most of the major error sources if proper care is taken in receiver design.

One of the goals of a laboratory test program will be to measure the magnitude of this error source for expected variations in signal level and doppler shift at the receiver input.

Satellite Oscillator

The statistics for the oscillator error model are derived in Reference 9. The error is represented as a range error in feet or a numerically equivalent time error in nanoseconds:

$$\Delta R(t) = C_o + C_1 t + C_2 t^2 + \epsilon(\tau)$$

where the polynomial terms have the following physical significance:

$C_o = c\phi_o$ where ϕ_o = initial oscillator phase error

$C_1 = c\frac{\Delta f}{f_o}$ where $\frac{\Delta f}{f_o}$ = frequency accuracy of oscillator

$C_2 = c\frac{\dot{\Delta f}}{f_o}$ where $\frac{\dot{\Delta f}}{f_o}$ = aging rate of oscillator

where c is the velocity of light. $\epsilon(\tau)$ is the residual in oscillator time prediction ahead to $+\tau$ from such a quadratic polynomial based on observations of the oscillator at -2τ, τ, and 0 times. The polynomial terms will generally be recovered in the regression so are described in terms of a priori statistics. For example, for an oscillator with a frequency accuracy of one part in 10^{10} and an aging rate of 1 part in 10^{11} per day,

	Mean	Standard Deviation
C_o (ft)	0	∞
C_1 (ft/sec)	0	0.1
C_2 (ft/sec^2)	0	10^{-7}

The residual error ϵ is known to be quite accurately represented as $1/f^3$ or "flicker frequency modulation" noise. It may be described statistically in terms of the short time variate difference function

$$\sigma_{\Delta R}(\tau) = \sqrt{\langle [\epsilon(t) - \epsilon(t - \tau)]^2 \rangle}$$
$$= K_3 \tau$$

where typically for a good oscillator

$$K_3 \approx 4.8 \text{ ft/hr}$$

The constant K_3 does not appear to deteriorate nearly as rapidly as the usual "quality number" of an oscillator. That is, a garden variety "10^{-6}" oscillator may be nearly as good in this respect as a high precision, "10^{-10}" oscillator.

The oscillator residual error will be correlated over all ranges and over a period τ, since every τ hours users are furnished a new estimate of the oscillator drift.

User Oscillator

The range error in feet due to the user oscillator is also characterized by

$$\Delta R(t) = C_o + C_1 t + C_2 t^2 + \epsilon(\tau)$$

The residual ϵ is a slowly varying term which for the short durations involved in the range difference measurements by users can be lumped into the C_o term. In processing the range difference measurements, it can be shown that the C_o and C_1 terms cancel and the C_2 term has a negligible effect on the range difference error.

A user makes a series of pseudo-range measurements from his position to each satellite

$R_1 (t_1)$

$R_2 (t_2)$

.
.
.

$R_1 (t_1 + T)$

where

t_1 = time at which user measures range from first satellite

t_2 = time at which user measures range from second satellite

T = time between transmissions from the same satellite, i.e., the frame time for all satellite transmissions

Under the assumption of a constant velocity between users and the satellite during the range measurement intervals, $R_1 (t_1)$ can be extrapolated to time t_2 as follows:

$$\bar{R}_1 (t_2) = R_1 (t_1) + \frac{t_2 - t_1}{T} \left[R_1 (T + t_1) - R_1 (t_1) \right]$$

The range difference from the two satellites at time t_2 can now be formed. (The dot over the Δ is used to distinguish the range difference symbol from the error symbol used previously)

$$\dot{\Delta} R_{12} (t_2) = \bar{R}_1 (t_2) - R_2 (t_2)$$

The error in the range difference measurement due to the user oscillator can now be determined

$$\begin{aligned} \Delta \left[\dot{\Delta} R_{12} (t_2) \right] &= \Delta \bar{R}_1 (t_2) - \Delta R_2 (t_2) \\ &= C_o + C_1 (t_1 - t_o) + C_2 (t_1 - t_o)^2 + \frac{t_2 - t_1}{T} \Big[C_o + \\ &\quad C_1 (T + t_1 - t_o) + C_2 (T + t_1 - t_o)^2 - C_o - C_1 (t_1 - t_o) - \\ &\quad C_2 (t_1 - t_o)^2 \Big] - C_o - C_1 (t_2 - t_o) - C_2 (t_2 - t_o)^2 \end{aligned}$$

where t_o is the time at which the oscillator was set to zero frequency error. Simplifying the expression shows that the C_o and the C_1 terms cancel and the error reduces to

$$\Delta\left[\dot{\Delta}R_{12}\,(t_2)\right] = C_2\left[T\,(t_2 - t_1) - (t_2 - t_1)^2\right]$$

For the BINOR code transmissions, T equals 12 seconds while $t_2 - t_1$ is approximately (neglecting transient time differences between different satellites which is small) equal to the time between two satellite transmissions or about 1.5 seconds.

For a user oscillator with an aging rate of one part in 10^9 per 12 seconds, C_2 is 1/12 ft/sec^2. The range difference error then is about 1.25 feet, which is negligible compared to other error sources.

Multipath

The error due to multipath will depend on the range signal modulation characteristics (for the BINOR code, the clock frequency) and the statistics of the multipath signal at the receiver. The multipath error is expected to be no worse than 45 ft-rms at a 10-degree elevation angle for the received signal. This number is based on a 320 kHz clock frequency for the BINOR code and expected ratios of the direct-to-indirect (or multipath) received signal with the proposed user antenna. The multipath error is subject to change depending on both the receiver and antenna designs and subsequent results of testing of these items. The multipath error should be uncorrelated for all range measurements and, as such, can be considered random.

REFERENCES

1. "Study of a Navigation and Traffic Control Technique Employing Satellites," Volumes I through IV, prepared under Contract NAS 12-539, for NASA/ERC, TRW Report No. 08710-6012-R000, December 1967.

2. Martin and Carroll, "Tropospheric Refraction Corrections and Their Residual Errors," Technical Document Report MTC-TDR-64-3, AFMTC, 15 February 1964.

3. J. J. Freeman, "Final Report on Ionospheric Correction to Tracking Parameters," Contract NAS 5-9782, 3 November 1965.

4. A. J. Mallinckrodt, "Ionospheric Error Modelling," TRW Memorandum 8800.3.5-8, 27 June 1968.

5. "Ionospheric Predictions," U.S. Department of Commerce, E.S.S.A. Monthly.

6. A. J. Mallinckrodt, "Ionospheric Error Correlation Model," TRW Memorandum 8800.3.5-7, 11 June 1967.

7. A. J. Mallinckrodt, "Distribution Function of Ionospheric Errors," TRW Memorandum 7222.2-419, 23 February 1968.

8. C. C. Chen, "Ionospheric Effect on Range Difference Error," TRW Memorandum 7244-105, 9 November 1967.

9. "High Power L-Band Transmitter and Ultrastable Oscillator for the NAVSTAR Satellites," Appendix C, prepared under Contract NAS 12-539 for NASA/ERC, TRW Report No. 08710-6021-R0-00, September 1968.

APPENDIX B

USE OF EXISTING SATELLITES FOR TEST PROGRAM

This appendix examines the possibilities of employing one or more satellites presently operating in orbit to achieve some of the NAVSTAR test objectives, in view of the possible economic benefits. The types of tests of interest are those which can demonstrate the accuracy of the BINOR range measurement in a realistic NAVSTAR user and/or NAVSTAR ground station environment, and which will provide data on the relative magnitudes and correlations of terms in the error model, including effects of the user aircraft environment.

For these types of tests, it appears desirable to have a satellite whose signal approximates that of NAVSTAR in frequency, signal level at the earth's surface, bandwidth, and if possible, modulation format. Since ionospheric effects vary as the inverse of the frequency squared, signals far removed from L-band will not provide realistic simulation of NAVSTAR. Satellites which do not provide sufficient radiated power to duplicate the expected ground received signal level of NAVSTAR cannot be used in tests involving the low-gain NAVSTAR user antennas. Since ranging bandwidth and modulation format are correlated with multipath effects, satellites which cannot simulate these characteristics of NAVSTAR will be of limited value.

Satellites which might be employed are listed in Table B-1. The data used in compiling this table was taken from past issues of the TRW Space Log, the files of H. T. Seaborn, editor of the TRW Space Log, and past issues of Aviation Week and Space Technology. The information is current as of publication of the winter 1967-68 Space Log; it is not known if any of the listed satellites have become inoperative since that time.

Table B-1 shows that there are no satellites operating in the 1500-1600 MHz region. The satellites with links operating near this frequency are OGO's 4 and 5, Syncoms II and III, and OGO-6 and TTS-2, which will be orbited later this year. (TTS-1 decayed from orbit about June 1, 1968 and hence is not shown in Table B-1.) OGO-6, the Syncoms and TTS-2

Table B-1. Satellites with Potential Application to the Navstar Test Program

Satellite	Responsible Agency	Purpose	Orbit Parameters	Uplink Frequency (MHz)	Downlink Frequency (MHz)	Other Pertinent Characteristics
Intelsat 1 (Early Bird)	Comsat	Commercial communication	Synchronous	6000	4000	10 W ERP, 25 MHz BW
Intelsat 2A (Lani Bird)	Comsat	Commercial communication	Synchronous	6000	4000	36 W ERP, 130 MHz BW
Intelsat 2B (Pacific 1)	Comsat	Commercial communication	Synchronous	6000	4000	36 W ERP, 130 MHz BW
Intelsat 2C (Atlantic 2)	Comsat	Commercial communication	Synchronous	6000	4000	36 W ERP, 130 MHz BW
Intelsat 2D (Pacific 2)	Comsat	Commercial communication	Synchronous	6000	4000	36 W ERP, 130 MHz BW
IDCSP 1-18	DOD/DCA	Military communication	Synchronous	8000	7275	10 W ERP, low channel capacity
Syncom II	DOD	Military communication	Synchronous	7360	1820	8 W ERP, 5 MHz BW
Syncom III	DOD	Military communication	Synchronous	7360	1820	8 W ERP, 10 MHz BW
DODGE	Navy	Gravity gradient experiment	Synchronous		240 136	No command link
DATS-1	Air Force	Despun antenna experiment	Synchronous	8000	7275	Very low ERP
LES-1	Air Force	Experimental Comsat	1700 n mi circular	8300	7700	0.2 W ERP
LES-2	Air Force	Experimental Comsat	1700 n mi perigee 9400 n mi apogee	8300	7700	0.2 W ERP
LES-3	Air Force	UHF communications experiment	100 n mi perigee 20,000 n mi apogee		300	30 W ERP
LES-4	Air Force	Multipath experiments	100 n mi perigee 21,000 n mi apogee	8300	7700	2 W ERP
LES-5	Air Force	Tactical UHF communication experiments	Synchronous	400	225	Not available
ATS-1	NASA	Communication and weather experiments	Synchronous	149 6000	135 4000	13 db antenna gain
ATS-2	NASA	Gravity gradient experiment	100 n mi perigee 7000 n mi apogee	6000	4000	14 [illegible] antenna gain, 25 kHz BW
ATS-3	NASA	Earth photography	Synchronous	6000	4000	1000 W ERP *** BW= 3 MHz
Echo-2	NASA	Passive Comsat	642 n mi perigee 816 n mi apogee			Satellite in partially collapsed state
ARIEL-3	United Kingdom	Space environment experiments	350 n mi circular	136	137	0.25 W transmitter power
SECOR-9	Army	Geodetic survey	2400 n mi circular	224.5	449	Not available
OSCAR-4	Air Force	Amateur radio Comsat	100 n mi perigee 21,000 n mi apogee	155	432	10 W ERP, 10 kHz BW
OGO-4	NASA	Geophysical experiments	Polar orbit 250 n mi perigee 500 n mi apogee	1800	2253	0.3 W ERP, 200 kHz BW
OGO-5	NASA	Geophysical experiments	250 n mi perigee 90,000 n mi apogee	1800	2253	0.3 W ERP, 200 kHz BW
ATS-4*	NASA	Technology experiments	Synchronous***	149 6000	135 6000	Unknown, presumed similar to ATS-3
ATS-5*	NASA	Technology experiments	Synchronous***	6000	6000	Unknown, presumed similar to ATS-3
TTS-2*	NASA	Checkout of USBS network	225 n mi perigee*** 400 n mi apogee	2070	2250	0.5 W ERP, 500 kHz BW
OGO-6*	NASA	Geophysical experiments	250 n mi Circular Polar***	2270	1705	0.5 W ERP, 3 MHz BW

*To be launched prior to 1970 **Estimate ***Planned

can transpond a baseband of several megacycles. All remaining satellites, with the exception of Echo-2, are at frequencies unsuitable for simulation of the NAVSTAR signal. Echo-2 is in a semi-collapsed state, not providing the amount of reflective surface it was designed for, and an unreasonably large ground transmitter and antenna would be required to bounce a strong enough signal off of it so that the result level of the reflected signal at the earth's surface would be of use in the contemplated tests.

Syncom II and III each provide an effective radiated power of about 8 watts, and with the space loss from synchronous orbit at 1820 MHz, the level of the syncom signal at the earth's surface is in the vicinity of -150 dbm. The Syncoms therefore cannot be used in tests where it is desired to employ the NAVSTAR user antenna (0-db gain) in a realistic environment such as an aircraft. Additionally, both Syncoms are presently under the operational control of DOD, and their availability for experimental purposes is questionable.

TTS-2, the second satellite to be used for checkout of the Apollo USBS network, will be similar to TTS-1, with a rated transmitter output power of 0.5 watt and an antenna gain of about -1 db. The TTS-2 orbit is planned as 250 x 400 n mi at this time, and assuming a 3-db polarization loss from the linearly-polarized TTS antenna to the circularly-polarized NAVSTAR user antenna, the available signal level at a range of 250 n mi from TTS-2 will be -128 dbm, slightly less than the desired value. Since it would be required to locate the NAVSTAR equipment directly under the perigee point of the TTS orbit to obtain just a few seconds of marginal data, the use of TTS-2 in a NAVSTAR experiment appears unattractive.

A similar situation exists with OGO's 4 and 5. With these satellites the closest approach to earth is about 250 n mi, the effective radiated power is about 0.3 watt, and the downlink frequency is 2253 MHz, resulting in an available signal level of -130 dbm at the point on the earth directly under perigee. There is an additional problem with the use of OGO 4 or 5 for a NAVSTAR experiment; the instrumentation system which supports OGO's 4 and 5 is the Goddard Range and Range Rate system, a quasi-coherent CW system employing side tones to obtain unambiguous

range. The bandwidth of this ranging modulation may be varied depending on the transponder employed, and for OGO's 4 and 5, the transponders have 200 kHz bandwidths, too small to accommodate the BINOR code.

OGO-6 is more attractive; the transponder bandwidth is 3 MHz, the effective radiated power is 0.5 watt, and the downlink frequency (1705 MHz) is the closest to the NAVSTAR frequency of any existing or proposed satellite. In its planned circular orbit, OGO-6 will provide -130 dbm of signal level to a station at a range of 350 n mi, about 3 db below the signal level anticipated for NAVSTAR and probably the lowest value which can be considered for test purposes. In a 250-mile circular orbit, a satellite will be within 350 miles of a ground station (or an aircraft) which lies on the satellite ground trace for only about 100 seconds. If the receiving terminal is displaced 240 miles to either side of the ground trace, the satellite will never be within 350 n mi range and the available signal level will never be greater than -130 dbm. There are presently four stations, located in Australia, Madagascar, Alaska, and North Carolina. Since it will be desirable to make extensive tests with aircraft simulating NAVSTAR users against this satellite, the first three locations can probably be ruled out by logistics and weather considerations. Thus, NAVSTAR tests with OGO-6 would probably be constrained to the Roseman, North Carolina area, with a maximum of 100 seconds of data per pass available if the satellite passes directly overhead.

Although a test program could be defined under these constraints, the combination of short data spans, long periods between passes, and marginal signal levels (which prohibit flexibility in testing) are thought to outweigh the advantages which might be accrued by such a program. However, it is felt that USBS PRN range code data taken with the TTS-2 could be of some value to the NAVSTAR program. The PRN data might be extrapolated to predict BINOR ranging results. The PRN data will contain virtually no multipath errors, no oscillator errors, and, with the high S/N available with the large antennas, small receiver noise errors. The primary errors in the PRN measurements will be ionospheric, tropospheric, quantization and receiver drift, and if the last two sources can be calibrated and the first two measured together, scaled to L-band and

compensated to reflect a BINOR rather than PRN measurement, it is felt that such data might be useful in predicting BINOR ranging accuracy and understanding the range error model at L-band.

In addition, existing synchronous or near-synchronous satellites such as the IDCSP's and the two Syncoms may be used with directional ground antennas and large aircraft (such as the Apollo ARIA aircraft) to demonstrate position location or navigation using range difference measurements from a network of tracked satellites. An example of such a demonstration test is described in Section 3.4.

APPENDIX C

PROCEDURE TO DETERMINE VALUES OF TEST PARAMETERS

Noise Bandwidth

The noise bandwidth of a device is defined as the width of an ideal rectangular bandpass characteristic having the same area and peak value as the power gain versus frequency characteristic of the device. Analytically, the noise bandwidth B may be expressed as:

$$B = \frac{1}{2\pi} \int_0^\infty \frac{W(\omega)}{W_m} \, d\omega$$

where $W(\omega)$ is the power gain as a function of frequency, W_m is the maximum power gain, and ω is the angular frequency.

The device to be measured must terminate in the proper load and the signal generator at the input must have the proper output impedance. If the device is active, the output level of the signal generator must be adjusted to insure linear (unsaturated) operation.

The signal generator frequency is adjusted to obtain a maximum reading on a voltmeter at the output of the device. This reading is the zero-db reference for subsequent voltmeter readings. The device bandpass characteristics above and below the reference frequency are then measured by recording readings of the signal generator frequency which produce -1 db, -3 db, -6 db, -9 db, and -12 db readings on the voltmeter. Next, the voltmeter readings are normalized (normalized power in watts) by utilizing the following conversion table:

0 db (reference)	= 1.0
- 1 db	= 0.795
- 3 db	= 0.5
- 6 db	= 0.250
- 9 db	= 0.125
-12 db	= 0.0625

Finally, the bandpass characteristic of the device (frequency as a function of normalized output power in watts) is plotted on linear graph paper. By subtracting the lower half-power frequency reading from the upper half-power frequency reading, the 3 db bandwidth is determined. By graphical integration of the area under the plot, the noise bandwidth is determined.

Tracking Loop Noise Bandwidth

The two-sided noise bandwidth of a second order phase lock loop is:

$$2\,B_L = \frac{4\xi^2 + 1}{4\xi}\,\omega_n$$

where

ξ = loop damping factor

ω_n = loop natural frequency in radians/sec

Both ω_n and ξ are dependent on the loop gain which in turn varies with the signal level at the loop phase detector input. If a limiter precedes the phase detector, the loop noise bandwidth changes with input signal-to-noise ratio as follows:

$$2\,B_L = 2\,B_{LO}\left(\frac{4\xi_o^2\,\frac{\alpha}{\alpha_o} + 1}{4\xi_o^2 + 1}\right)$$

where

α = limiter suppression factor at any input SNR

α_o = limiter suppression factor at nominal given input SNR

ξ_o = damping ratio of loop at nominal given input SNR

$2\,B_{LO}$ = loop noise bandwidth at nominal given input SNR

The limiter suppression factor varies with input SNR as:

$$\frac{\alpha}{\alpha_o} = \left(\frac{\frac{4}{\pi} + (SNR)_o}{\frac{4}{\pi} + (SNR)_i} \right)^{\frac{1}{2}}$$

where

$(SNR)_o$ = nominal given input signal-to-noise ratio (usually loop threshold)

$(SNR)_i$ = input signal-to-noise ratio

Normally the loop damping ratio at threshold is designed for a value of $1/\sqrt{2}$. Therefore, the above equations simplify to:

$$2 B_{LO} = \frac{3}{2\sqrt{2}} \omega_{no}$$

$$2 B_L = \frac{2}{3} \left(\frac{\alpha}{\alpha_o} + \frac{1}{2} \right) (2 B_{LO}) = \frac{1}{\sqrt{2}} \left(\frac{\alpha}{\alpha_o} + \frac{1}{2} \right) \omega_{no}$$

By measuring ω_{no}, the loop noise bandwidth can be determined at any input signal-to-noise ratio. Figure C-1 shows the test setup to measure ω_{no}. The test actually measures the transfer function $|1 - H(s)|$, where H(s) is the closed loop transfer function. An FM signal generator is frequency modulated with an audio signal generator whose output frequency is adjustable. The frequency output from the FM signal generator is adjusted to the loop center frequency. The signal level is set to equal the value which will occur at the specified nominal input signal-to-noise ratio for the loop in order to measure ω_{no} and not some other value of ω_n. The audio signal generator frequency is varied (keeping the output amplitude constant) and the rms voltage at the output of the phase detector is measured.

The measured transfer function analytically is equal to

$$|1 - H(s)| = \frac{1}{\sqrt{1 + \left(\frac{\omega_{no}}{\omega}\right)^4 + 2(2\xi^2 - 1)\left(\frac{\omega_{no}}{\omega}\right)^2}}$$

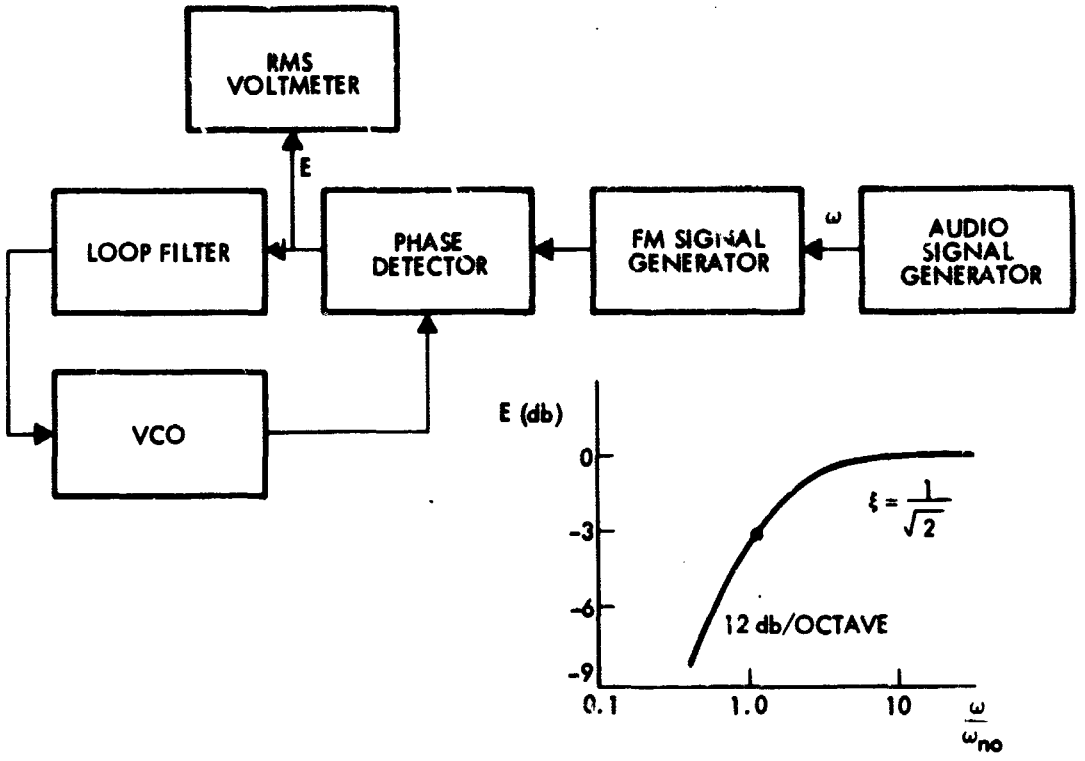

Figure C-1. Test Setup to Measure Loop Bandwidth

and is seen to have a high pass filter characteristic. For a loop damping ratio of $1/\sqrt{2}$, ω_{no} is equal to the audio generator frequency at which the rms voltage decreases 3 db relative to the high frequency out of band response. Figure C-1 shows a sketch of the response curve $|1 - H(s)|$ for a loop damping ratio of $1/\sqrt{2}$.

Predetection SNR (IF)

Figure C-2 shows the test setup to measure IF signal-to-noise ratio in a receiver. First the receiver input is terminated with a 50-ohm load by means of the switch. The noise power P_n in the IF is measured and recorded by the true or calorimetric power meter. The meter must have a frequency response equal to the IF bandwidth. Next the switch is turned to the precision attenuator output. The attenuator is then adjusted to obtain twice the power reading on the meter as previously. Therefore,

$$P_s + P_n = 2P_n \text{ , or}$$

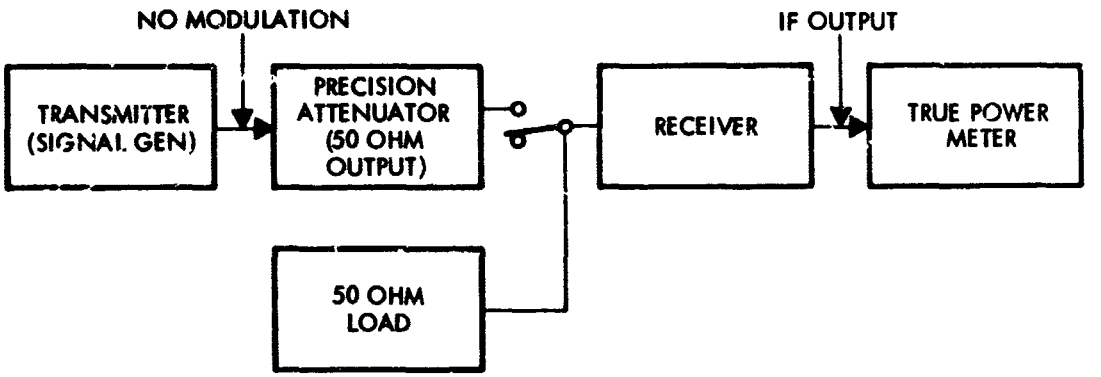

Figure C-2. Test Setup to Measure IF Signal-to-Noise Ratio

$$\frac{P_s}{P_n} = 1 \text{ (0 db signal-to-noise ratio)}$$

The attenuator setting thus obtained results in a 0 db signal-to-noise ratio in the receiver IF. Other SNR's are obtained by adjusting the attenuator setting from the 0 db reference setting. Care must be taken to insure that the signal from the attenuator output does not exceed the dynamic range of the receiver. If the signal level to obtain the 0 db reference exceeds the receiver dynamic range or the meter does not have an adequate frequency response for the IF bandwidth, a narrow calibrated noise bandwidth filter can be used in front of the meter. The 0 db reference signal-to-noise ratio is now equivalent to a lower IF signal-to-noise ratio by the following simple relationship:

$$(\text{IF SNR})_{db} = 0 \text{ db} - 10 \log \left(\frac{B_{IF}}{B_M} \right)$$

where

B_M = calibrated noise bandwidth of filter preceding meter

B_{IF} = IF noise bandwidth

Both noise bandwidths can be measured by the method described at the beginning of the appendix.

APPENDIX D

COMPUTER PROGRAM FOR ANTENNA MULTIPATH RECEPTION

This appendix describes a program to compute the expected direct/indirect (ground reflected) multipath ratio of a received satellite signal as a function of the following variables:

- Measured antenna response to vertical, horizontal, right-hand, and left-hand polarization in the direct and indirect directions
- Incident polarization
- Ground electrical parameters, conductivity and dielectric constant
- Ground physical parameter equivalent to wave height for diffuse reflection

The program divides into the following parts:

- Determination of the antenna basic polarization parameters from the basic pattern measurements
- Determination of ground reflection coefficient for a smooth ground, modification for the scatter loss to give the net specular component, and the resulting reflected signal strength and polarization of the indirect specular component
- Computation of the antenna response to the direct and indirect components

The basic relations involved in these computations are derived in the following sections. Program operating instructions are given.

Polarization Analysis

An arbitrarily polarized wave may be represented in terms of its horizontal and vertical components as

$$E = a\,\bar{1}_h + b\,\bar{1}_v$$

where a, b are complex coefficients, and $\bar{1}_h$, $\bar{1}_v$ are unit time varying vectors, e^{jwt}, in the horizontal and vertical directions. Here the overbar denotes a spatial vector. The power in this wave is the sum of the

powers in the two orthogonal components.

$$|E|^2 = |a|^2 + |b|^2$$

Unit right- and left-handed rotating circular vectors may be defined by

$$\overline{I}_r = \frac{1}{\sqrt{2}} \left(\overline{I}_h - j \overline{I}_v \right)$$

$$\overline{I}_\ell = \frac{1}{\sqrt{2}} \left(\overline{I}_h + j \overline{I}_v \right)$$

Now the response R of any antenna to any incident polarization can only be a linear form in the polarization components, i.e., for the incident wave $\overline{E}$,

$$R = |ah + bv| \qquad \text{(D-1)}$$

where h and v are complex constants specifying the antenna characteristic response to horizontal and vertical inputs in any given direction.

If we denote magnitudes of these quantities by the corresponding capitals:

$$A = |a|$$

$$B = |b|$$

$$H = |h|$$

$$V = |v|$$

and define the reference and relative phases by

$$a = A e^{j\epsilon}$$

$$b = B e^{j(\epsilon + \beta)}$$

$$h = H e^{j\delta}$$

$$v = V e^{j(\delta + \gamma)}$$

Then for the magnitude response, from (D-1),

$$R^2 = A^2 H^2 + B^2 V^2 - 2\,AHBV \cos(\gamma + \beta) \qquad (D\text{-}2)$$

Now if on the antenna pattern range we measure the response of this antenna to unit horizontal, vertical, and (for generality) k unit right- and left-handed circular polarizations, we have

$$M_h^2 = R^2 \,(A = 1,\ B = 0)$$
$$= H^2 \qquad (D\text{-}3)$$

$$M_v^2 = R^2 \,(A = 0,\ B = 1)$$
$$= V^2 \qquad (D\text{-}4)$$

$$M_r^2 = R^2 \left(A = B = \frac{k}{\sqrt{2}},\ \beta = 90^\circ\right)$$
$$= \frac{k^2}{2}\left[H^2 + V^2 + 2\,HV \sin\gamma\right] \qquad (D\text{-}5)$$

$$M_\ell^2 = R^2 \left(A = B = \frac{k}{\sqrt{2}},\ \beta = -90^\circ\right)$$
$$= \frac{k^2}{2}\left[H^2 + V^2 - 2\,HV \sin\gamma\right] \qquad (D\text{-}6)$$

From these four relations we may then solve for the fundamental antenna polarization parameters

$$H = M_h \qquad (D\text{-}7)$$

$$V = M_v \qquad (D\text{-}8)$$

$$\sin\gamma = \frac{M_r^2 - M_\ell^2}{2\,(M_r^2 + M_\ell^2)} \left(\frac{M_h}{M_v} + \frac{M_v}{M_h}\right) \qquad (D\text{-}9)$$

and incidentally

$$k^2 = \frac{M_r^2 + M_\ell^2}{M_h^2 + M_v^2} \qquad \text{(D-10)}$$

In order to more easily specify the incident wave we may define

$$\alpha \equiv \arctan \frac{A}{B}$$

so for a unit incident wave

$$A = \sin \alpha$$

$$B = \cos \alpha$$

so the unit incident wave is completely described (except for the, irrelevant, common phase) in terms of the parameters α and β.

The four principal polarizations are then representable as follows:

	α (deg)	β (deg)	
Vertical	0	45	←(actually arbitrary)
Horizontal	90	45	←(actually arbitrary)
Right-hand circular	45	90	
Left-hand circular	45	-90	

Reflection Analysis

For incident and reflected waves defined in the sense of Figure D-1 and for a specular reflector of conductivity σ and dielectric constant ϵ, the reflection coefficient for a wave incident at an elevation angle Ψ from the horizontal is given by the following relations. Let

$$x = \frac{\sigma}{2\pi f \epsilon_o}$$

$$N = \epsilon - i x$$

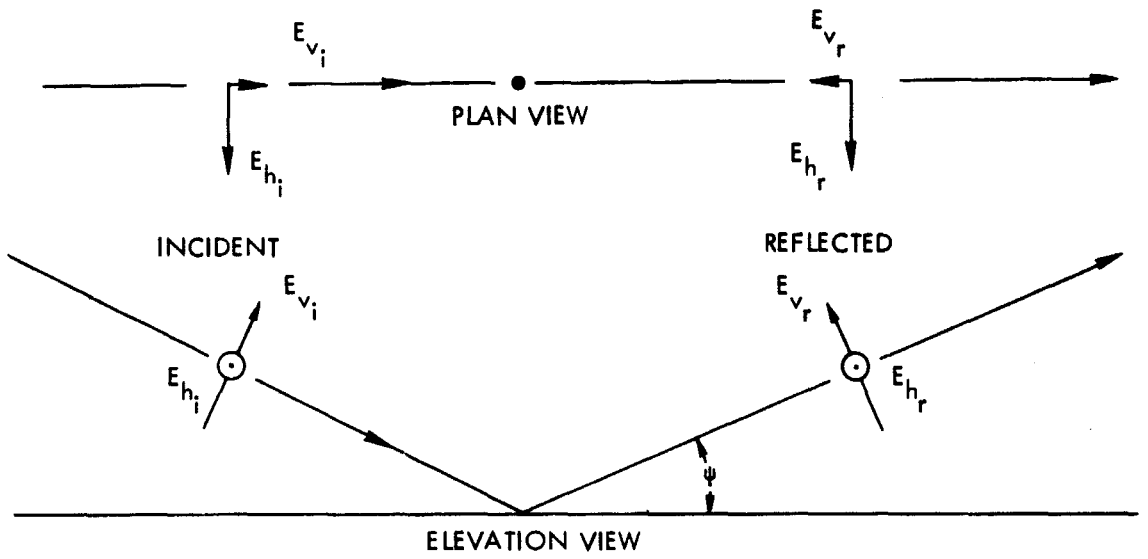

$$R_v = \frac{E_{v_r}}{E_{v_i}} \qquad R_h = \frac{E_{h_r}}{E_{h_i}}$$

NOTE THAT WITH THESE SIGN CONVENTIONS, IF THE COMPLEX VERTICAL AND HORIZONTAL REFLECTION COEFFICIENTS ARE EQUAL, THE SENSE OF ROTATION IS PRESERVED.

Figure D-1. Sign Conventions for Reflection Coefficient

where

ϵ = relative dielectric constant of the ground

ϵ_o = permittivity of free space

f = frequency, MHz

σ = conductivity, EMU

Then

$$x = 1.79731 \cdot 10^{-5} (\sigma/f)$$

Let

$$Q = \sqrt{N - \cos^2 \Psi} \quad \text{(complex)}$$

where

Ψ = elevation angle from horizon

Then the reflection coefficient for vertically or horizontally polarized waves are of the form (Reference 1)

$$R_v = \frac{N \sin\Psi - Q}{N \sin\Psi + Q} \tag{D-11}$$

$$R_h = \frac{\sin\Psi - Q}{\sin\Psi + Q} \tag{D-12}$$

Reduced to real numbers these relations can be expressed in the following steps. Let

$$p = \text{Re}(Q) = \left(\frac{\left[x^2 + (\epsilon - \cos^2\Psi)^2 \right]^{\frac{1}{2}} + (\epsilon - \cos^2\Psi)}{2} \right)^{\frac{1}{2}}$$

$$q = \text{Im}(Q) = -\frac{x}{2p}$$

Then if we define

U_1 = Re (numerator)

$$= \begin{cases} \epsilon \sin\Psi - p & \text{for vertical polarization} \\ \sin\Psi - p & \text{for horizontal polarization} \end{cases}$$

U_2 = Im (numerator)

$$= \begin{cases} -x \sin\Psi - q & \text{vertical} \\ -q & \text{horizontal} \end{cases}$$

U_3 = Re (denominator)

$$= \begin{cases} \epsilon \sin\Psi + p & \text{vertical} \\ \sin\Psi + p & \text{horizontal} \end{cases}$$

U_4 = Im (denominator)

$$= \begin{cases} -x \sin\Psi + q & \text{vertical} \\ -q & \text{horizontal} \end{cases}$$

Then in either case

$$|R| = \frac{U_1^2 + U_2^2}{U_3^2 + U_4^2} \qquad \text{(D-13)}$$

$$\phi = \measuredangle R = \arctan\left[\frac{U_2 U_3 - U_1 U_4}{U_1 U_3 + U_2 U_4}\right] \qquad \text{(D-14)}$$

where ϕ is defined in the principal range:

$$\begin{cases} -\pi < \phi < 0 \ . & \text{for vertical polarization} \\ -\pi > \phi > -2\pi & \text{for horizontal polarization} \end{cases}$$

Scattering Loss

When the reflecting surface is not perfectly smooth the effective reflection coefficient is reduced below that for a smooth surface by a scattering loss factor. The controlling parameter is the so-called Rayleigh parameter

$$p = \frac{h\Psi}{\lambda}$$

where

h = rms surface deviation from a smooth plane (within, say, the first Fresnel zone) or wave height (ft)

Ψ = elevation angle or angle of grazing incidence (radians)

λ = carrier wavelength (ft)

For $p \ll 1$ the surface may be considered smooth but otherwise there is a theoretical (References 2-4) loss factor (voltage basis)

$$F = \exp\left[-8\pi^2 p^2\right] \qquad \text{(D-15)}$$

This factor has been confirmed experimentally by Beard (Reference 4) for values of R up to about 0.1. The effect of the scattering loss is to multiply the effective smooth earth reflection coefficient by F so that

$$R' = R \cdot F \qquad \text{(D-16)}$$

Modification of Polarization Parameters by Reflection

If the incident wave is described by the parameters of Equation (D-2),

$$A,\ B,\ \beta$$

and the reflection properties, modified for scatter loss by Equations (D-13), (D-14), (D-16),

$$R_v',\ \phi_v,\ R_h',\ \phi_n$$

Then after reflection

$$A' = A \cdot R_h'$$

$$B' = B \cdot R_v'$$

$$\beta' = \beta + \phi_v - \phi_h$$

and the antenna response is determined by Equations (D-2), (D-7), (D-8), and (D-9).

Program Description

A computer program has been written which uses the Tymshare, Inc. basic language. In order to compute the direct/indirect multipath ratio, antenna pattern measurements must be available which consist of responses to vertical, horizontal, right-hand circular, and left-hand circular incident polarizations, at conjugate angles above and below the horizon. The program data entries must be made in the following manner. Two successive data entries contain first the four gain responses of the antenna at an elevation angle Ψ and an azimuth angle Θ. Next the four gain responses are entered for the same azimuth angle Θ and an elevation angle $-\Psi$. These two entries provide the data to compute the multipath ratio for a direct signal arriving at an elevation angle Ψ and an azimuth angle Θ.

The program interprets successive data as corresponding direct and indirect responses and automatically computes the ratio response. If Ψ is entered as a positive number the incident ray is treated as a direct ray and is unaffected by reflection. If Ψ is negative, the incident ray is treated as a reflected ray and is modified by the reflection coefficient for that elevation angle.

The parameters f, ϵ, σ, and h must be specified for a particular case. The total data entry is as follows:

Line	Data	
9	F7	{ 1 = full print 0 = no headers
10	f	frequency, MHz
	ϵ	relative dielectric constant
	σ	conductivity, EMU
	h	wave height, ft
20	α	arctan A/B, degrees
	β	degrees
30	V7	scale factors on the input
	H7	polarization data. Thus
	R7	$V_{voltage} = 10^{[V_{data} \cdot V_7 + G1]/20}$
	L7	V7, H7, R7, L7 are dimensionless
	G1	scale factors, G1 is in db
31	Θ	azimuth, degrees
	Ψ	elevation, degrees
	V	response to vertical incident } db, down scaled
	H	response to horizontal incident } db, down scaled
	R	response to right incident } db, down scaled
	L	response to left incident } db, down scaled
32	Same as 31	
.	Same as 31	
.	Same as 31	

Line	Data	
32	Same as 31	
98	Same as 31	
99	1, 1	End of data designation

REFERENCES

1. Kerr, "Propagation of Short Radio Waves," V-13, MIL Radiation Lab Series, McGraw-Hill, 1951.

2. H. Davies, "The Reflection of Electromagnetic Waves from a Rough Surface," Proc. IEE, Pt. 4, Monograph No. 90, pp. 1-6, January 1954.

3. W. S. Ament, "Toward a Theory of Reflection by a Rough Surface," Proc. IRE, Vol. 41, pp. 142-146, January 1953.

4. C. I. Beard, "Coherent and Incoherent Scattering of Microwaves from the Ocean," IRE Trans. Cent. and Prop., pp. 470-483, September 1961.

APPENDIX E

GEOMETRIC CONSIDERATIONS FOR MULTIPATH

In this appendix the geometry of multipath reception in an aircraft is considered for two cases. One case assumes a synchronous satellite as the signal source and the other assumes simulation of the satellite by an aircraft or balloon as a signal source. The geometry is shown in Figure E-1. In the synchronous satellite case $h_1 >> h_2$. With the simulated satellite this is not necessarily true. However, to provide realistic multipath measurements the simulated satellite should give similar values for the following parameters:

- The magnitude of the angles of arrival of the direct signal and the multipath signal at the receiver, θ and ϕ, respectively, to provide similar conditions for antenna reception.
- The difference in path length between the multipath ray and the direct ray, $R_1 + R_2 - R_D$, to keep the space loss difference and the phase difference between the two rays similar at various receiving altitudes.
- The time rate of change of path length difference to keep the multipath induced phase and amplitude rates on the received signal similar.
- The area of the first fresnel zone of the multipath ground reflection point. This parameter is of interest if the reflection area is smooth as defined by the Rayleigh criterion, i.e.,

$$h << \frac{\lambda}{\sin \phi}$$

where h = rms roughness of surface, and λ = wavelength (0.6 foot at L band). For example, at a reflection angle ϕ = 10 degrees, an ocean state of waves 1 to 2 feet high from peak to trough (assuming sinusoidal wave motion) satisfies the Rayleigh criterion for smoothness. Therefore the fresnel zone is significant in the multipath considerations for relatively calm ocean states.

Since multipath occurs primarily at low elevation angles, the above parameters are of interest only in the region $10^\circ \leq \theta \leq 20^\circ$. Aircraft signal reception below 10 degrees is generally not of interest in the Navstar system.

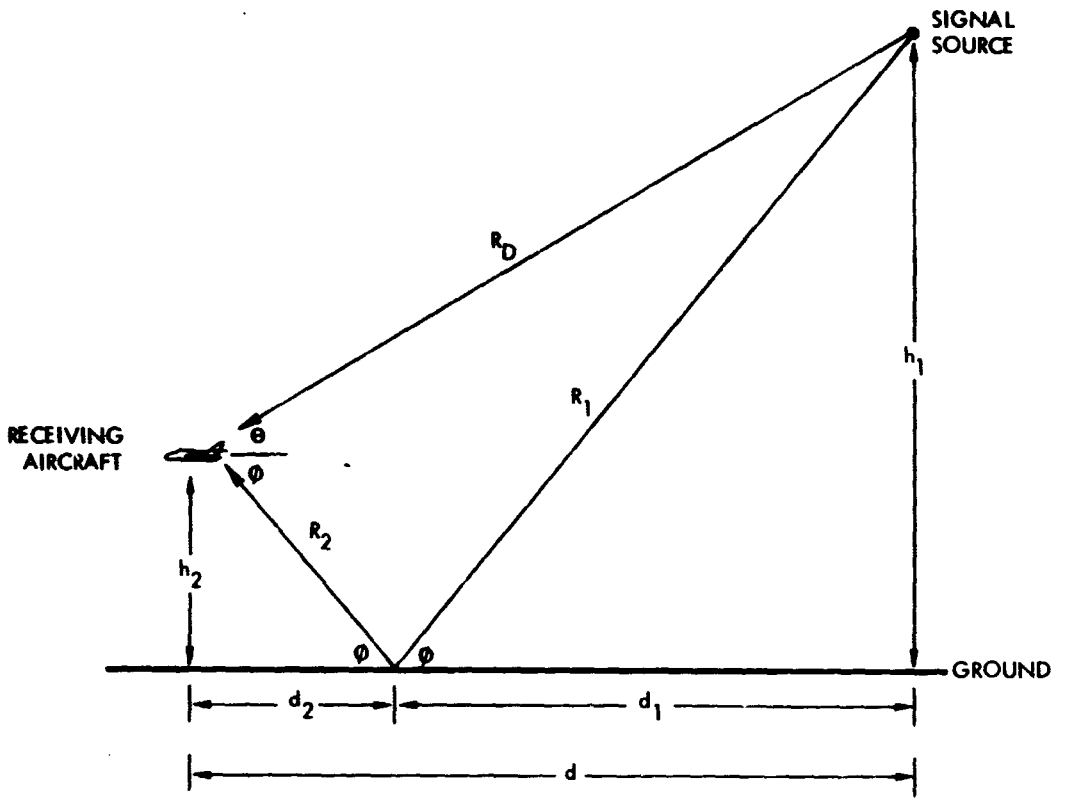

Figure E-1. Geometry for Multipath

The derivations of the geometric differences for multipath reception at an aircraft when a synchronous satellite signal source is simulated by another aircraft or a balloon indicate that good simulation of the multipath is possible if the following conditions are met. The signal source must be at least five times higher than the receiving aircraft; if the source is seven to ten times higher the angle of arrivals of the direct ray above the horizon and the multipath ray below the horizon become nearly equal. In addition, to maintain multipath amplitude and phase change rates which are not too much greater than for the synchronous satellite the relative ground velocity or equivalently the doppler between the receiving aircraft and the signal source must be very low (less than 50 ft/sec).

1. ANGLE OF ARRIVAL

The two angles of arrival can be derived as functions of the two heights h_1 and h_2 as follows. For the angle of arrival of the direct ray,

$$\tan \theta = \frac{h_1 - h_2}{d}$$

For the angle of arrival of the multipath ray,

$$\sin \phi = \frac{h_2}{R_2} = \frac{h_1}{R_1}$$

Consequently

$$R_1 + R_2 = \frac{h_1 + h_2}{\sin \phi}$$

Multiplying each side by cos ϕ,

$$(R_1 + R_2) \cos \phi = \frac{h_1 + h_2}{\tan \phi}$$

Since $d = (R_1 + R_2) \cos \phi$, then

$$\tan \phi = \frac{h_1 + h_2}{d}$$

Combining the equations for tan ϕ and tan θ, the relationship between the two angles becomes

$$\tan \theta = \left(\frac{h_1 - h_2}{h_1 + h_2}\right) \tan \phi$$

Defining k as the ratio h_1/h_2

$$\boxed{\tan \phi = \left(\frac{k + 1}{k - 1}\right) \tan \theta}$$

For the synchronous satellite $k >> 1$ and the two angles become equal. Figure E-2 plots ϕ for elevation angles of 10 and 20 degrees as a function of k. The plots show that the two angles differ by 5 degrees at θ = 10 degrees and 8.5 degrees at θ = 20 degrees for k = 5. For

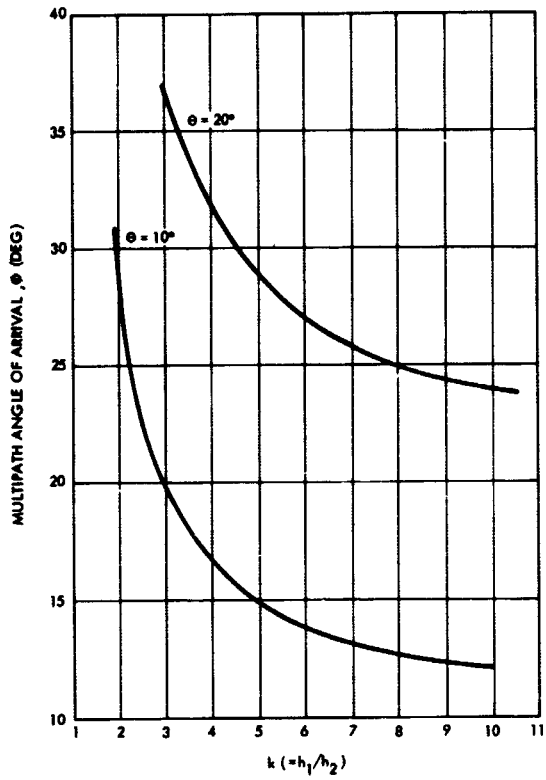

Figure E-2. Angle of Arrival of Multipath Ray

smaller k the difference increases rapidly. Therefore it can be concluded that the signal source should be at a minimum five times higher than the receiving aircraft to keep the two angles approximately equal, since for the synchronous satellite they are actually equal. Values of k from 7 to 10 are preferred.

2. PATH LENGTH DIFFERENCE

The path length difference, $R_1 + R_2 - R_D$ (see Figure E-1) is derived as follows.

$$R_D \cos\theta = (R_1 + R_2)\cos\phi$$

$$R_1 \sin\phi = R_D \sin\theta + h_2$$

$$R_2 \sin\phi = h_2$$

The last two equations combine to form

$$(R_1 + R_2) \sin \phi = R_D \sin \theta + 2h_2$$

Forming the sum of the squares yields

$$(R_1 + R_2)^2 = (R_D \sin \theta + 2h_2)^2 + (R_D \cos \theta)^2$$

$$= R_D^2 + 4h_2 R_D \sin \theta + 4h_2^2$$

Therefore, the path length difference, Δ, equals

$$\Delta = (R_1 + R_2) - R_D = R_D \left\{ \sqrt{1 + 4\left(\frac{h_2}{R_D}\right) \sin \phi + 4\left(\frac{h_2}{R_D}\right)^2} - 1 \right\}$$

which can be put in another form by the following substitution

$$R_D = \frac{h_1 - h_2}{\sin \theta} = \frac{(k - 1) h_2}{\sin \theta}$$

Therefore,

$$\Delta = \frac{(k - 1) h_2}{\sin \theta} \left\{ \sqrt{1 + \frac{4k}{(k - 1)^2} \sin^2 \theta} - 1 \right\}$$

For $k \geq 5$ and $\theta \leq 20$ degrees, the square root quantity in the last equation can be represented by the first order term in the series expansion

$$\sqrt{1 + u} \approx 1 + \frac{u}{2}$$

with very small error. Therefore

$$\boxed{\Delta \approx \frac{2k h_2 \sin \theta}{k - 1}}$$

For a synchronous satellite, $k >> 1$ and Δ becomes

$$\Delta = 2h_2 \sin \theta$$

For k = 5, the receiving aircraft must fly at 80 percent of its altitude in the synchronous satellite case to obtain the same multipath phase difference at the receiver.

To obtain the difference in space loss between the direct and multipath rays, the ratio $\left[(R_1 + R_2)/R_D\right]^2$ is formed

$$\left(\frac{R_1 + R_2}{R_D}\right)^2 = 1 + \frac{4k}{(k-1)^2} \sin^2 \theta$$

Again for the synchronous case $k \gg 1$ showing that the space loss is the same for the two rays. For the case k = 5 and θ = 20 degrees the worst case to be considered

$$\left(\frac{R_1 + R_2}{R_D}\right)^2 = 1.146 \text{ or } 0.6 \text{ db}$$

That is, the space loss difference between the two rays is only 0.6 db in this case as compared to 0 db for the synchronous satellite.

3. TIME RATE OF CHANGE OF PATH LENGTH DIFFERENCE

Because of the motion of the receiving aircraft and the signal source the path length difference will change with time. In the case of the synchronous satellite, the satellite will be assumed to be stationary while the receiving aircraft will have a horizontal velocity component, $\dot{d}$, and a vertical component, $\dot{h}_2$. With a balloon or aircraft signal source, $\dot{d}$ represents the relative horizontal velocity between the receiving aircraft and the signal source and $\dot{H}$ the relative vertical velocity (note: $H = h_1 - h_2$).

For the synchronous satellite case, differentiating the expression $\Delta = 2h_2 \sin \theta$,

$$\dot{\Delta} = 2\left[\dot{h}_2 \sin \theta + h_2 \dot{\nu}\right]$$

where $\nu = \sin\theta$ has been used. The time derivative $\dot{\nu}$ is obtained as follows

$$\nu = \sin\theta = \frac{H}{R_D}$$

Then

$$\dot{\nu} = \frac{1}{R_D}\left[\dot{H} - \dot{R}_D \sin\theta\right]$$

and

$$R_D = H^2 + d^2$$

$$\dot{R}_D = \left(\frac{H}{R_D}\right)\dot{H} + \left(\frac{d}{R_D}\right)\dot{d} = \dot{H}\sin\theta + \dot{d}\cos\theta$$

Finally

$$\dot{\nu} = \frac{1}{R_D}\left[\dot{H}\cos^2\theta - \frac{\dot{d}}{2}\sin 2\theta\right]$$

Substituting this result in the first equation for $\dot{\Delta}$

$$\dot{\Delta} = 2\dot{h}_2 \sin\theta + \frac{2h_2}{R_D}\left[\dot{H}\cos^2\theta - \frac{\dot{d}}{2}\sin 2\theta\right]$$

Since for a stationary satellite

$$\dot{H} = -\dot{h}_2$$

then $\dot{\Delta}$ reduces to

$$\dot{\Delta} = 2\dot{h}_2\left[\sin\theta - \left(\frac{h_2}{R_D}\right)\cos^2\theta\right] - \dot{d}\left(\frac{h_2}{R_D}\right)\sin 2\theta$$

This expression simplifies further to

$$\dot{\Delta} = 2\dot{h}_2 \sin\theta - \dot{d}\left(\frac{h_2}{R_D}\right)\sin 2\theta$$

since for the synchronous case

$$\frac{h_2}{R_D} << \sin\theta \quad \text{for} \quad \theta \geq 10 \text{ degrees}$$

Therefore the path length difference varies with time as follows:

1) For the vertical velocity component

$$\dot{\Delta}_v = 2\dot{h}_2 \sin\theta$$

2) For the horizontal velocity component

$$\dot{\Delta}_h = \dot{d}\left(\frac{h_2}{R_D}\right)\sin 2\theta$$

As an example, assume the SST flying at 70,000 feet or about 12 nautical miles. R_D for the synchronous satellite will be about 20,000 nautical miles. Assume $\dot{d}$ is 3000 ft/sec and $\dot{h}_2$ is about 300 ft/min (autopilot control). Using the worst case elevation angle θ = 20 degrees, the path length difference rates are

vertical: 3.4 ft/sec

horizontal: 1.2 ft/sec

For the simulated satellite case, differentiating the expression

$$\Delta \approx \frac{2kh_2 \sin\theta}{k-1}$$

yields

$$\dot{\Delta} \approx \frac{2\dot{k}h_2 \sin\theta}{(k-1)^2} + \frac{2k}{k-1}\left(\dot{h}_2 \sin\phi + h_2\dot{\nu}\right)$$

Also

$$\dot{k} = \frac{d}{dt}\left(\frac{h_1}{h_2}\right) = \frac{h_2\dot{h}_1 - h_1\dot{h}_2}{h_2^2} = \frac{\dot{h}_1}{k} - \frac{k\dot{h}_2}{h_2}$$

Substituting for $\dot{\nu}$ and $\dot{k}$

$$\dot{\Delta} \approx \frac{2k(k-2)}{(k-1)^2}\,\dot{h}_2 \sin\theta \left[1 + \frac{\dot{h}_1}{k(k-2)\dot{h}_2} + \frac{\dot{H}}{(k-2)\dot{h}_2}\cos^2\theta\right]$$

$$- \frac{k\dot{d}}{(k-1)^2}\sin\theta\sin 2\theta$$

In the worst case, $|\dot{H}| = |2\dot{h}_2|$, $|\dot{h}_1| = |\dot{h}_2|$ and for low elevation angles $\cos^2\theta \approx 1$. Then $\dot{\Delta}$ simplifies to

$$\dot{\Delta} \approx \frac{2k(k-2)}{(k-1)^2}\,\dot{h}_2 \sin\theta \left[1 + \frac{1}{k(k-2)} + \frac{2}{k-2}\right]$$

$$- \frac{k\dot{d}}{(k-1)^2}\sin\theta\sin 2\theta$$

Taking the vertical velocity component first and setting $k = 5$

$$\dot{\Delta}_v \sim 3.2\,\dot{h}_2 \sin\theta$$

Comparing this to the synchronous satellite case $\dot{\Delta}_v$ is seen to be higher but not significantly so.

For the horizontal component

$$\dot{\Delta}_h \approx \frac{k\dot{d}}{(k-1)^2}\sin\theta\sin 2\theta$$

Comparing this to $\dot{\Delta}_h$ for the synchronous satellite shows that the horizontal velocity component for this case, even for values of $k = 10$ instead of 5, must be considerably smaller than for the synchronous satellite. To obtain the same horizontal rate of 1.2 ft/sec as in the SST example,

$\dot{d}$ has to be only about 17 ft/sec for k = 5. Note that in this case $\dot{d}$ is not the absolute velocity of the receiving aircraft but its velocity relative to the signal source. Nevertheless, this represents a severe constraint even for rates two or three times the synchronous case because of the difficulty in controlling the relative velocity to that precision between two aircraft or an aircraft and a free floating balloon. A tethered balloon signal source would ease the problem.

4. FRESNEL ZONE

The area of the first fresnel zone at the ground reflection point of the multipath ray is defined as the locus of all ground reflection points for which the path length from the signal source to the receiving aircraft is $\lambda/2$ greater than the minimum path length which occurs at the specular reflection point. Figure E-3 shows the geometry from which the fresnel zone area is calculated as represented by the ground dimensions x and y. The distance involved can be expressed by

$$R_1 = \sqrt{h_1^2 + d_1^2} \qquad R_2 = \sqrt{h_2^2 + R_2^2}$$

$$R_1' = \sqrt{h_1^2 + (d_1 + x)^2} \qquad R_2' = \sqrt{h_2^2 + (d_2 - x)^2}$$

By appropriate expansions to the second order in x

$$R_1' = R_1 \left[1 + \frac{1}{2} \left(\frac{2x d_1 + x^2}{R_1^2} \right) - \frac{1}{8} \left(\frac{4x^2 d_1^2}{R_1^4} \right) + \ldots \right]$$

$$R_2' = R_2 \left[1 - \frac{1}{2} \left(\frac{2x d_2 - x^2}{R_2^2} \right) - \frac{1}{8} \left(\frac{4x^2 d_2^2}{R_2^4} \right) + \ldots \right]$$

The path length difference Δ is given by

$$\Delta = (R_1' + R_2') - (R_1 + R_2) = \frac{x^2}{2} \left[\frac{1}{R_1} \left(1 - \frac{d_1^2}{R_1^2} \right) + \frac{1}{R_2} \left(1 - \frac{d_2^2}{R_2^2} \right) \right]$$

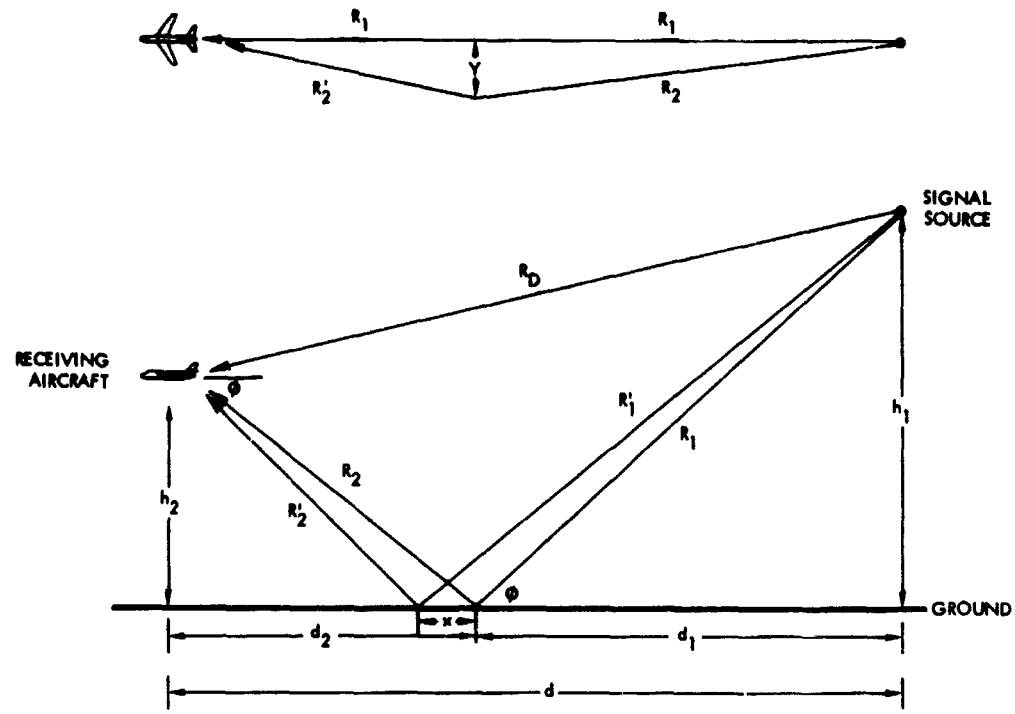

Figure E-3. Geometry for Fresnel Zone Determination

Since

$$\frac{d_1}{R_1} = \frac{d_2}{R_2} = \cos \phi$$

and

$$\frac{h_1}{R_1} = \frac{h_2}{R_2} = \sin \phi$$

the path length difference simplifies to

$$\Delta = \frac{x^2}{2}\left(\frac{1}{h_1} + \frac{1}{h_2}\right) \sin^3 \phi$$

For the first fresnel zone $\Delta = \lambda/2$ so that the dimension x equals

$$x = \sqrt{\frac{\lambda}{\left(\frac{1}{h_1} + \frac{1}{h_2}\right) \sin^3 \phi}}$$

or

$$\boxed{x = \sqrt{\frac{k \lambda h_2}{(k + 1) \sin^3 \phi}}}$$

In the synchronous satellite case $k >> 1$, and

$$x = \sqrt{\frac{\lambda h_2}{\sin^3 \phi}}$$

For the simulated case with $k = 5$

$$x = \sqrt{\frac{0.835 \lambda h_2}{\sin^3 \phi}}$$

The y dimension is derived as follows. The distances involved here are

$$R_1' = \sqrt{R_1^2 + y^2} \qquad R_2' = \sqrt{R_2^2 + y^2}$$

Again by appropriate expansions to the second order in y

$$R_1' = R_1 \left(1 + \frac{y^2}{2R_1^2} - \ldots\right)$$

$$R_2' = R_2 \left(1 + \frac{y^2}{2R_2^2} - \ldots\right)$$

The path length difference Δ equals

$$\Delta = (R_1' + R_2') - (R_1 + R_2) = \frac{y^2}{2}\left(\frac{1}{R_1} + \frac{1}{R_2}\right)$$

Since $\Delta = \lambda/2$

$$y = \sqrt{\frac{\lambda}{\frac{1}{R_1} + \frac{1}{R_2}}} = \sqrt{\frac{\lambda}{\left(\frac{1}{h_1} + \frac{1}{h_2}\right)\sin\phi}}$$

or

$$\boxed{y = \sqrt{\frac{k\lambda h_2}{(k+1)\sin\phi}}}$$

The y dimension behaves in the same manner as the x dimension as a function of altitude. Since the area of the first fresnel zone is proportional to x y, the area will decrease by the factor 0.835 from the synchronous satellite case when the altitude of the signal source is five times that of the receiving aircraft. It can be concluded that $k \geq 5$ is sufficient to provide similar fresnel zones for the two cases.